Supporting Information

For

Bisubstrate Reagent Orchestrating Adenosine Triphosphate and L-Tyrosine making Tyrosyl Adenylate: Partial Mimicking of Tyrosyl tRNA Synthetase

Harpreet Singh, Baljit Kaur, Harpreet kaur, Palwinder Singh*

Department of Chemistry and Centre for Advanced Studies, University with Potential for Excellence – Guru Nanak Dev University, Amritsar-143005. India

Table of contents

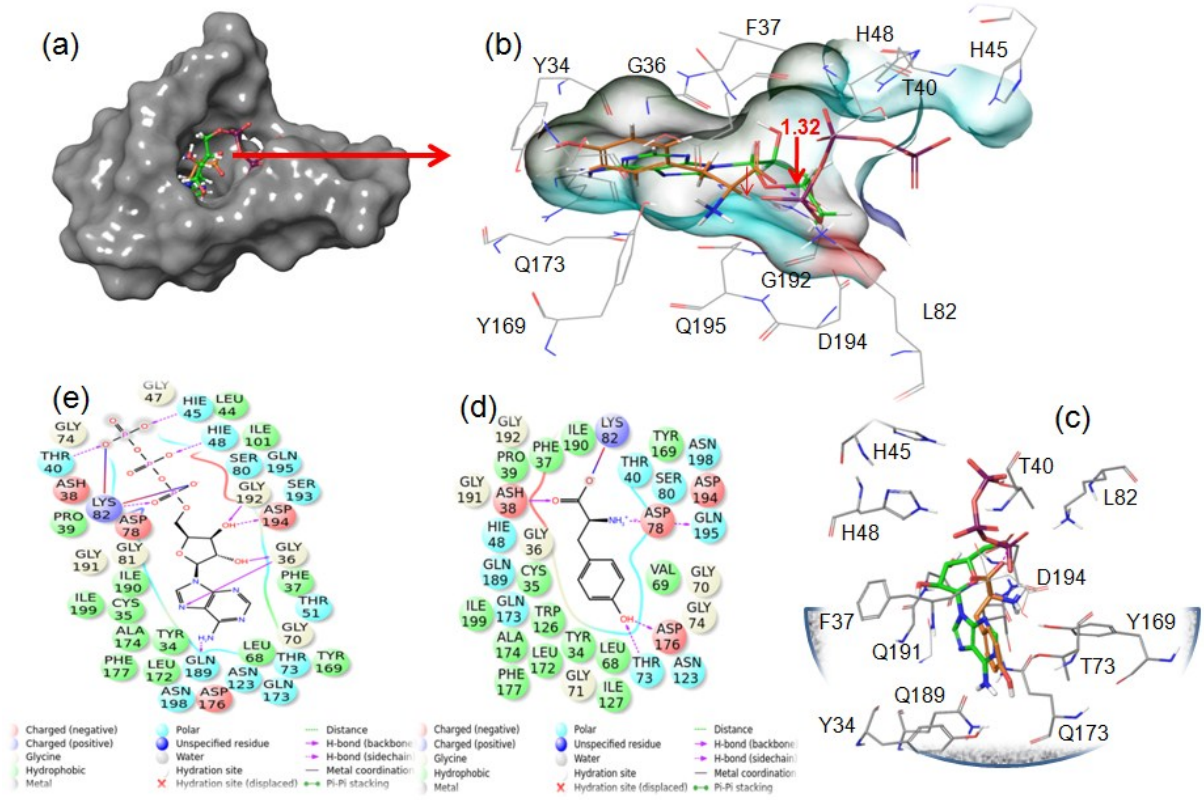

Figure S1. Structural analysis of TyrTS: (a) Total enzyme showing the active site pocket carrying L-Tyr and ATP. ATP was docked in the crystal structure of the enzyme – L-Tyr complex (PDB id 4TS1) using Schrodinger software package. (b) The active site of the enzyme is expanded to show the proximity of L-Tyr and ATP. The carboxyl group of Tyr approaches to the phosphorus centre of ATP at a distance of 1.32 Å (dotted line in red). The adenine and phenolic units are placed in the hydrophobic region constituted by Phe, Gly, Tyr residues. Light green: hydrophobic, blue: polar positive, red: polar negative. (c) Active site pocket showing placement of adenine and phenolic units of ATP and L-Tyr in the hydrophobic pocket constituted by F37, Y34, Y169. (d) 2d view showing interactions of L-Tyr in the active site pocket. (e) 2d view showing interactions of ATP in the active site pocket.

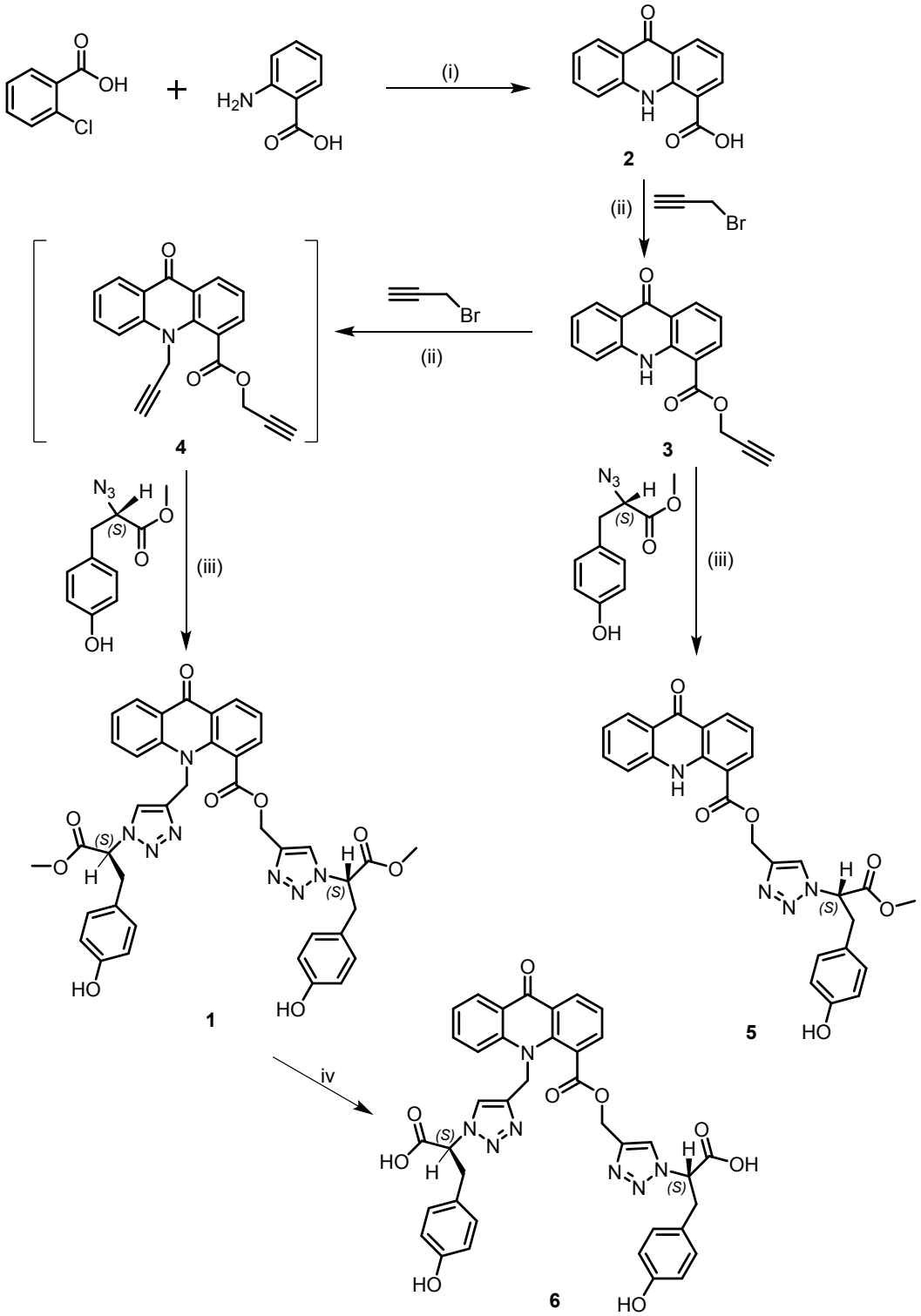

Reaction condtions: (i) (a) K_2CO_3, CuO, isoamyl alcohol, reflux, 42 h; (b) Conc. H_2SO_4, Heat
(ii) K_2CO_3, Propargyl Bromide, KI, DMF, 60 ^oC, overnight.
(iii) $CuSO_4.5H_2O$, Sodium Ascorbate, t-butanol:H_2O (9:1 v/v), 24 h, 60 ^oC.
(iv) LiOH (2 equiv), acetone - water (2:1 v/v)

Scheme S1

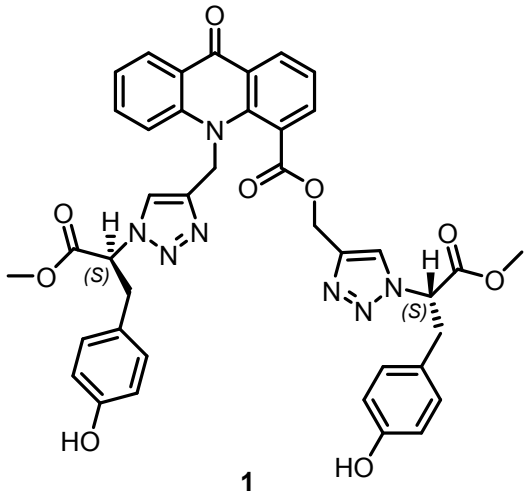

1

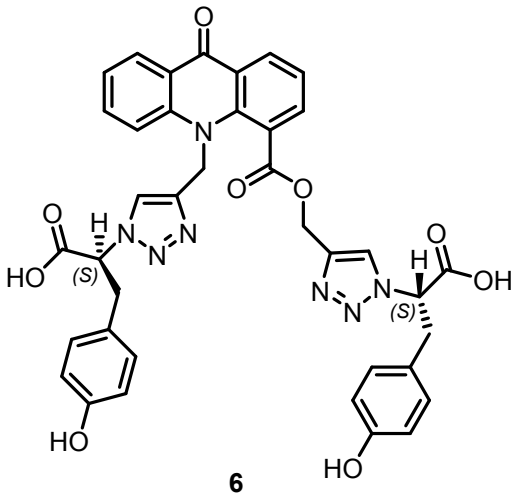

6

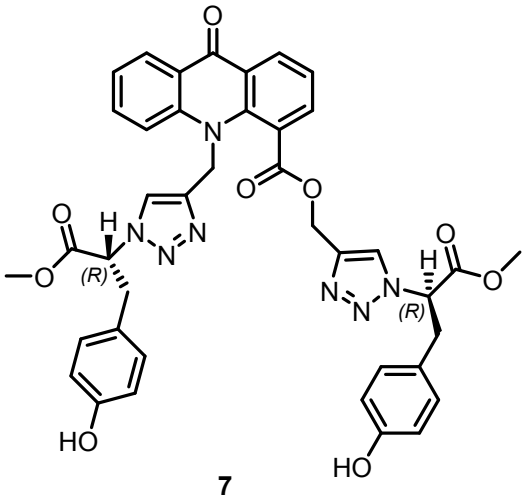

7

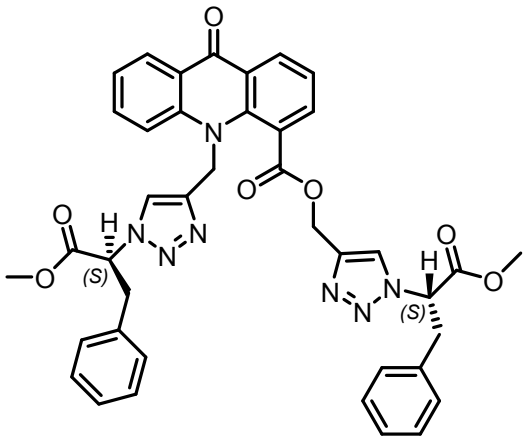

8

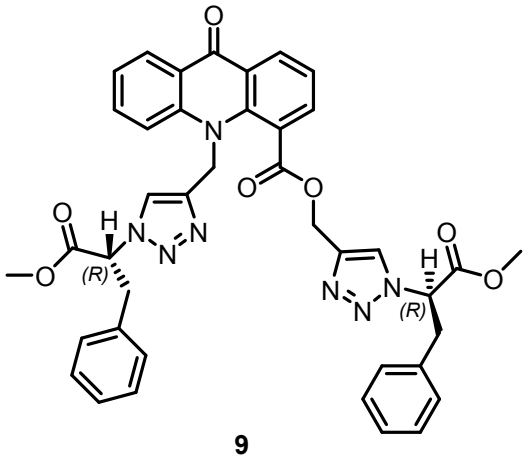

9

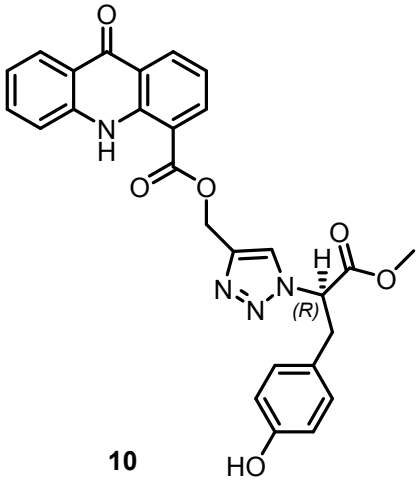

10

Chart S1

General Note

Melting points were determined in capillaries and are uncorrected. ^{1}H and ^{13}C NMR spectra were recorded on a Bruker 500 and 125 MHz NMR spectrometer, respectively, using $CDCl_3$ and/or DMSO-d_6 as solvent. Chemical shifts are given in ppm with TMS as an internal reference. *J* values are given in hertz. Signals are abbreviated as singlet, s; doublet, d; double−doublet, dd; triplet, t; and multiplet, m. In ^{13}C/DEPT-135 data, +ve sign corresponds to signals due to CH_3, CH groups while -ve signs symbolize signals of CH_2 groups and signals of quaternary carbon are absent (ab) in DEPT-135 spectra. Column chromatography was performed with silica 60-120 mesh, and reactions were monitored by thin layer chromatography (TLC) with silica plates precoated with silica gel GF-254 (Qualigens, India). Some of the reactions with the biomodel reagent and enzymatic reactions were monitored with HRMS/LC-MS. IR and UV-vis, Flourescence spectral data were recorded on FTIR Agilent CARY 630 and BIOTEK Synergy H1 Hybrid Reader instruments, respectively.

Synthesis of 9-oxo-9,10-dihydroacridine-4-carboxylic acid (2)

Mixture of 2-chlorobenzoic acid (10 g, 58.62 mmol), anthranilic acid (8.04 g, 58.62 mmol), K_2CO_3 (12.14 g, 87.94 mmol) and CuO (0.69 g, 8.79 mmol) in isoamyl alcohol was refluxed for 36 h. Isoamyl alcohol was distilled off on rotary evaporator and hot water was added to the resulting mixture followed by filtration. To the filtrate conc. HCl was added to cause precipitation. The solid product obtained after filtration was dried. The solid product was taken in a beaker and concentrated H_2SO_4 (100 mL) was added and heated on water bath for 4 h. Reaction mixture was then cooled to room temperature and poured into distilled water resulting in the formation of precipitates that were filtered to obtain 9-oxo-9,10-dihydroacridine-4-carboxylic acid; green solid, mp >300 ºC. $\bar{\upsilon}$ (cm^{-1}): 3226 (NH), 2881 (OH), 1690 (CO). ^{1}H NMR (400 MHz, DMSO-d_6) δ 5.84-7.16 (br, 1H, exchangeable with D_2O), 7.29-7.35 (m, 2H), 7.76 (d, *J* = 3.1 Hz, 2H), 8.21 (d, *J* = 7.9 Hz, 1H), 8.41-8.43 (m, 1H), 8.51 (d, *J* = 7.9 Hz, 1H), 11.93 (s, 1H, exchangeable with D_2O). ^{13}C NMR (101 MHz, DMSO-d_6) δ 114.97 (C), 118.63 (+ve, CH), 119.97 (+ve, CH), 120.23 (C), 120.60 (C), 122.01 (+ve, CH), 125.62 (+ve, CH), 132.41 (+ve, CH), 134.10 (+ve, CH), 136.89 (+ve, CH), 139.91 (C), 141.20 (C), 169.14 (C), 176.52 (C). HRMS (micro TOF-QII, MS, ESI): Calcd for $C_{14}H_9NO_3$ $[M+H]^+$ 240.0655, found 240.0529.

Synthesis of prop-2-yn-1-yl 9-oxo-9,10-dihydroacridine-4-carboxylate (3)

9-oxo-9,10-dihydroacridine-4-carboxylic acid (1 g, 4.18 mmol) was dissolved in 30 ml DMF in a round bottom flask (100 mL) fixed with a guard tube. K_2CO_3 (577 mg, 4.18 mmol),

propargyl bromide (0.37 ml, 4.18 mmol) and catalytic amount of KI were added in sequence. Reaction was allowed to stir overnight at 60 ºC. After the completion of reaction (TLC), ethyl acetate was added to the reaction mixture, washed with distilled water. Organic layer was then washed with saturated solution of $NaHCO_3$, dried over Na_2SO_4 and concentrated under vacuum. The residue was purified by washing with diethyl ether to yield yellow solid. Yield 36%. $\bar{\upsilon}$ (cm^{-1}): 3257 (NH), 3201 (CH), 1694 (CO). ^{1}H NMR (500 MHz, $CDCl_3$) δ 2.60 (t, *J* = 2.4 Hz, 1H), 5.02 (d, *J* = 2.1 Hz, 2H), 7.32-7.26 (m, 2H), 7.39 (d, *J* = 8.2 Hz, 1H), 7.67-7.71 (m, 1H), 8.43-8.48 (m, 2H), 8.74-8.75 (m, 1H), 11.59 (s, 1H). ^{13}C NMR (126 MHz, $CDCl_3$) δ 52.93 (-ve, CH_2), 75.70 (+ve, CH), 112.85 (C), 117.60 (+ve, CH), 119.95 (+ve, CH), 121.60 (C), 122.47 (C), 122.57 (+ve, CH), 127.08 (+ve, CH), 134.08 (+ve, CH), 134.57 (+ve, CH), 136.86 (+ve, CH), 140.04 (C), 141.91 (C), 167.50 (C), 177.70 (C). HRMS (micro TOF-QII, MS, ESI): Calcd for $C_{17}H_{11}NO_3$ 278.0811 $[M+H]^+$, found 278.0844.

Synthesis of prop-2-yn-1-yl 9-oxo-10-(prop-2-yn-1-yl)-9,10-dihydroacridine-4-carboxylate (4)

Taken in a round bottom flask fixed with a guard tube, compound **3** (100 mg, 0.36 mmol) was dissolved in 10 ml DMF. K_2CO_3 (75 mg, 0.54 mmol), propargyl bromide (0.05 ml, 0.54 mmol) and catalytic amount of KI were added in sequence. Reaction was allowed to stir overnight at 60 ºC. After the completion of reaction (TLC), the reaction mixture was diluted with ethyl acetate and washed with distilled water. Organic layer was separated and passed through Na_2SO_4 and distilled off under reduced pressure to yield solid that was used without further purification.

Synthesis of methyl 2-azido-3-(4-hydroxyphenyl)propanoate

L-tyrosine methyl ester hydrochloride (500 mg, 2.56 mmol) was dissolved in MeOH (13 mL). K_2CO_3 (846.56 mg, 3.07 mmol), $CuSO_4$ (6.36 mg, 1 mol %) and imidazole sulphonyl azide hydrochloride (ISA.HCl) (643.89 mg, 3.07 mmol) were added to the reaction mixture and it was stirred for 6 h at room temperature. After the completion of the reaction, it was quenched with water and extracted with ethyl acetate. Organic layer was separated and dried over Na_2SO_4 and concentrated under vacuum. The residue was purified by column chromatography as pale yellow liquid, yield 90%, ^{1}H NMR (400 MHz, $CDCl_3$) δ 2.92-3.13 (m, 2H), 3.78 (s, 3H), 4.03 (dd, *J* = 8.7, 5.5 Hz, 1H), 5.03 (s, 1H), 6.79 (dd, *J* = 6.4, 2.3 Hz, 2H), 7.09 (dd, *J* = 6.4, 1.8 Hz, 2H), 7.26 (s, 1H). ^{13}C NMR (101 MHz, $CDCl_3$) δ 36.84 (-ve, CH_2), 52.65 (+ve, OCH_3), 63.44 (+ve, CH), 115.54 (+ve, CH), 127.99 (C), 130.42 (+ve, CH),

154.91 (C). HRMS (micro TOF-QII, MS, ESI): Calcd for $C_{10}H_{11}N_3O_3$ 239.1139 $[M+NH_4]^+$, found 239.0970.

Synthesis of (1-(3-(4-hydroxyphenyl)-1-methoxy-1-oxopropan-2-yl)-1*H*-1,2,3-triazol-4-yl)methyl 9-oxo-9,10-dihydroacridine-4-carboxylate (5)

Compound **3** (100 mg, 0.36 mmol) was dissolved in 18 mL t-butanol. To this solution sodium ascorbate (3.57 mg, 5 mol %) in 1 mL water, $CuSO_4.5H_2O$ (1.79 mg, 2 mol %) in 1 mL water and methyl 2-azido-3-(4-hydroxyphenyl)propanoate (79.78 mg, 0.36 mmol) were added in sequence and the reaction was stirred for 14 h at 60 ºC. Reaction was monitored with TLC. After the completion of reaction, it was diluted with water and extracted with ethyl acetate. The organic layer was dried over Na_2SO_4 and distilled under reduced pressure to yield solid compound that was purified by washing with diethyl ether to yield yellowish solid. Yield 61%. Mp 197-200 ^oC; $[\alpha]_D^{25}$ = -65^o (0.5, DMSO). $\bar{\upsilon}$ (cm^{-1}): 3293 (OH), 1742 (CO). ^1H NMR (500 MHz, DMSO-d_6) δ 3.40-3.48 (m, 2H), 3.71 (s, 3H), 5.53 (d, *J* = 4.64 Hz, 2H), 5.81 (dd, *J* = 10.41, 5.3 Hz, 1H), 6.53 (d, *J* = 8.2 Hz, 2H), 6.91 (d, *J* = 8.2 Hz, 2H), 7.35-7.41 (m, 2H), 7.79-7.87 (m, 2H), 8.25 (d, *J* = 7.9 Hz, 1H), 8.37 (d, *J* = 7.6 Hz, 1H), 8.41 (s, 1H), 8.58 (d, *J* = 7.9 Hz, 1H), 9.23 (s, 1H, exchangeable with D_2O), 11.60 (s, 1H, exchangeable with D_2O). ^{13}C NMR (126 MHz, DMSO-d_6) δ 3.46 (-ve, CH_2), 53.35 (+ve, OCH_3), 59.11 (-ve, CH_2), 63.88 (+ve, CH), 114.63 (C), 115.53 (+ve, CH), 119.09 (+ve, CH), 120.84 (+ve, CH), 122.24 (C), 123.00 (+ve, CH), 125.70 (+ve, CH), 126.06 (C), 126.43 (+ve, CH), 130.34 (+ve, CH), 133.54 (+ve, CH), 134.71 (+ve, CH), 137.10 (+ve, CH), 140.52 (C), 141.28 (C), 141.87 (C), 156.60 (C), 166.80 (C), 169.40 (C), 176.90 (C). HRMS (micro TOF-QII, MS, ESI): Calcd for $C_{27}H_{22}N_4O_6$ 499.1612 $[M+H]^+$, found 499.1453.

Synthesis of (1-(3-(4-hydroxyphenyl)-1-methoxy-1-oxopropan-2-yl)-1*H*-1,2,3-triazol-4-yl)methyl 10-((1-(3-(4-hydroxyphenyl)-1-methoxy-1-oxopropan-2-yl)-1*H*-1,2,3-triazol-4-yl)methyl)-9-oxo-9,10-dihydroacridine-4-carboxylate (1).

Compound **4** (50 mg, 0.16 mmol) was dissolved in 18 mL t-butanol. To this solution sodium ascorbate (12.57 mg, 40 mol %) in 1 mL distilled water, $CuSO_4.5H_2O$ (7.89 mg, 20 mol %) in 1 mL water and methyl 2-azido-3-(4-hydroxyphenyl)propanoate (70.15 mg, 0.31 mmol) were added in sequence and the reaction was stirred at 60 ºC for 20 h. After the completion of reaction (TLC), it was diluted with distilled water and extracted with ethyl acetate. Ethyl acetate was distilled off under reduced pressure to yield solid compound that was purified with column chromatography using ethyl acetate – hexane (7:3) as eluent to isolate the product, yield 10%. Mp 110-112 ^oC; $[\alpha]_D^{25}$ = -30^o (0.5, $CHCl_3$). ^1H NMR (400 MHz, $CDCl_3$) δ 3.14 (d, *J* = 6.7 Hz, 2H), 3.34-3.50 (m, 2H), 3.69 (s, 3H), 3.76 (s, 3H), 5.36 (m, 1H), 5.42-

5.46 (m, 4H), 5.54-5.61 (dd, *J* = 9.90, 5.41 Hz, 1H), 6.25 (d, *J* = 8.3 Hz, 2H), 6.45 (d, *J* = 8.8 Hz, 2H), 6.56 (d, *J* = 8.3 Hz, 2H), 6.73 (s, 1H), 6.77 (d, *J* = 8.45 Hz, 2H), 7.21 (d, *J* = 10.9 Hz, 1H), 7.24 (d, *J* = 7.75 Hz, 2H), 7.43-7.45 (m, 1H), 7.51 (t, *J* = 7.62 Hz, 1H), 7.77 (s, 1H), 8.03 (d, *J* = 6.87 Hz, 1H), 8.28 (d, *J* = 7.55 Hz, 1H), 8.51 (d, *J* = 7.90 Hz, 1H). ^{13}C NMR (101 MHz, $CDCl_3$) δ 37.62 (-ve, CH_2), 37.76 (-ve, CH_2), 49.54 (-ve, CH_2), 53.18 (+ve, OCH_3), 53.25 (+ve, OCH_3), 58.55 (-ve, CH_2), 64.22 (+ve, CH), 64.35 (+ve, CH), 115.79 (+ve, CH), 116.01 (+ve, CH), 118.62 (+ve, CH), 121.27 (C), 121.78 (+ve, CH), 122.87 (+ve, CH), 123.21 (+ve, CH), 123.91 (C), 124.92, 125.12 (C), 125.41 (C), 125.66 (C), 127.08 (CH), 129.61 (CH), 129.94 (CH), 131.54 (CH), 134.06 (CH), 137.23 (CH), 141.85 (C), 142.47 (C), 142.82 (C), 143.20 (C), 155.74 (C), 155.77 (C), 166.77 (C), 168.33 (C), 168.59 (C), 178.68 (C). HRMS (micro TOF-QII, MS, ESI): Calcd for $C_{40}H_{35}N_7O_9$ 758.2569 $[M+H]^+$, found 758.2670.

(*S*)-2-(4-((4-(((1-((*S*)-1-Carboxy-2-(4-hydroxyphenyl)ethyl)-1*H*-1,2,3-triazol-4-yl)methoxy)carbonyl)-9-oxoacridin-10(9*H*)-yl)methyl)-1*H*-1,2,3-triazol-1-yl)-3-(4-hydroxyphenyl)propanoic acid (6).

Compound **1** (30 mg, 0.039 mmol) was dissolved in acetone water 2 : 1 (5 mL acetone, 2.5 mL water) followed by the addition of LiOH (1.66 mg, 0.079 mmol). The reaction mixture was stirred at 35 ^{o}C and monitored with TLC. After the completion of the reaction, acetone was removed on rota-vapor and the reaction mixture was cooled in ice bath. 1N HCl was added to cause the precipitation and the precipitates were collected by vacuum filtration to procure pure product 35%. ^{1}H NMR (500 MHz, DMSO-d_6) δ 3.05-3.04 (m, 4H, 2xCH_2), 5.30-5.45 (m, 5H, 2xCH_2), 5.63 (br, 1H), 6.38-6.47 (m, 6H, ArH), 6.86 (d, 2H, ArH, *J*=5.94 Hz), 7.30 (t, *J*=6.38 Hz, 1H, ArH), 7.43 (t, *J*=7.57 Hz, 1H, ArH,), 7.68 (s, 2H, ArH), 7.98 (d, *J*=6.87 Hz, 1H, ArH), 8.04 (d, *J*=6.0 Hz, 1H, ArH), 8.17 (d, *J*=7.34 Hz, 1H, ArH), 8.35 (s, 1H), 8.45 (d, *J*=6.59 Hz 1H, ArH), 9.21 (s, 2xOH), 13.22-13.89 (br, OH). ^{13}C NMR (126 MHz, DMSO-d_6) δ 35.90 (CH_2), 36.10 (CH_2), 48.58 (CH_2), 58.54 (CH_2), 63.71 (CH), 63.86 (CH), 114.95 (CH), 119.11 (CH), 121.49 (CH), 121.84 (C), 122.36 (C), 123.68 (CH), 124.92 (CH), 125.21 (CH), 125.81 (C), 125.96 (CH), 126.03(C), 129.39 (CH), 129.68 (CH), 130.31 (CH), 133.60 (CH), 136.24 (CH), 141.04 (C), 141.64 (C), 142.50 (C), 143.03 (C), 155.83 (C), 155.97 (C), 166.51 (C=O), 169.47 (C=O), 169.73 (C=O), 176.84 (C=O). HRMS (micro TOF-QII, MS, ESI): Calcd for $C_{38}H_{31}N_7O_9$ 730.2256 [M+H], found 730.2250).

(1-((*R*)-3-(4-hydroxyphenyl)-1-methoxy-1-oxopropan-2-yl)-1*H*-1,2,3-triazol-4-yl)methyl 10-((1-((*R*)-3-(4-hydroxyphenyl)-1-methoxy-1-oxopropan-2-yl)-1*H*-1,2,3-triazol-4-

yl)methyl)-9-oxo-9,10-dihydroacridine-4-carboxylate (7). 17%, mp 105-107 ^{o}C; $[\alpha]_D^{25}$ = +40^{o} (0.5, $CHCl_3$).

(1-((S)-1-methoxy-1-oxo-3-phenylpropan-2-yl)-1H-1,2,3-triazol-4-yl)methyl 10-((1-((S)-1-methoxy-1-oxo-3-phenylpropan-2-yl)-1H-1,2,3-triazol-4-yl)methyl)-9-oxo-9,10-dihydroacridine-4-carboxylate (8). Compound 4 (150 mg, 0.476 mmol) was dissolved in 54 ml t-butanol. To this solution sodium ascorbate (37.72 mg, 40 mol %) in 3 ml distilled water, $CuSO_4$ .5H_2O (23.67 mg, 20 mol %) in 3 ml distilled water and methyl (*S*)-2-azido-3-phenylpropanoate (195.23 mg, 0.952 mmol) were added in sequence and the reaction was stirred at 60 ºC for 20 h and the reaction was monitored with TLC. After the completion of reaction, it was diluted with distilled water and extracted with ethyl acetate. Ethyl acetate was distilled off under reduced pressure to yield solid which was purified with column chromatography to isolate the product, 17%, mp 120-123 ^{o}C; $[\alpha]_D^{25}$ = -50^{o} (0.5, $CHCl_3$). $\bar{\upsilon}$ (cm^{-1}): 1746 (CO). ^{1}H NMR (400 MHz, $CDCl_3$) δ 3.35-3.16 (m, 2H, CH_2), 3.56-3.43 (m, 2H, CH_2), 3.64 (s, 3H, OCH_3), 3.72 (s, 3H, OCH_3), 5.48-5.28 (m, 5H, $2CH_2$, CH), 5.60 (dd, J = 8.7, 6.4 Hz, 1H), 6.69 (d, 2ArH, J = 6.9 Hz), 6.93 (s, 1H), 7.02 (d, 2ArH, J = 3.2 Hz), 7.17-7.06 (m, 6ArH), 7.34-7.28 (m, 2ArH), 7.41 (d, 1ArH, J = 8.2 Hz), 7.59-7.55 (m, 1ArH), 7.78 (s, 1H), 8.04 (dd, J = 7.5, 1ArH, 1.6 Hz), 8.43-8.40 (m, 1ArH), 8.66 (dd, 1ArH, J = 7.8, 1.4 Hz). ^{13}C NMR (101 MHz, $CDCl_3$) δ 38.36 (CH_2), 38.77 (CH_2), 49.98 (CH_2), 53.09 (CH), 53.14 (CH), 58.68 (CH_2), 64.01 (CH_3), 64.09 (CH_3), 118.55 (CH), 121.42 (CH), 121.49 (CH), 122.36 (CH), 122.59 (C), 124.11 (C), 124.43(CH), 125.61 (C), 127.21 (CH), 127.48 (CH), 127.57 (CH), 128.57 (CH), 128.74 (CH), 128.78 (CH), 128.85 (CH), 131.57 (CH), 133.68 (CH), 134.34 (C), 134.54 (C), 136.68 (CH), 142.00 (C), 143.00 (C), 143.27 (C), 143.38 (C), 166.97 (C), 168.25 (C), 168.52 (C), 178.09 (C). HRMS (micro TOF-QII, MS, ESI): Calcd for $C_{40}H_{35}N_7O_7$ $[M+Na]^+$, found 748.2466.

(1-((*R*)-1-Methoxy-1-oxo-3-phenylpropan-2-yl)-1*H*-1,2,3-triazol-4-yl)methyl 10-((1-((*R*)-1-methoxy-1-oxo-3-phenylpropan-2-yl)-1*H*-1,2,3-triazol-4-yl)methyl)-9-oxo-9,10-dihydroacridine-4-carboxylate (9). 20%, mp 116-119 ^{o}C; $[\alpha]_D^{25}$ = +40^{o} (0.5, $CHCl_3$).

(*S*)-(1-(3-(4-Hydroxyphenyl)-1-methoxy-1-oxopropan-2-yl)-1*H*-1,2,3-triazol-4-yl)methyl 9-oxo-9,10-dihydroacridine-4-carboxylate (10). 59%, mp 172-174 ^{o}C; $[\alpha]_D^{25}$ = +60^{o} (0.5, DMSO).

Reagent 1 mediated formation of tyrosyl adenylate

Solution of reagent **1** (1 mmol), ATP (1.2 mmol), $Mg(OAc)_2$ (16 mmol) and L-Tyr (1.2 mmol) in DMSO-H_2O (20 mL, 1:9 v/v) was stirred at 25±2 ^{o}C for 1.5h. The pH of the reaction mixture was maintained at 7.4 using 0.01N HCl. Formation of tyrosyl adenylate was detected in the HRMS of the reaction mixture. The reaction mixture was concentrated in

vacuum and the residue was purified with flash chromatography using ethyl acetate – methanol as the eluent. Reagent **1** and tyrAd were isolated in 90% and 65% respectively. TyrAd was obtained as thick oil; $[\alpha]_D^{25}$ = -18° (0.5, DMSO), ^{1}HNMR (400 MHz, DMSO-d_6+D_2O, 9:1) δ 8.43 (s, 2H), 8.09 (d, *J* = 4.6 Hz, 3H), 7.00 (d, *J* = 8.7 Hz, 2H), 6.63 (d, *J* = 8.7 Hz, 2H), 5.86 (d, *J* = 6.4 Hz, 1H), 4.60-4.49 (m, 2H), 4.15 (t, *J* = 3.9 Hz, 1H), 3.99-4.04 (m, 1H), 3.92 (d, *J* = 8.4 Hz, 1H), 3.76-3.78 (m, 1H), 3.38 (q, *J* = 4.3 Hz, 1H), 2.98 (dd, *J* = 14.4, 4.3 Hz, 1H), 2.72 (dd, *J* = 14.4, 8.5 Hz, 1H); ^{13}C DEPT NMR (101 MHz) δ 36.03 (-ve, CH_2), 49.18 (+ve), 56.32 (+ve), 64.04 (-ve, CH_2), 71.03 (+ve), 74.91 (+ve), 79.39 (+ve), 84.99 (+ve), 87.68 (+ve), 115.58 (+ve), 130.92 (+ve), 144.27 (+ve), 153.18 (+ve), 171.48 (C=O). HRMS (micro TOF-QII, MS, ESI): Calcd for $C_{19}H_{23}N_6O_9P$ 511.1336 $[M+H]^+$, found 511.1330.

Reaction between ATP and L-Tyr. A mixture of ATP (1 mmol) and L-Tyr (1.2 mmol) in different solvents (H_2O, DMF, ACN) in the presence of $Mg(OAc)_2$ was stirred at 25 – 100 °C for several hours. The reaction was monitored by recording HRMS at different time intervals. We did not observe the peak for tyrAd.

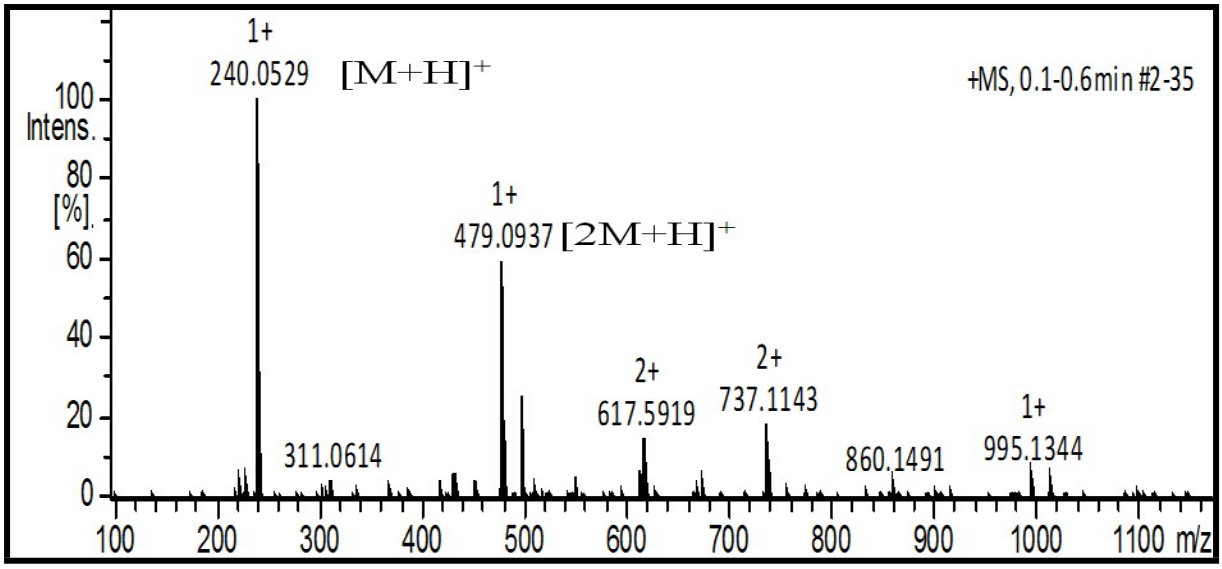

Figure S2. Mass spectrum of compound **2** with mass peak at *m/z* 240.0529 (calcd *m/z* 240.0655 $[M+H]^+$).

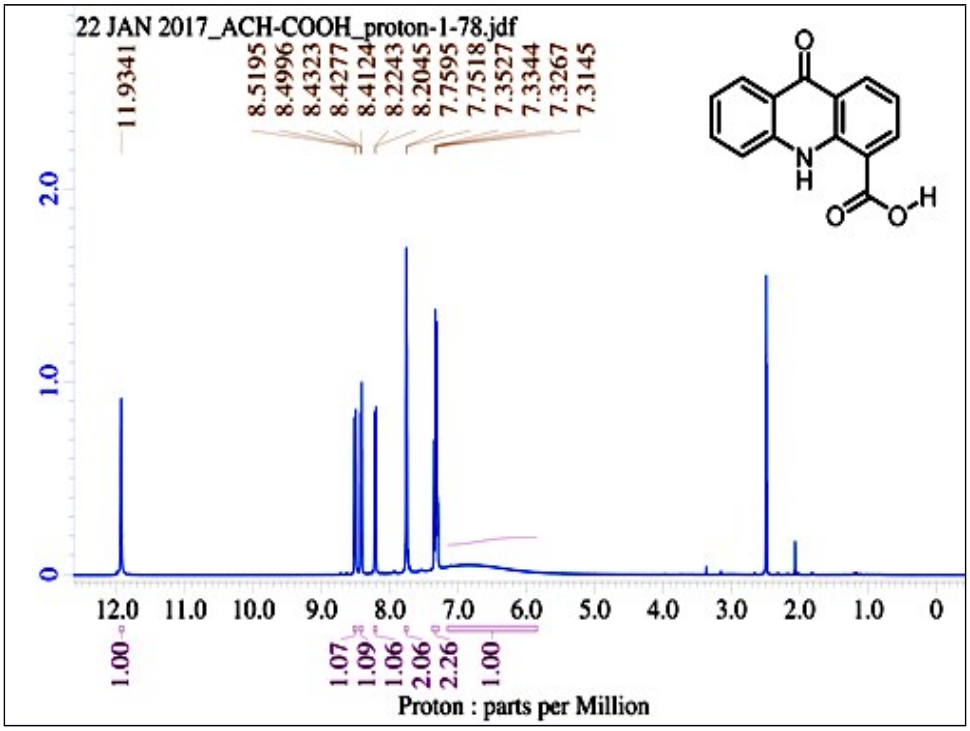

Figure S3. ^{1}H NMR spectrum of compound **2** (DMSO-d_6 as solvent).

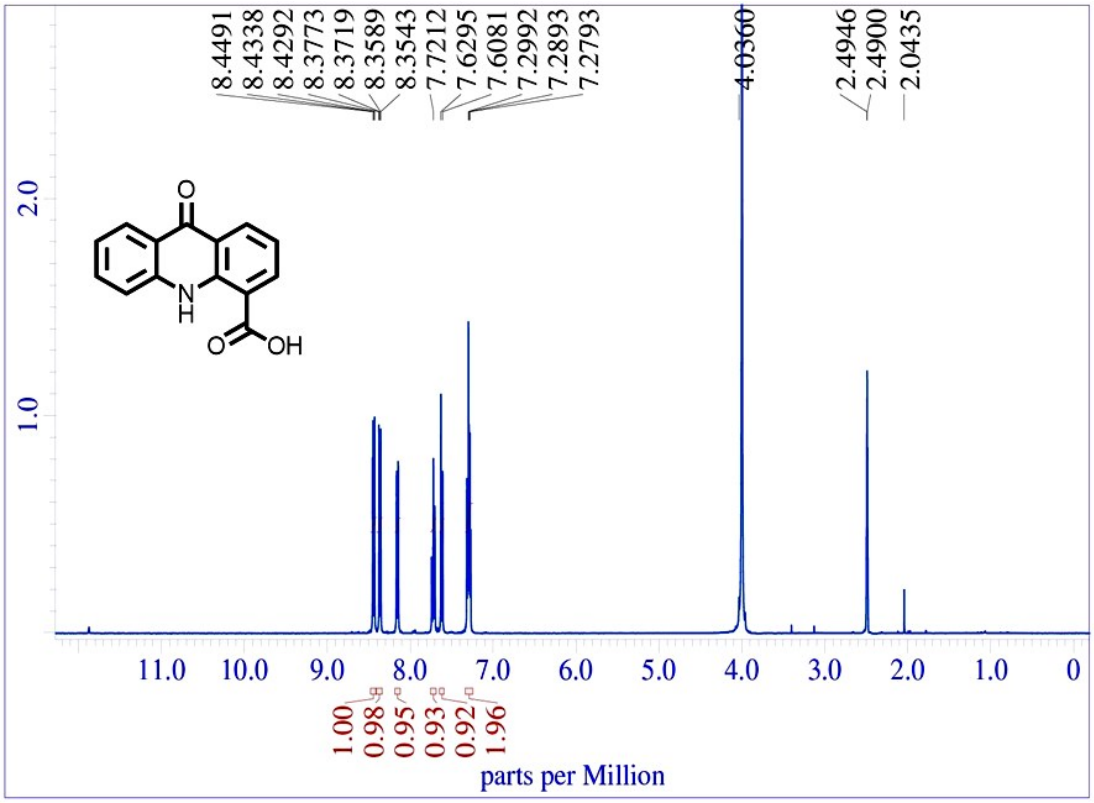

Figure S4. ^{1}H NMR spectrum of compound **2** (DMSO-d_6 as solvent) with one drop of D_2O for detecting exchangeable protons.

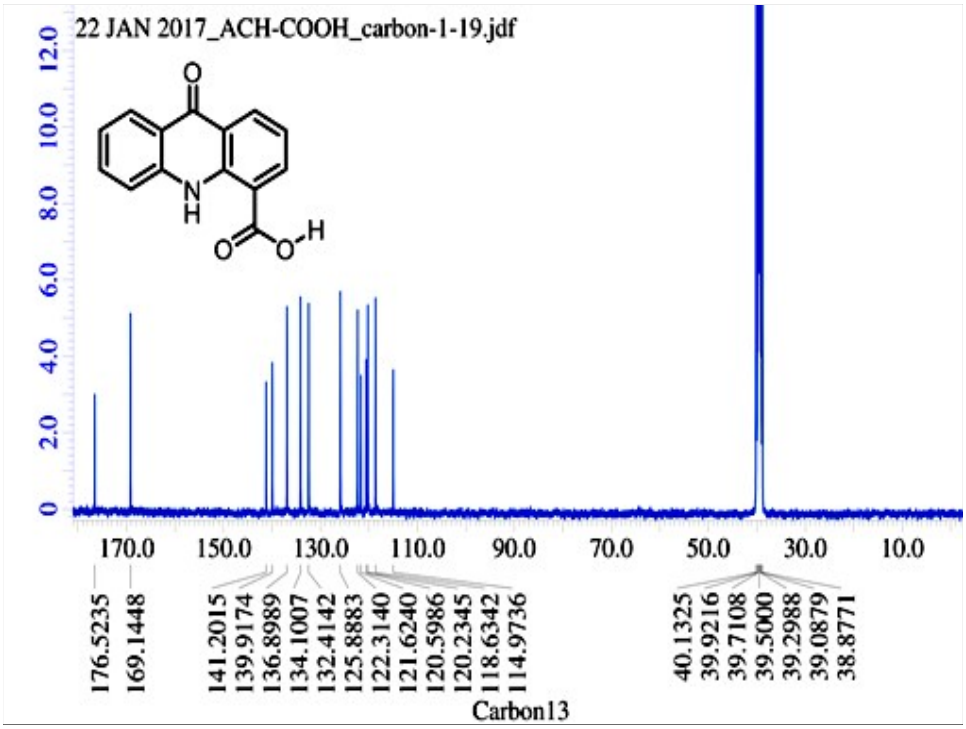

Figure S5. ^{13}C NMR spectrum of compound **2** (DMSO-d_6 as solvent).

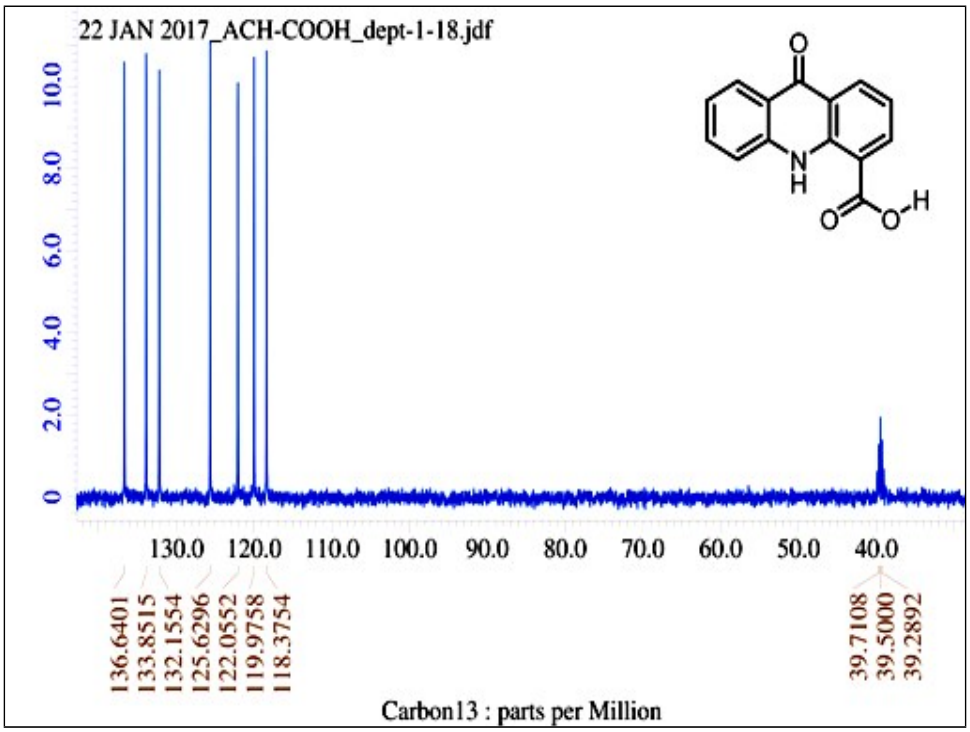

Figure S6. DEPT-135 NMR spectrum of compound **2** (DMSO-d_6 as solvent).

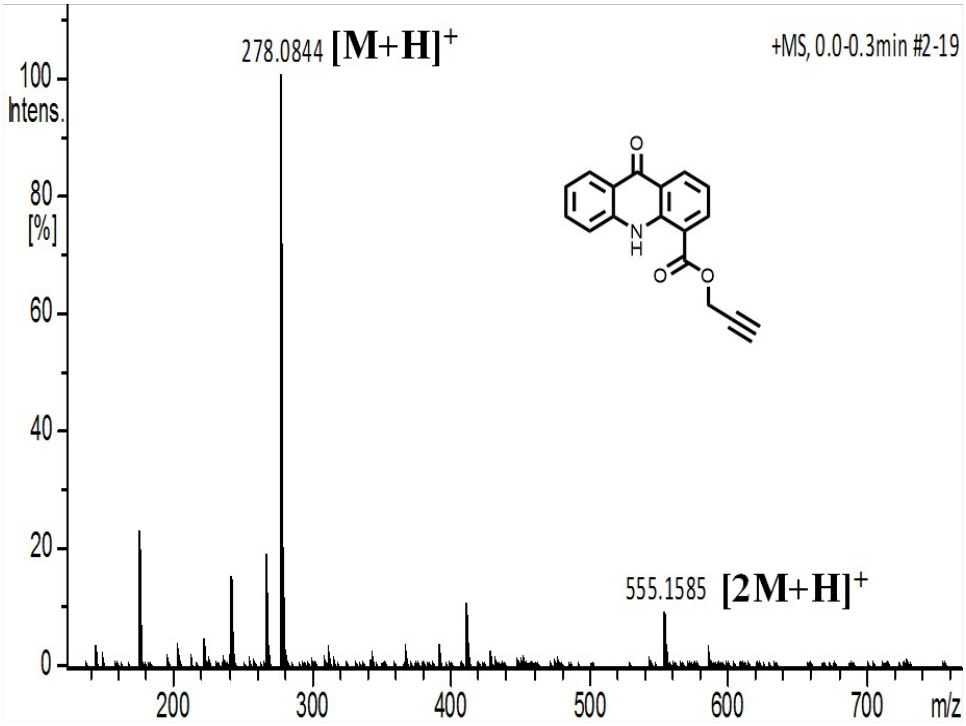

Figure S7. Mass spectrum of compound **3** with mass peak at *m/z* 278.0844 $[M+H]^+$, 555.1585 $[2M+H]^+$ (calcd *m/z* 278.0811 $[M+H]^+$, 555.1550 $[2M+H]^+$).

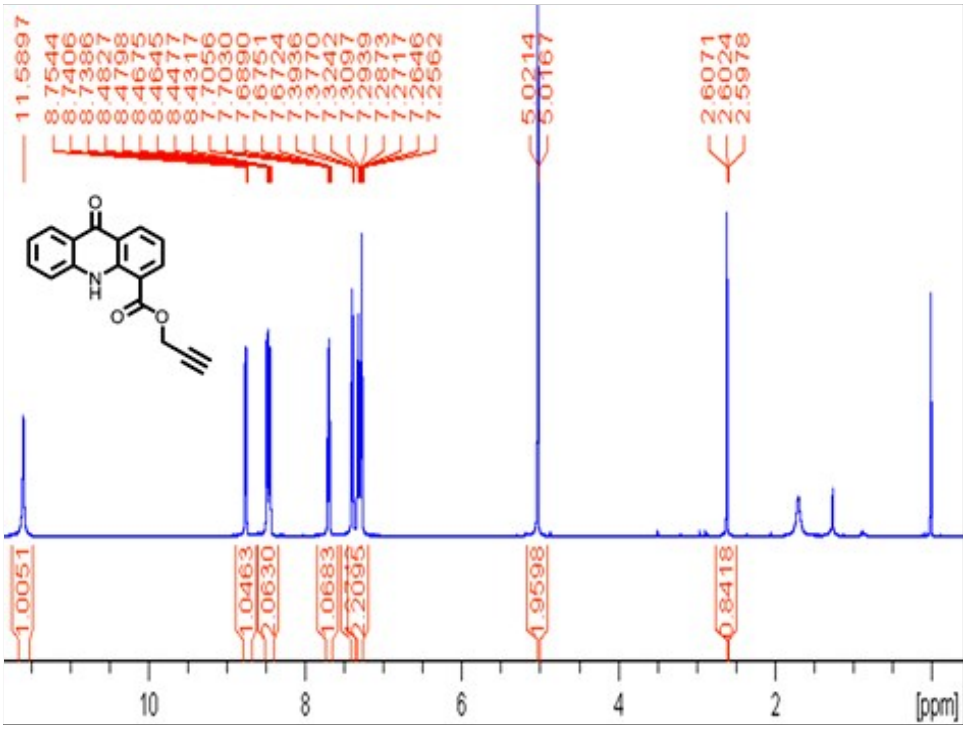

Figure S8. ^1H NMR spectrum of compound **3** ($CDCl_3$ as solvent).

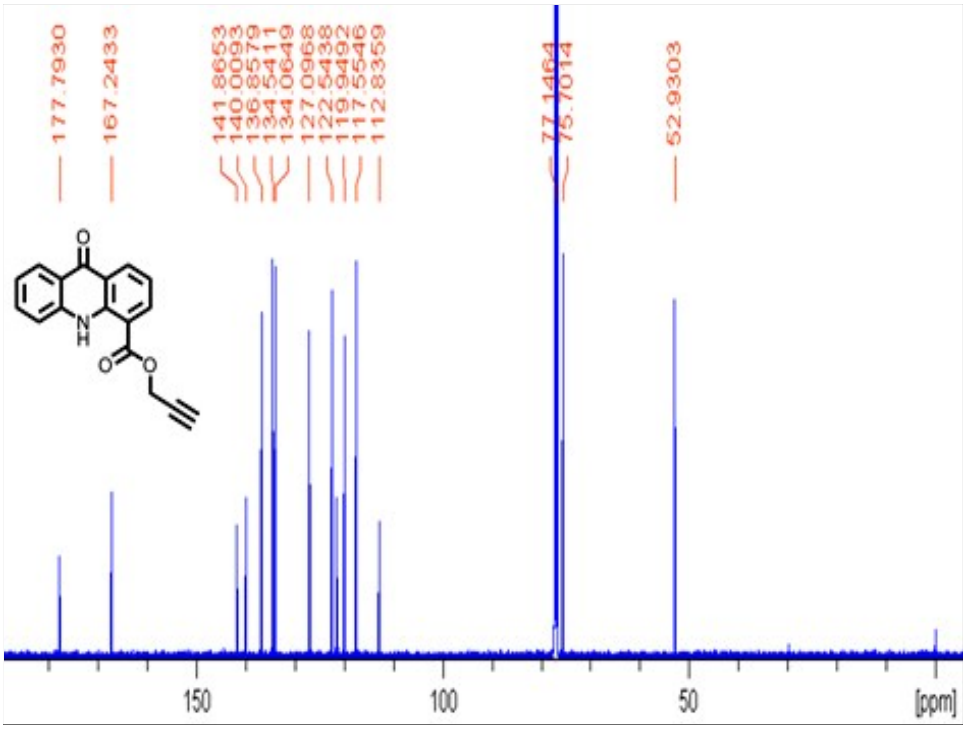

Figure S9. ^{13}C NMR spectrum of compound **3**.

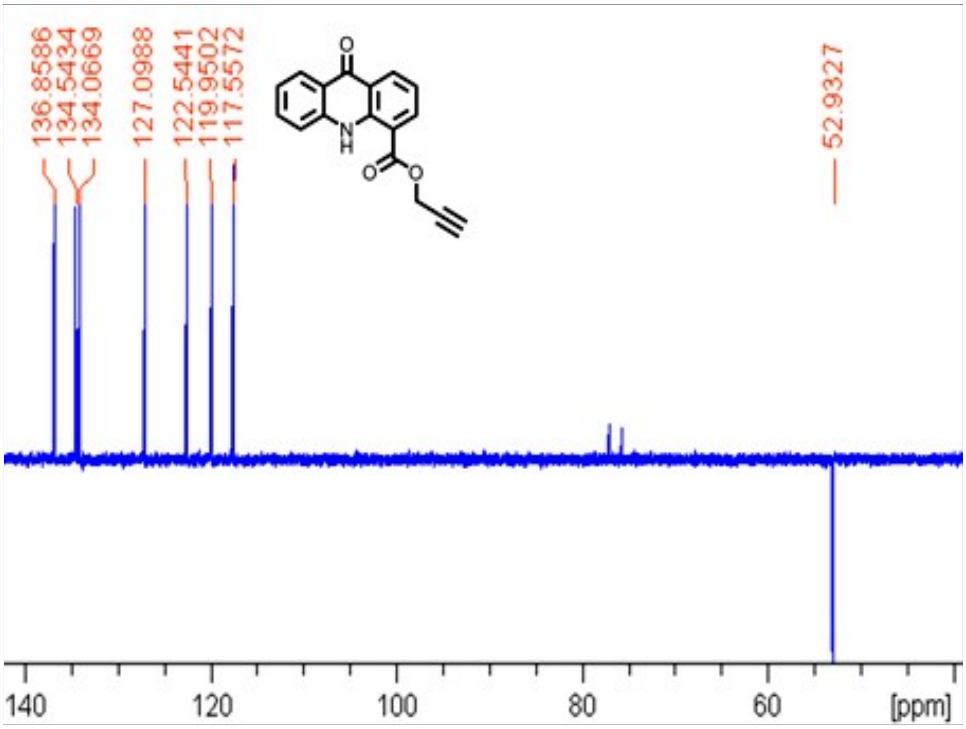

Figure S10. DEPT-135 NMR spectrum of compound **3**.

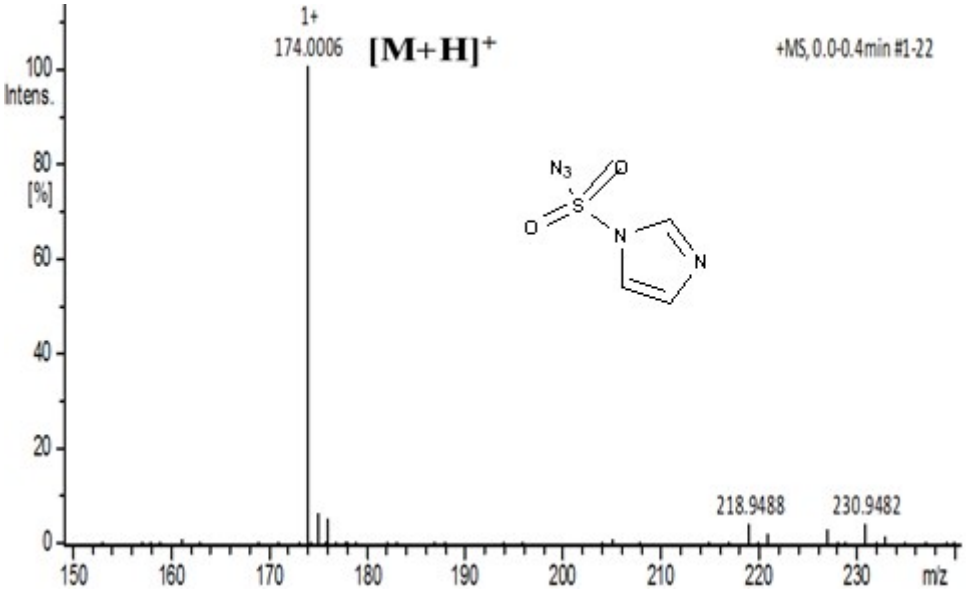

Figure S11. HRMS of the compound shown in the inset (calcd *m/z* 174.0080 $[M+H]^+$).

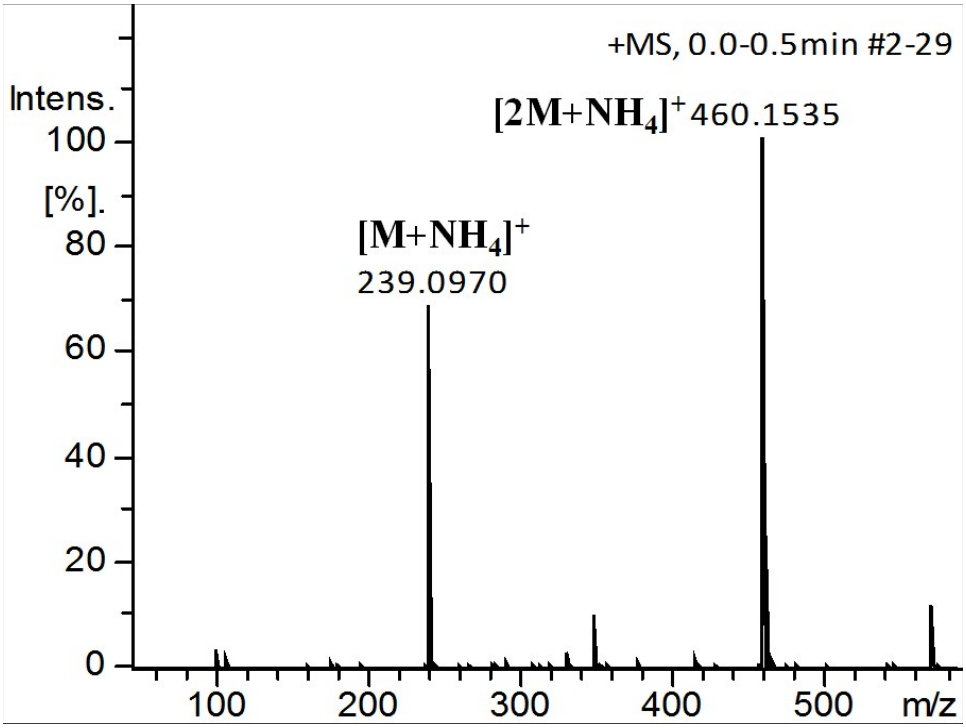

Figure S12. Mass spectrum of tyrosine azide with mass peak at *m/z* 239.0970 (calcd *m/z* 239.1139 $[M+NH_4]^+$).

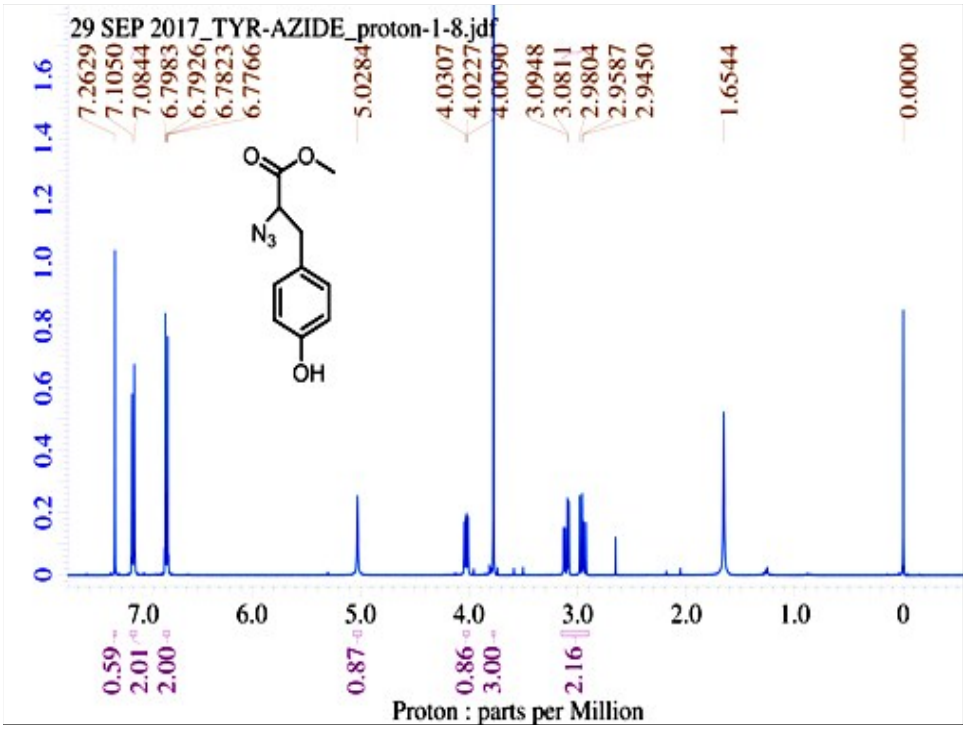

Figure S13. ^{1}H NMR spectrum of tyrosine azide ($CDCl_3$ as solvent).

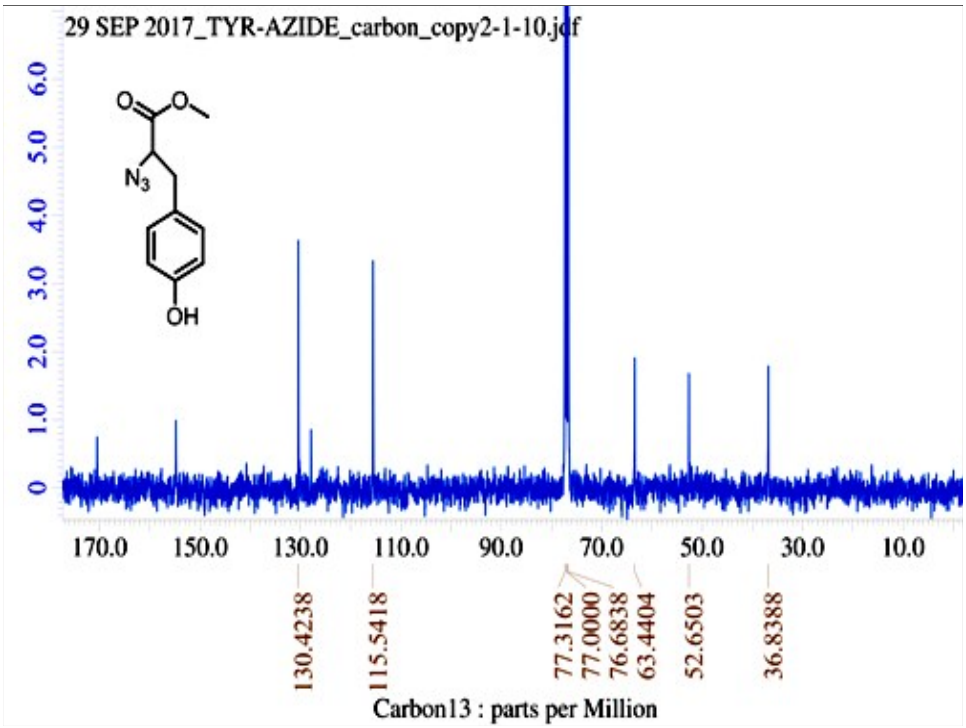

Figure S14. ^{13}C NMR spectrum of tyrosine azide ($CDCl_3$ as solvent).

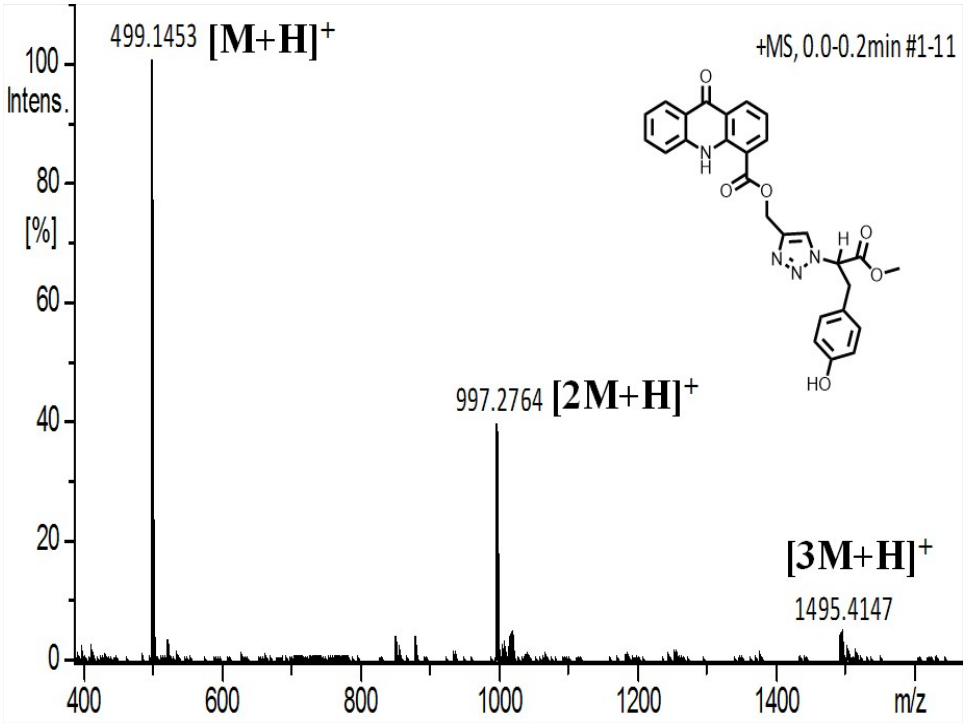

Figure S15. Mass spectrum of compound **5** with mass peaks at *m/z* 499.1453 $[M+H]^+$, 997.2764 $[2M+H]^+$, 1495.4147 $[3M+H]^+$ (calcd *m/z* 499.1612 [M+H], 997.3151 $[2M+H]^+$, 1495.4690 $[3M+H]^+$).

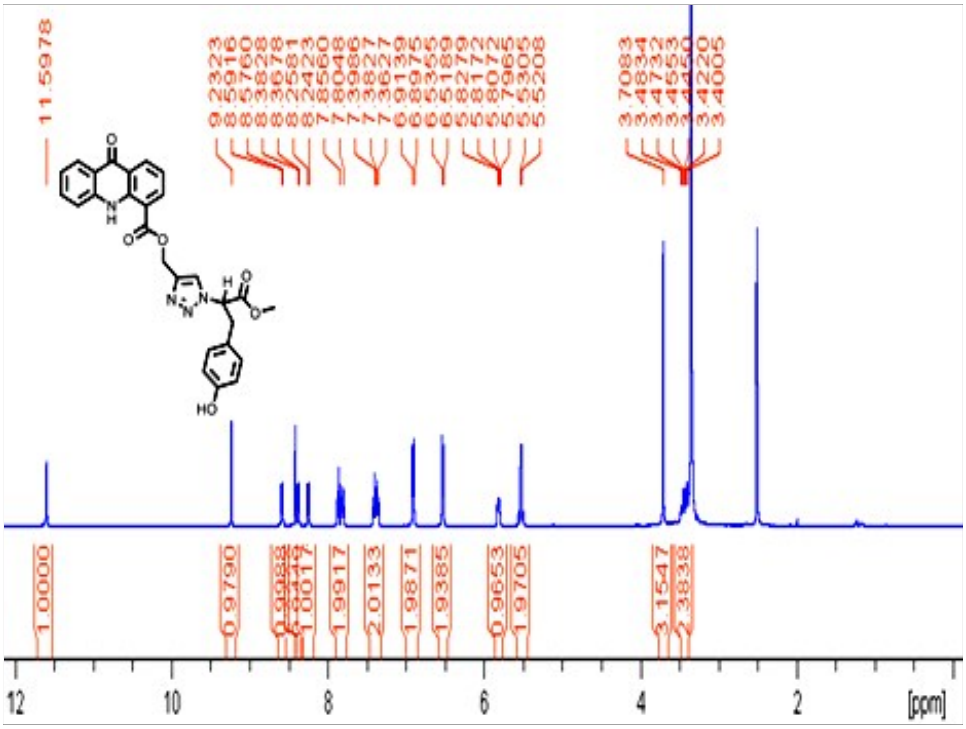

Figure S16. ^{1}H NMR spectrum of compound **5** (DMSO-d_6 as solvent).

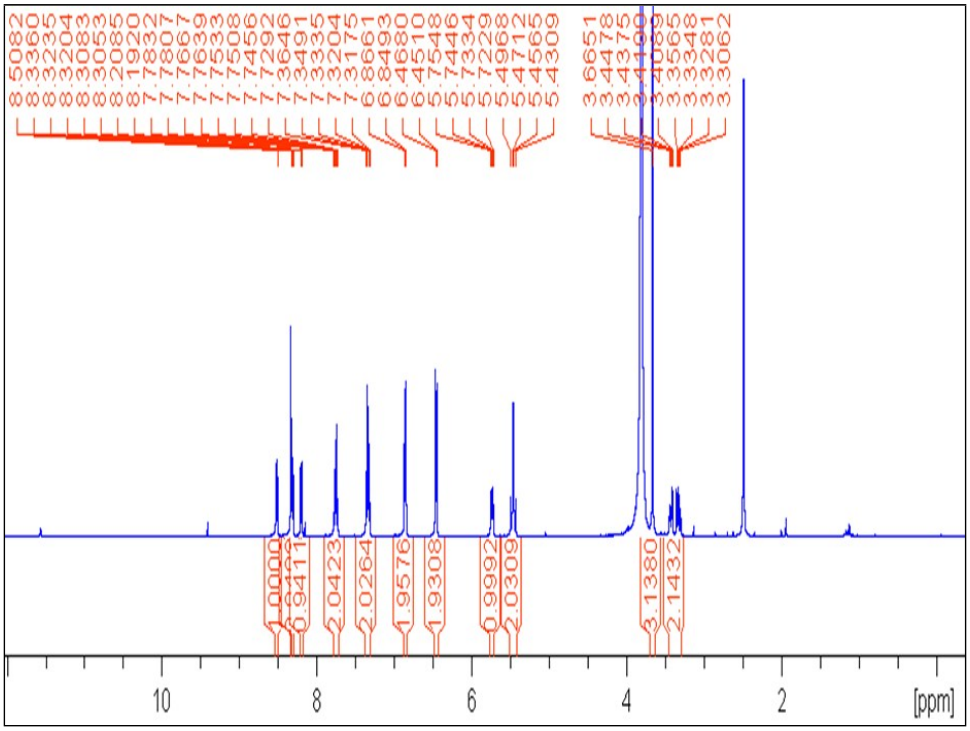

Figure S17. ^{1}H NMR spectrum of compound **5** (DMSO-d_6 as solvent) with one drop of D_2O for detecting exchangeable protons.

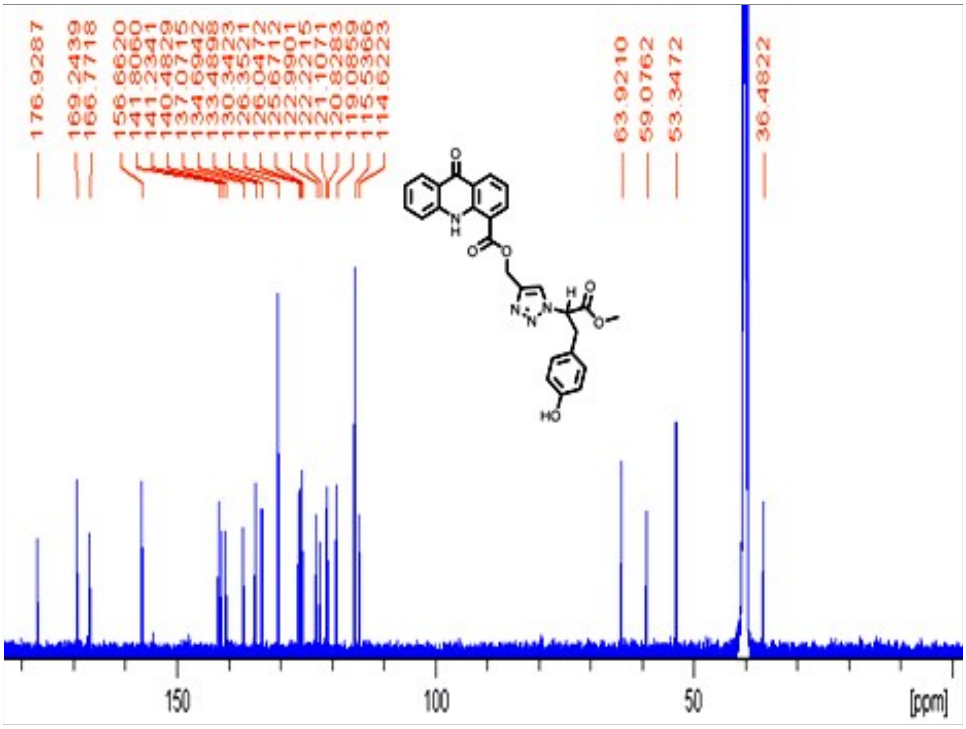

Figure S18. ^{13}C NMR spectrum of compound **5** (DMSO-d_6 as solvent).

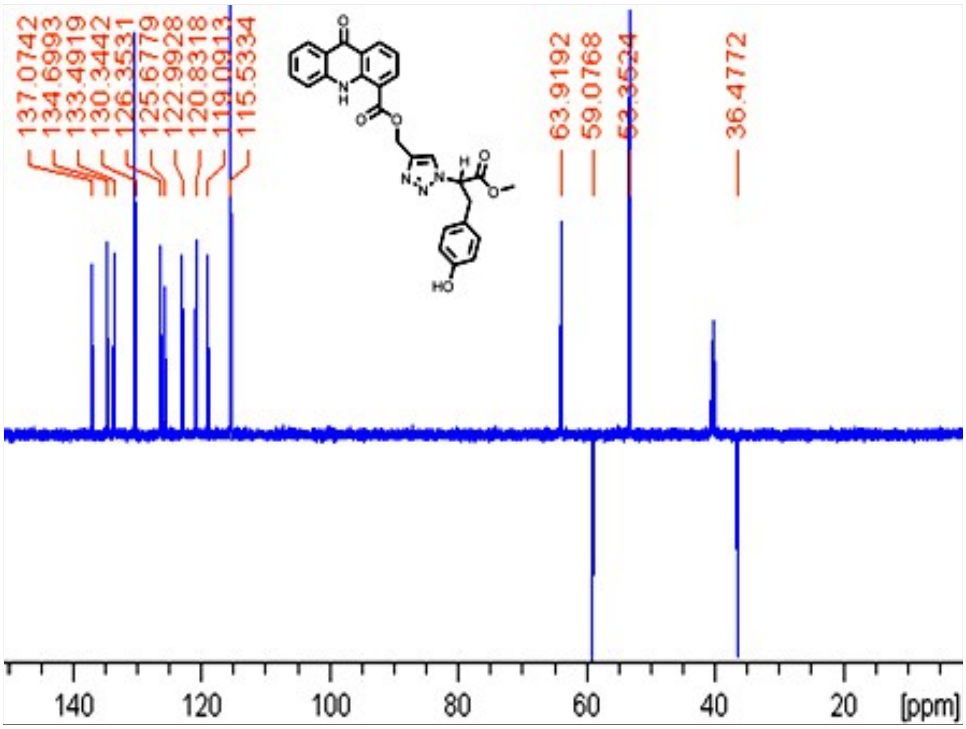

Figure S19. DEPT-135 NMR spectrum of compound **5** (DMSO-d_6 as solvent).

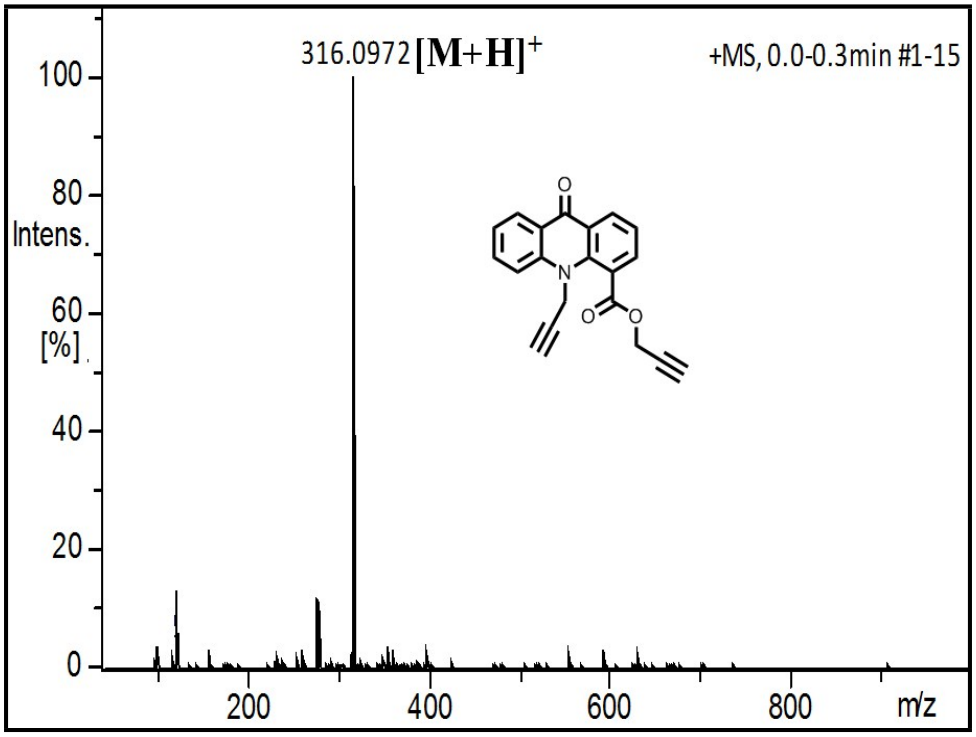

Figure S20. Mass spectrum of compound **4** with mass peak at *m/z* 316.0972 $[M+H]^+$ (calcd *m/z* 316.0968 $[M+H]^+$).

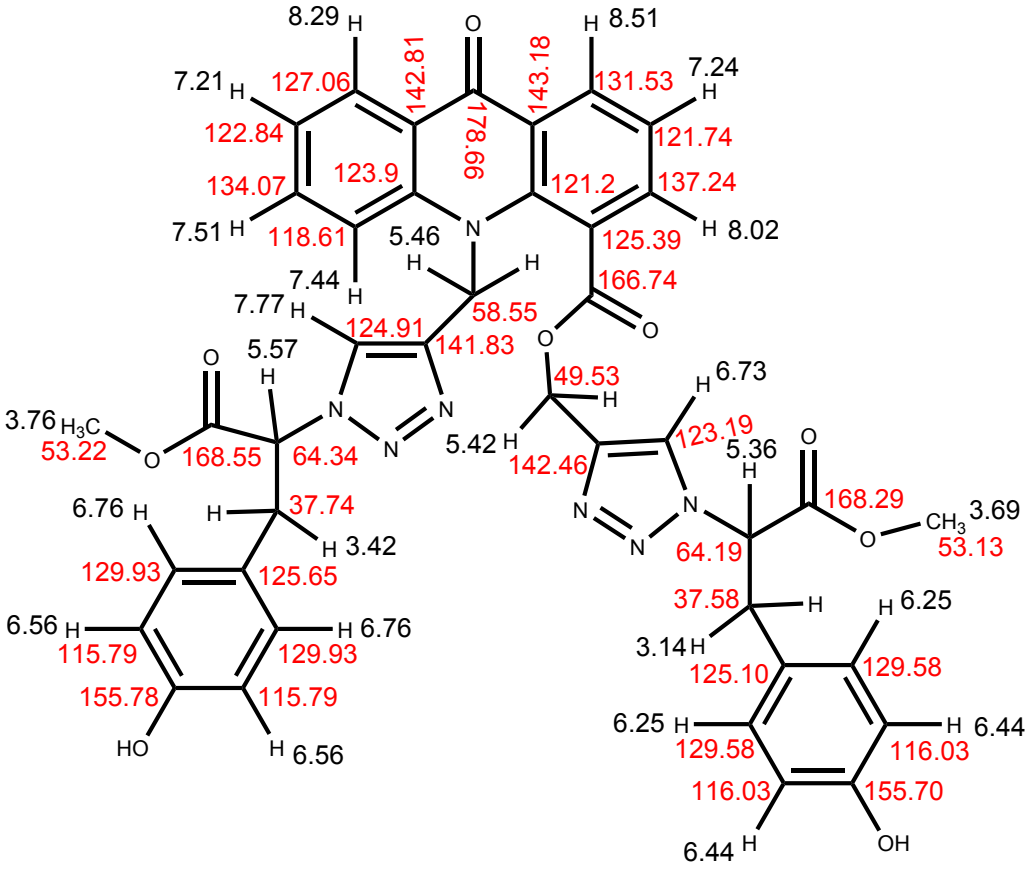

Figure S21. ^{1}H and ^{13}C NMR assignments to compound **1** ($CDCl_3$ as solvent).

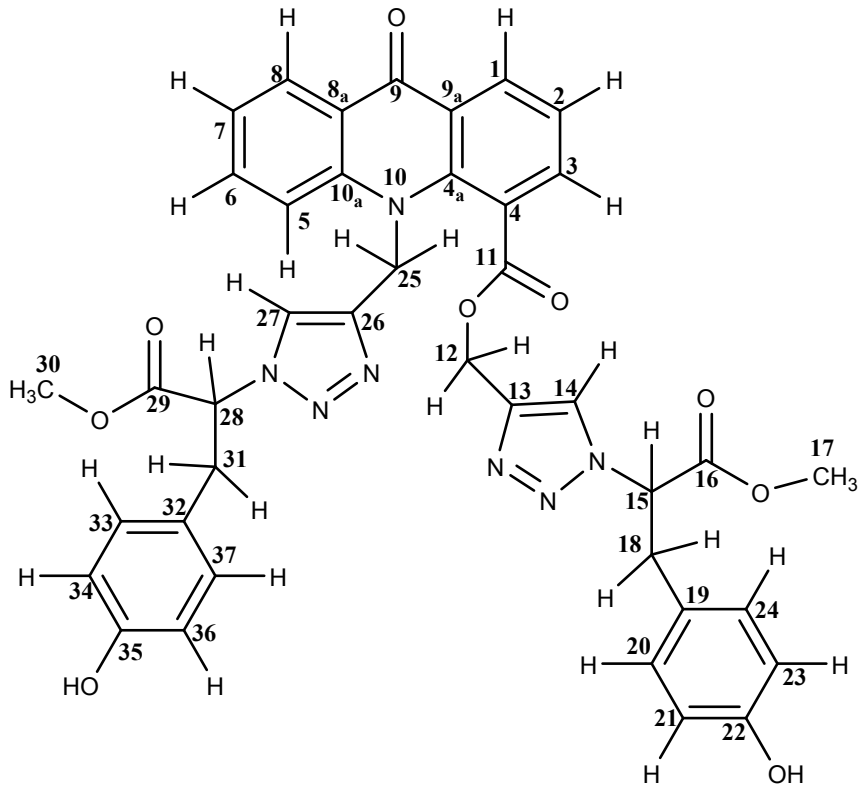

Figure S22. Numbering of compound **1** for NMR resonance assignments.

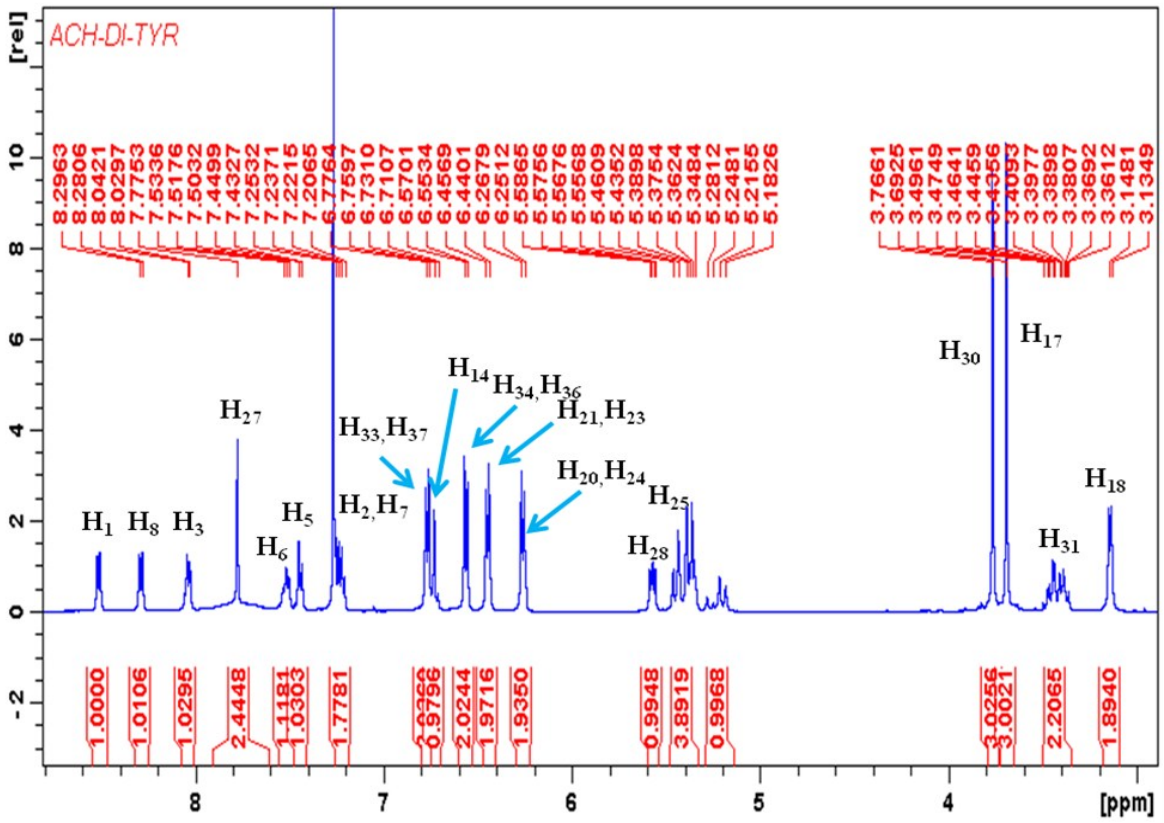

Figure S23. ^{1}H NMR spectrum of compound **1** ($CDCl_3$ solvent).

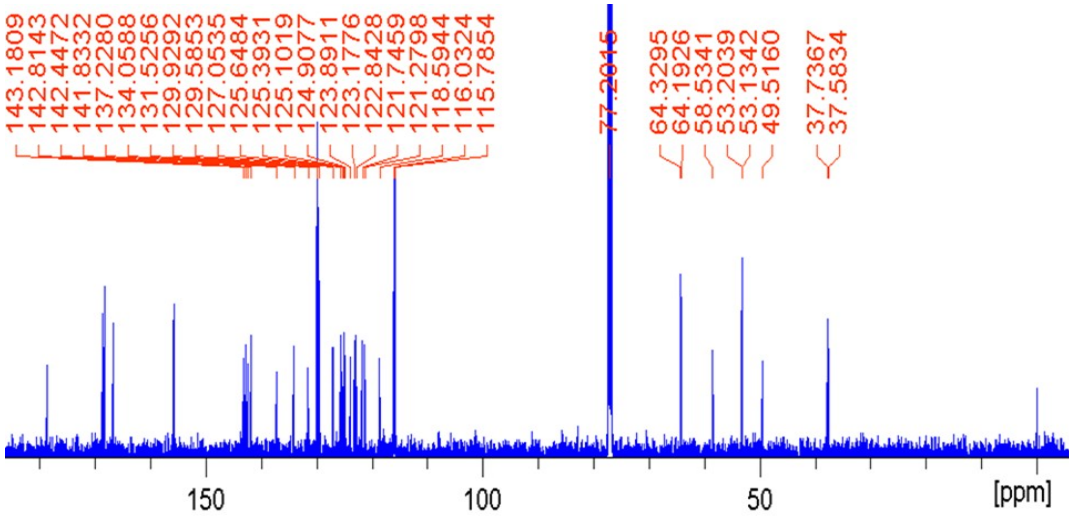

Figure S24. ^{13}C NMR spectrum of compound **1** ($CDCl_3$ solvent).

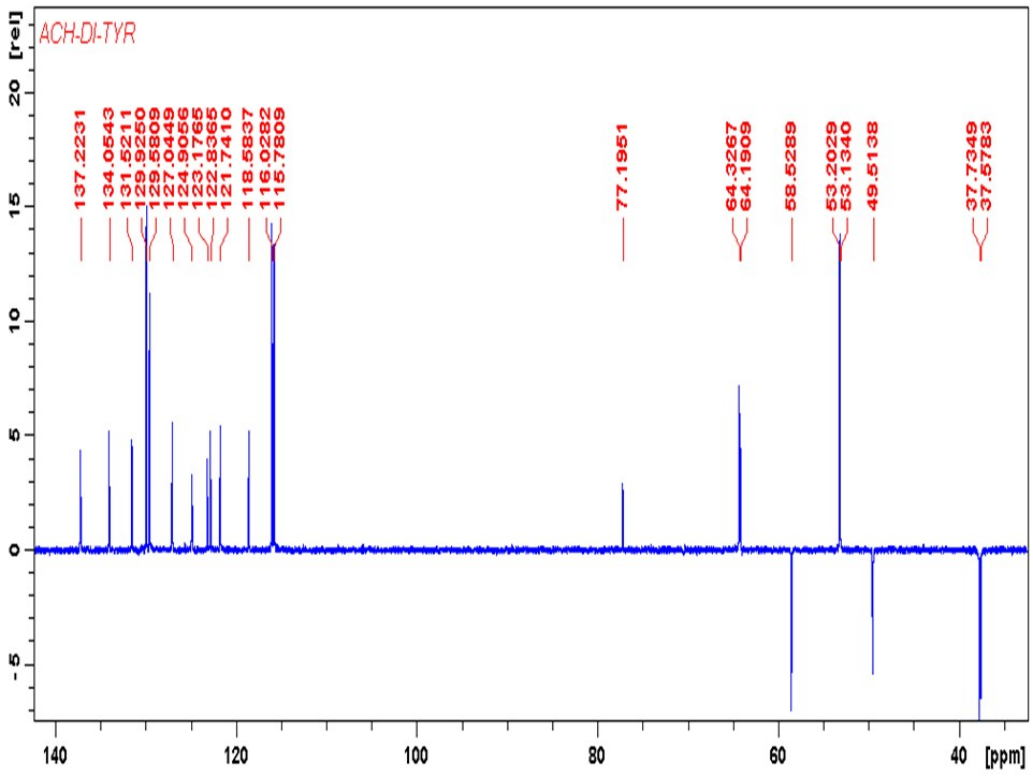

Figure S25. DEPT-135 NMR spectrum of compound **1** ($CDCl_3$ solvent).

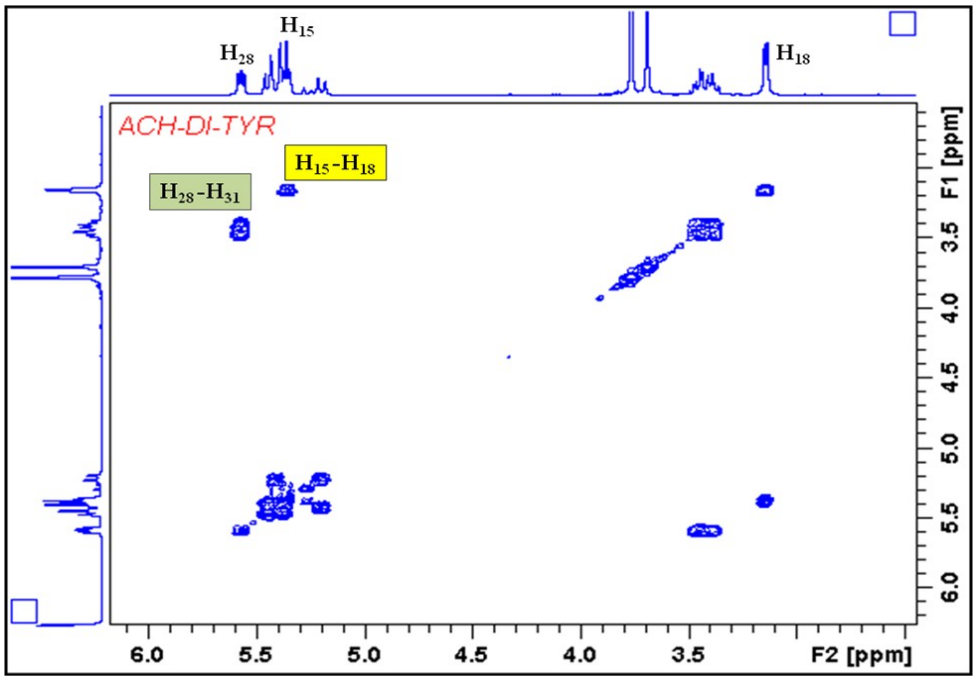

Figure S26. A part of ^{1}H-^{1}H COSY spectrum of compound **1** ($CDCl_3$ solvent).

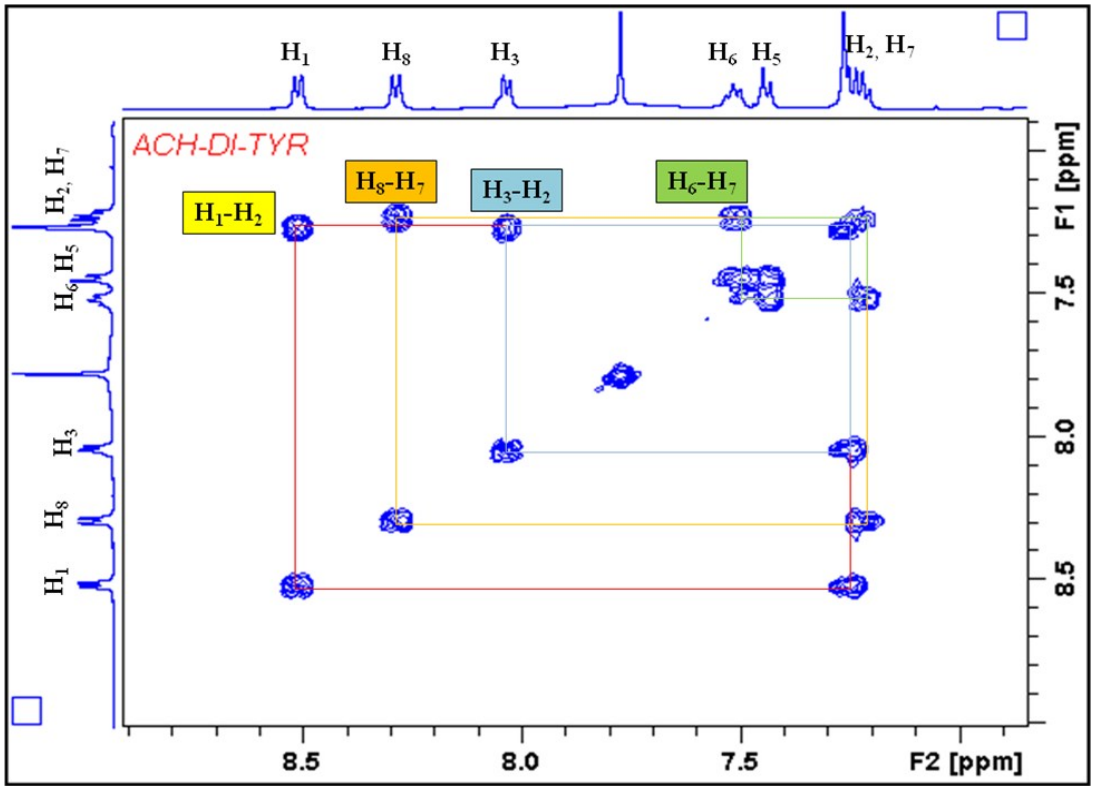

Figure S27. A part of ^{1}H-^{1}H COSY spectrum of compound **1** ($CDCl_3$ solvent).

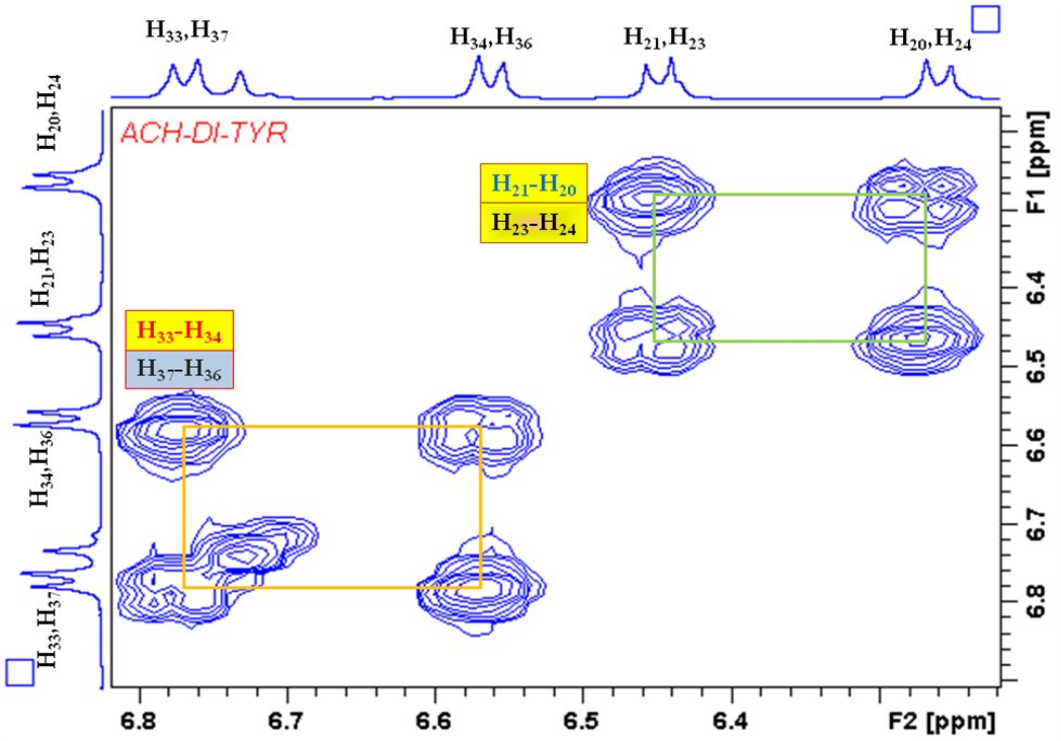

Figure S28. A part of ^{1}H-^{1}H COSY spectrum of compound **1** ($CDCl_3$ solvent).

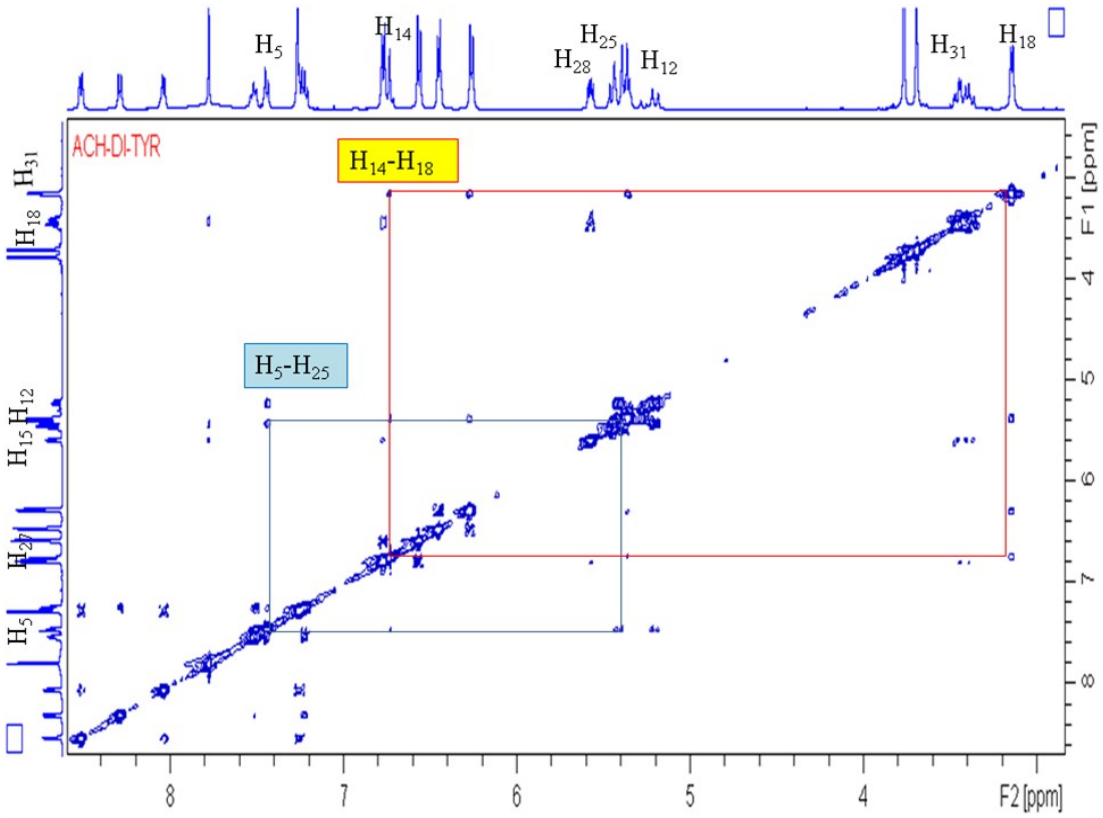

Figure S29. A part of ^{1}H-^{1}H NOESY spectrum of compound **1** ($CDCl_3$ solvent).

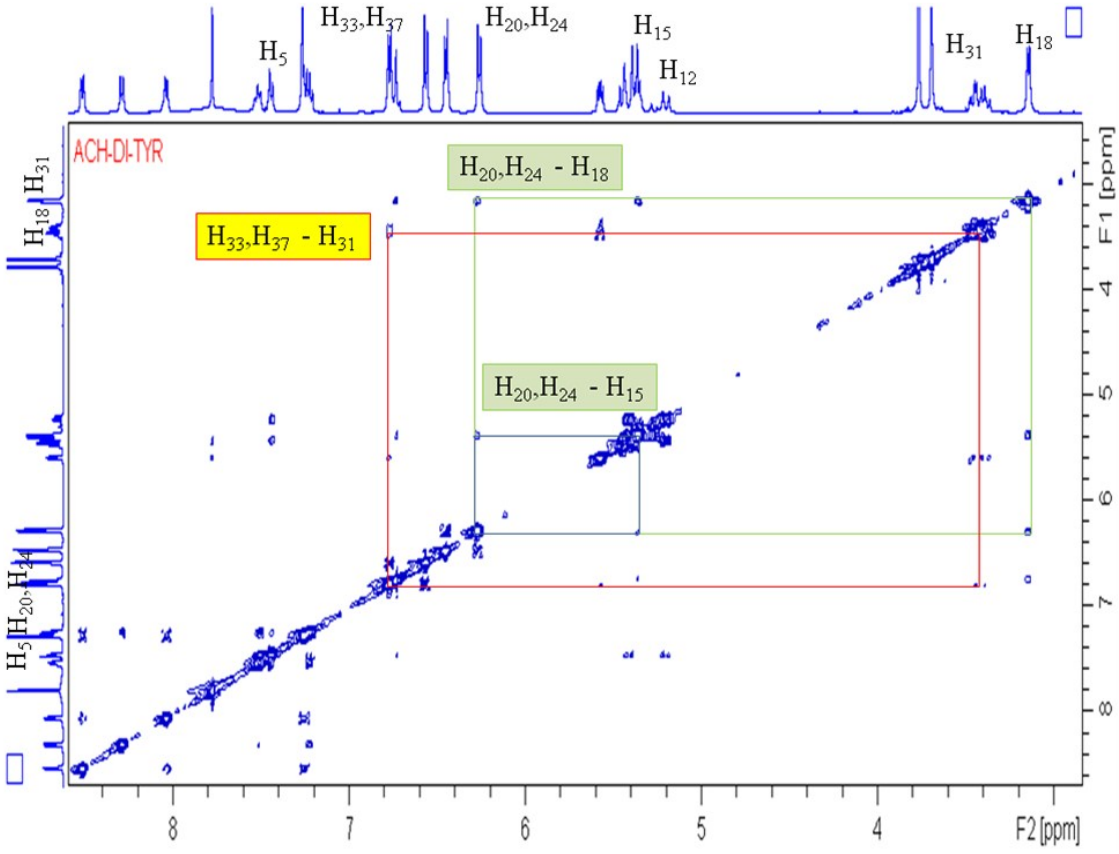

Figure S30. A part of ^{1}H-^{1}H NOESY spectrum of compound **1** ($CDCl_3$ solvent).

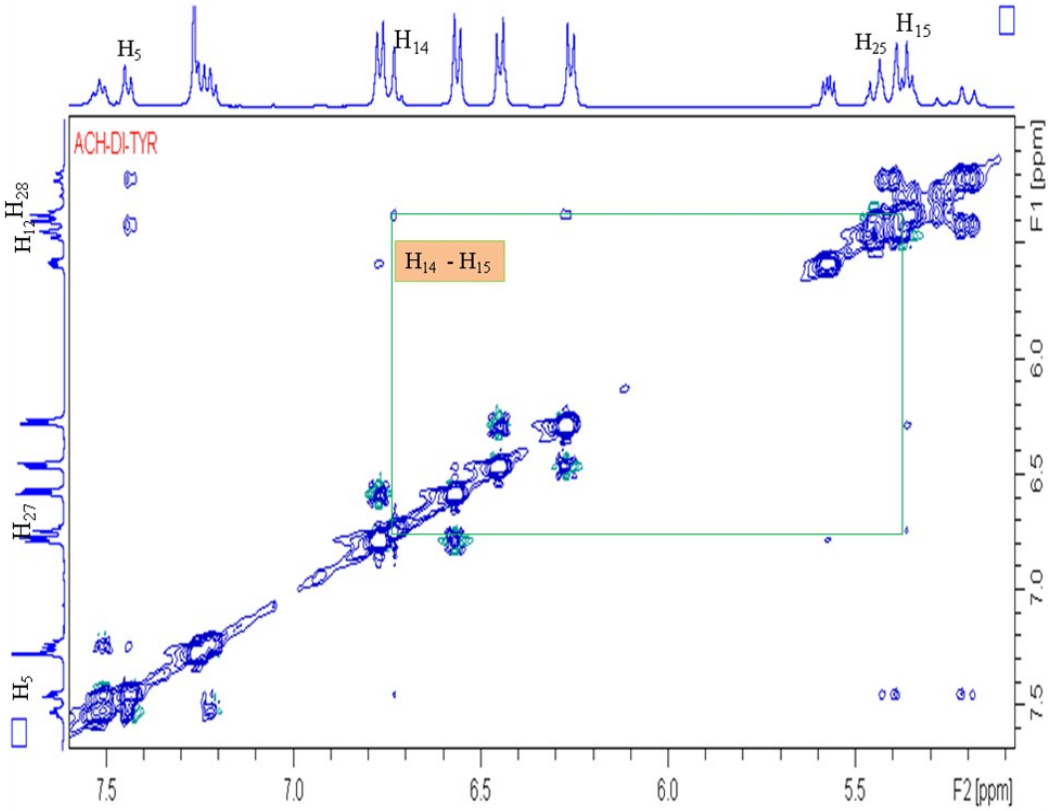

Figure S31. A part of ^{1}H-^{1}H NOESY spectrum of compound **1** ($CDCl_3$ solvent).

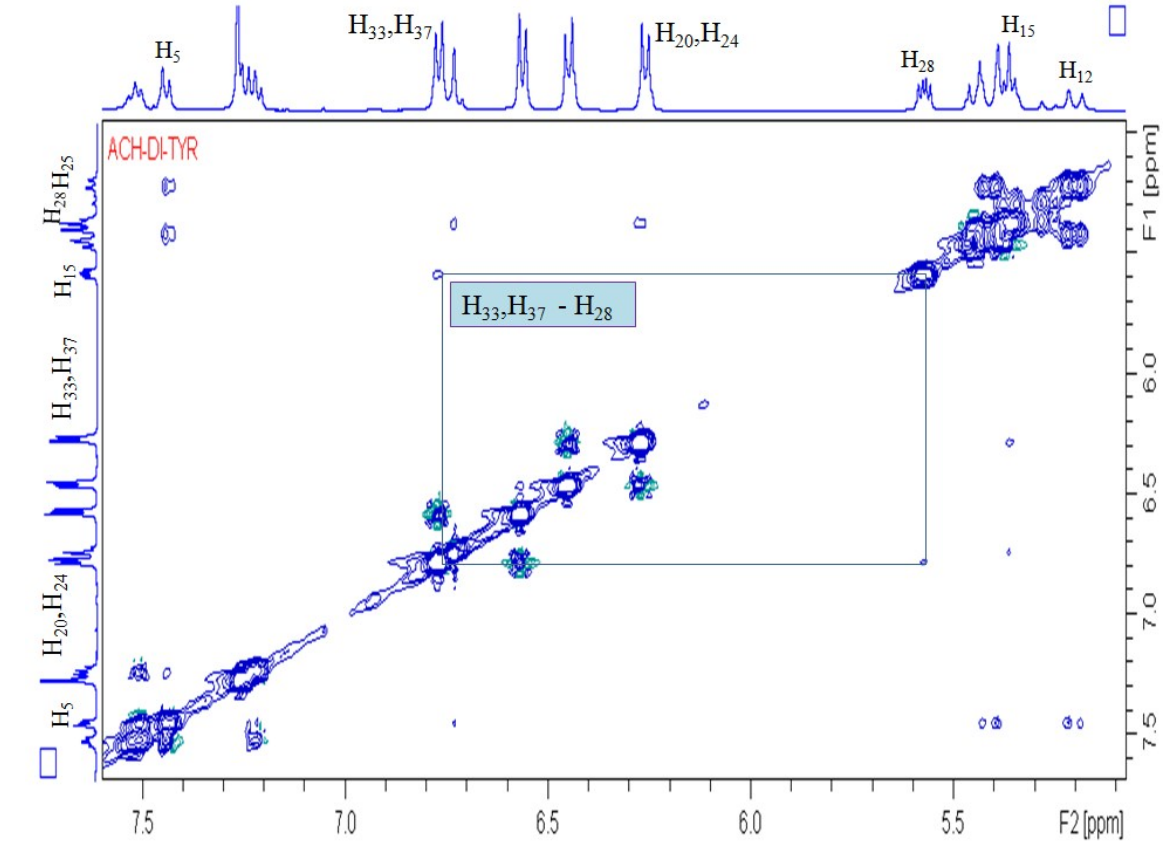

Figure S32. A part of ^{1}H-^{1}H NOESY spectrum of compound **1** ($CDCl_3$ solvent).

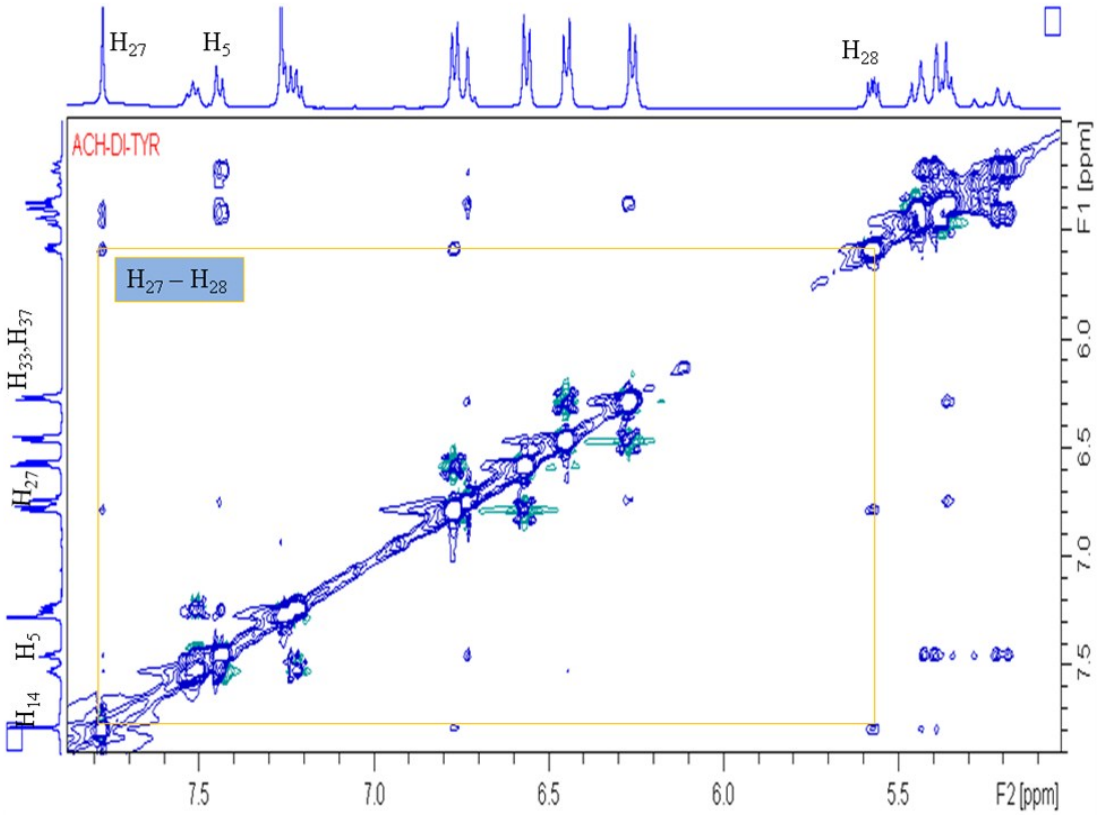

Figure S33. A part of ^{1}H-^{1}H NOESY spectrum of compound **1** ($CDCl_3$ solvent).

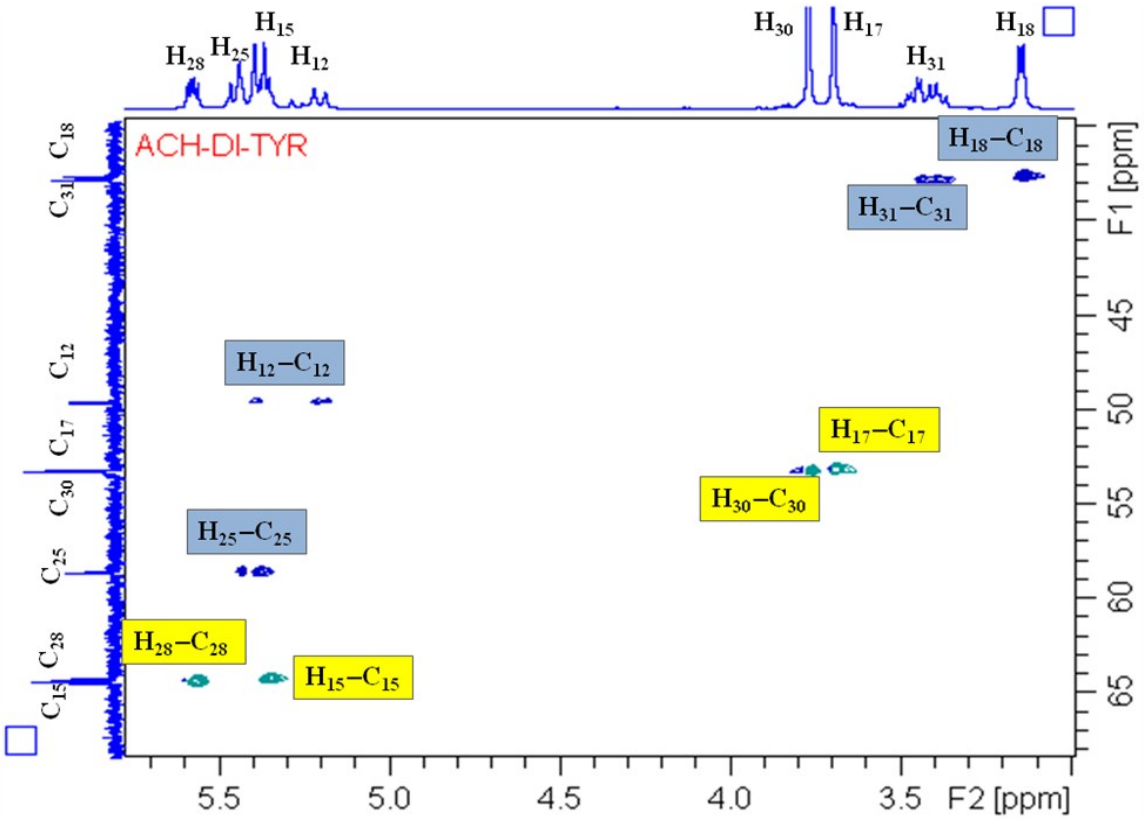

Figure S34. A part of ^{1}H-^{13}C HSQC NMR spectrum of compound **1** ($CDCl_3$ solvent).

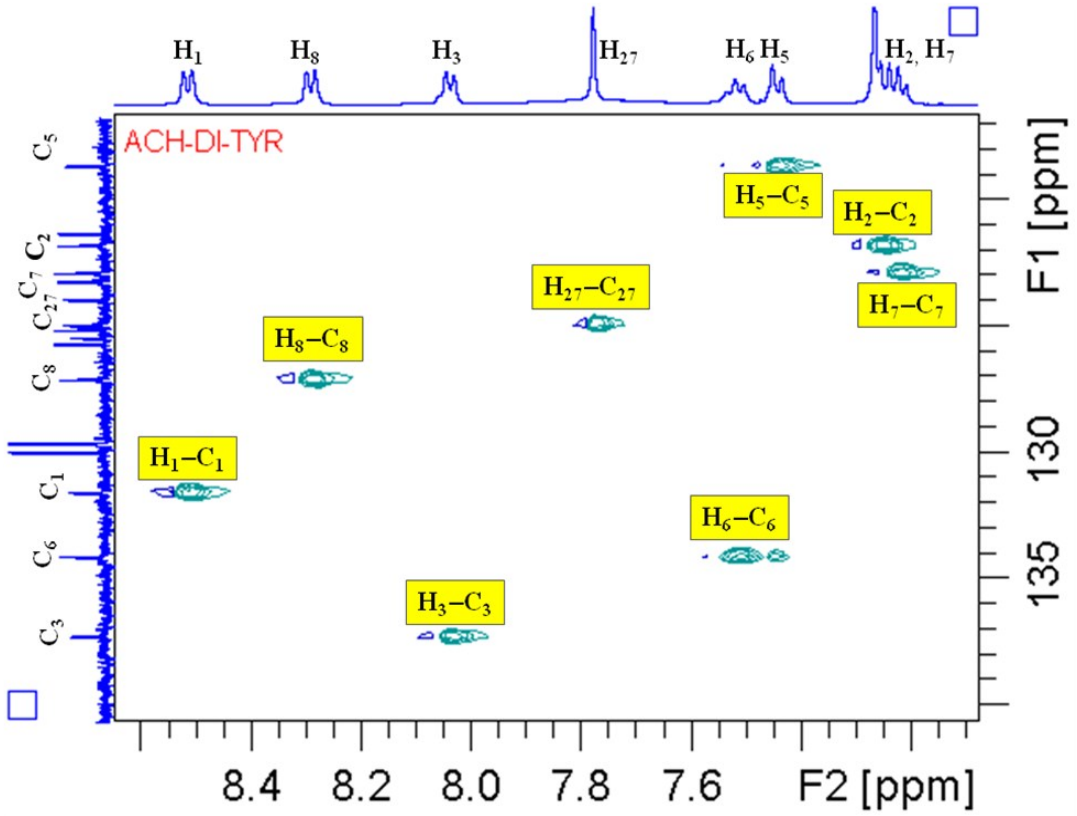

Figure S35. A part of ^{1}H-^{13}C HSQC NMR spectrum of compound **1** ($CDCl_3$ solvent).

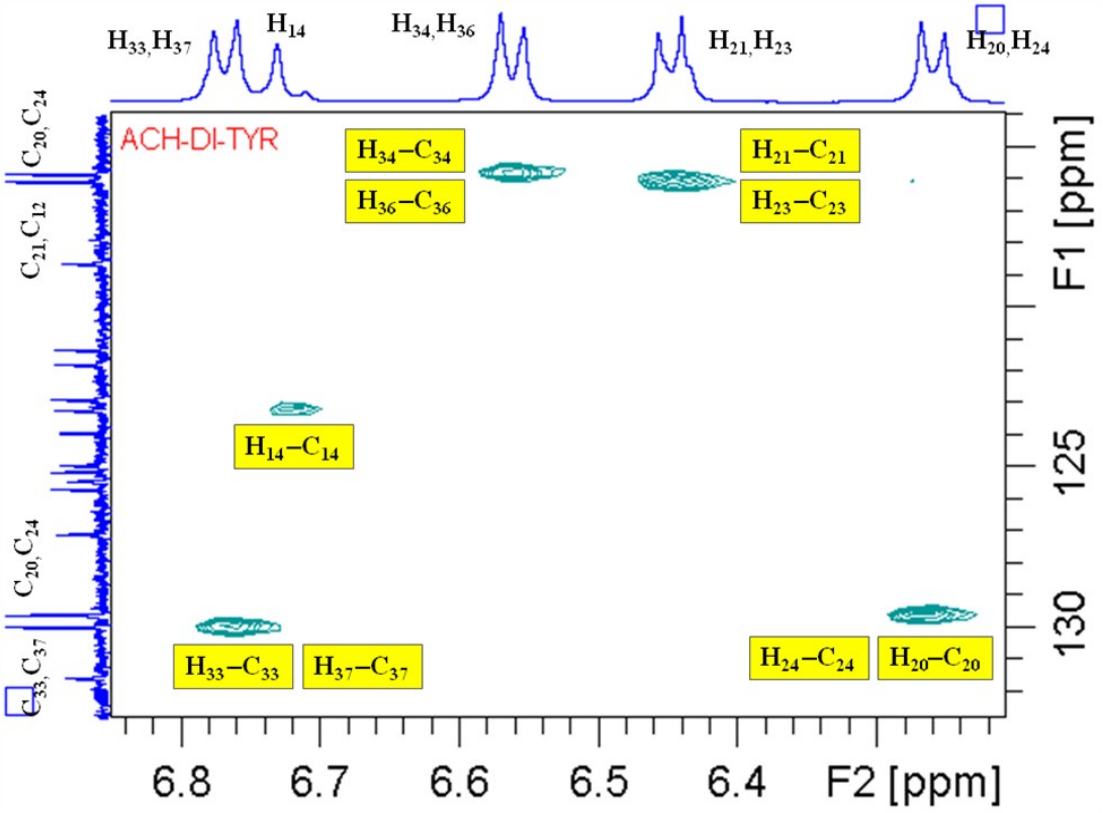

Figure S36. A part of ^{1}H-^{13}C HSQC NMR spectrum of compound **1** ($CDCl_3$ solvent).

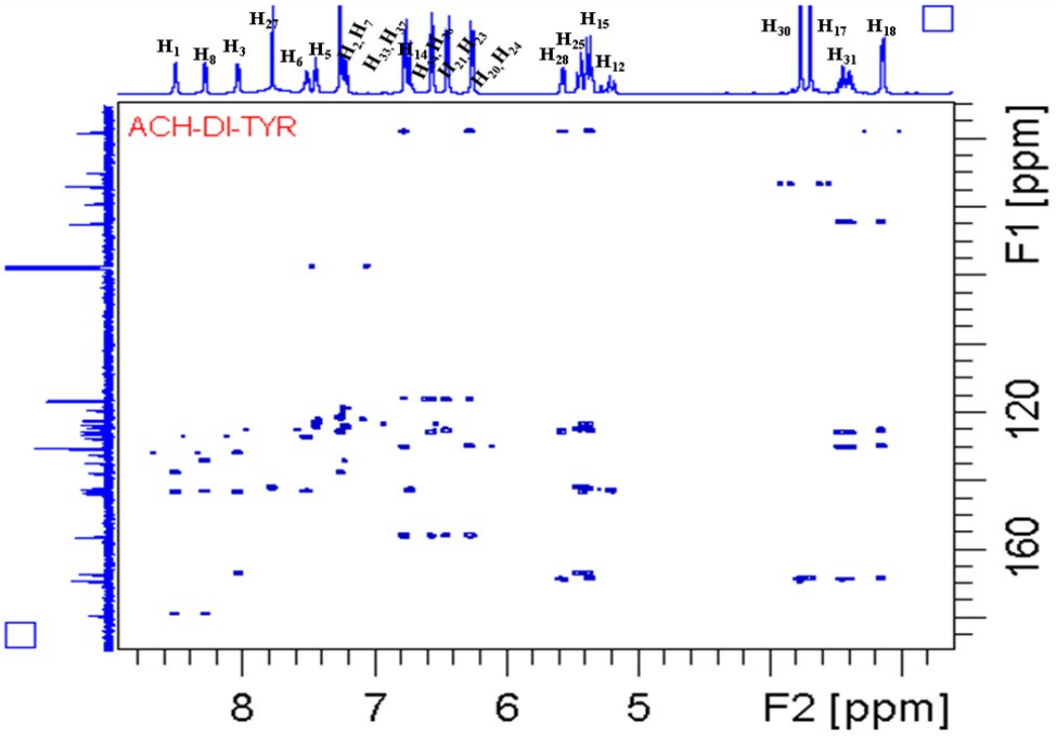

Figure S37. ^{1}H-^{13}C HMBC NMR spectrum of compound **1** ($CDCl_3$ solvent).

Since all the physic-chemical experiments with compound **1** were performed in DMSO-H_2O medium, NMR spectra of compound **1** was also recorded in DMSO-H_2O.

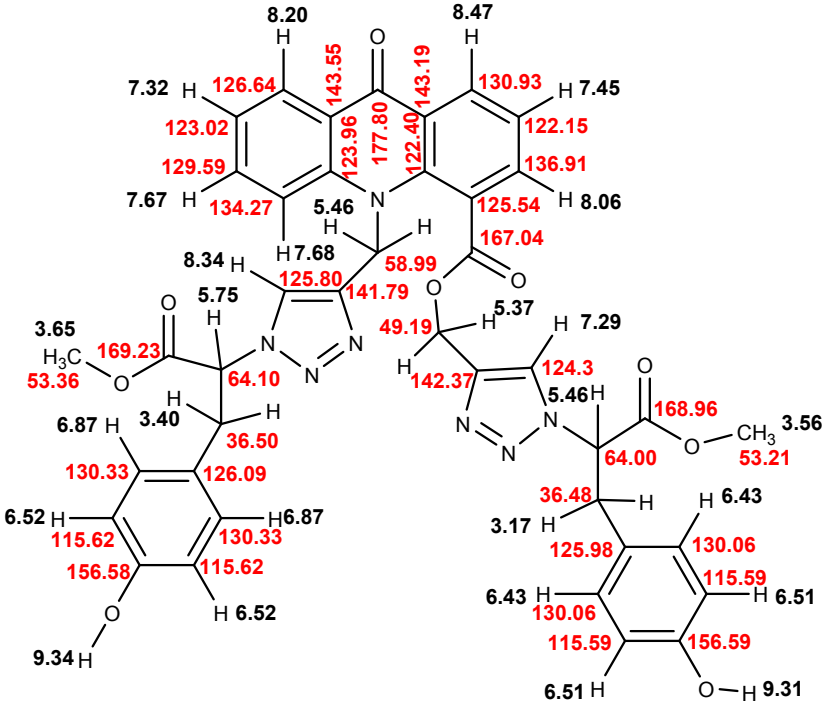

Figure S38. ^{1}H NMR assignments to compound **1** (DMSO-H_2O-DMSO-d_6 8:1:1 v/v).

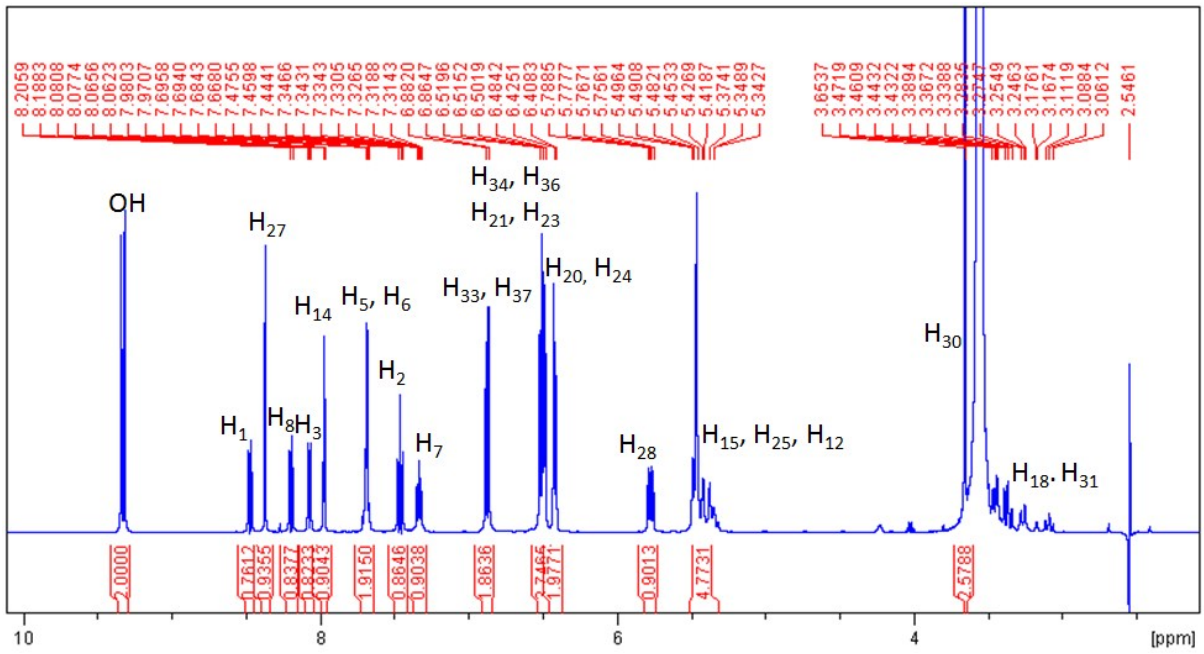

Figure S39 ^{1}H NMR spectrum of compound **1** (DMSO-H_2O-DMSO-d_6 8:1:1 v/v). The peak due to DMSO at δ 2.54 was suppressed.

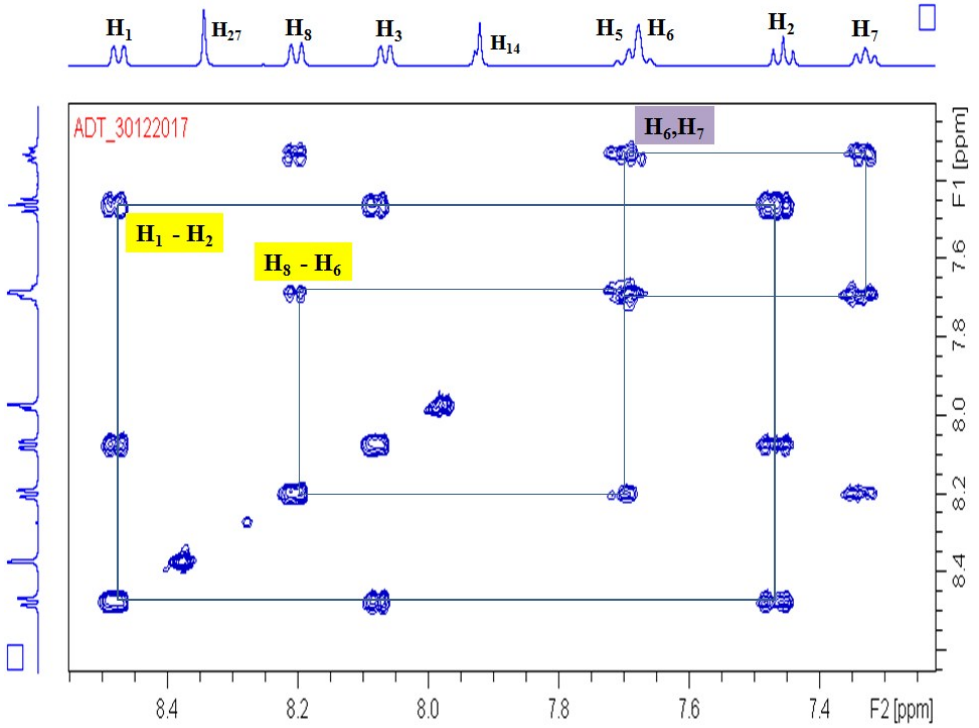

Figure S40. A part of ^{1}H-^{1}H COSY NMR spectrum of compound **1** (DMSO-H_2O-DMSO-d_6 8:1:1 v/v).

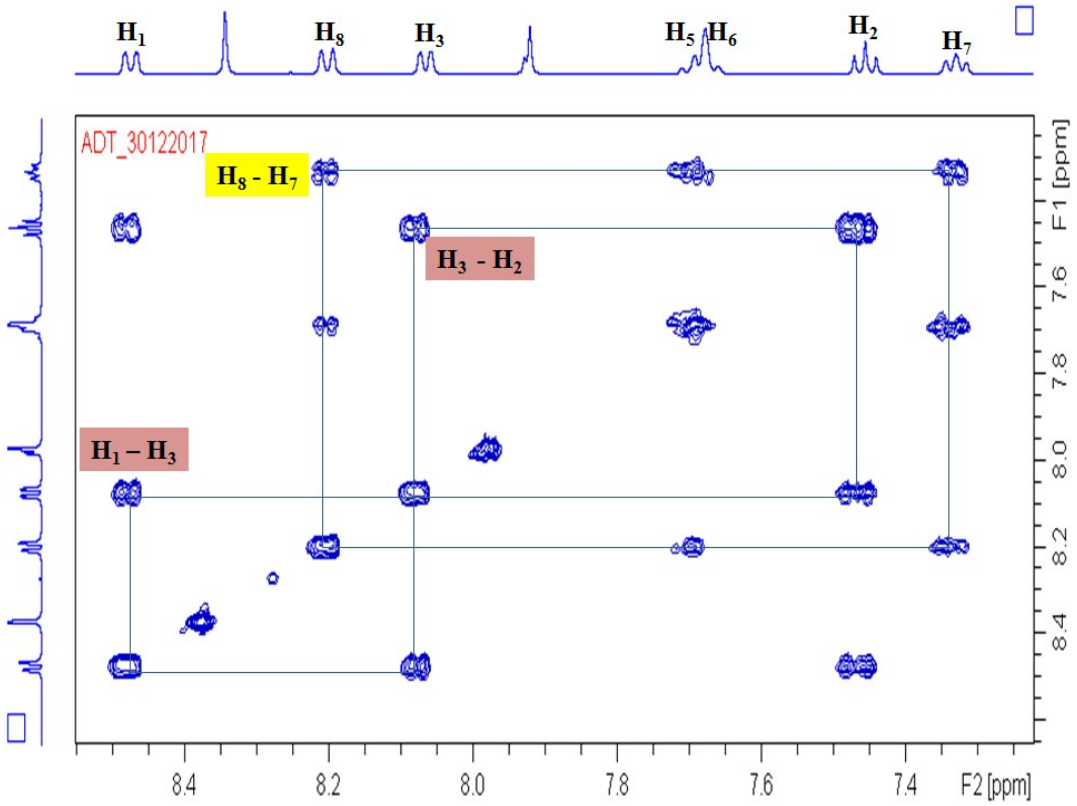

Figure S41. A part of ^{1}H-^{1}H COSY NMR spectrum of compound **1** (DMSO-H_2O-DMSO-d_6 8:1:1 v/v).

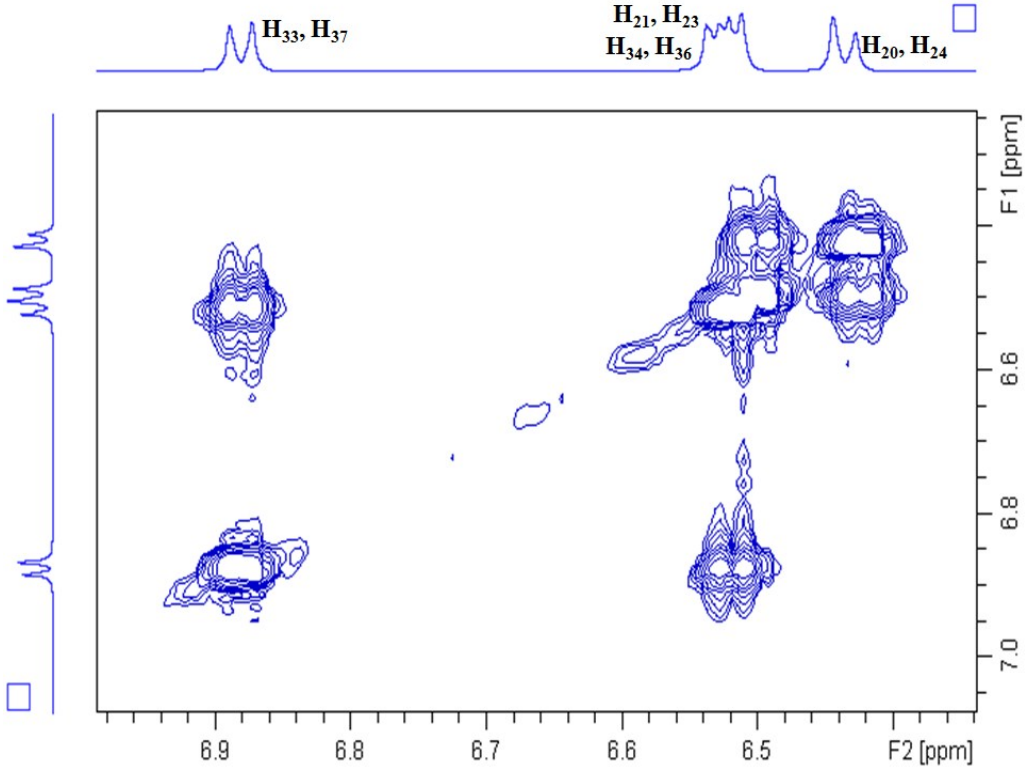

Figure S42. A part of ^{1}H-^{1}H COSY NMR spectrum of compound **1** (DMSO-H_2O-DMSO-d_6 8:1:1 v/v).

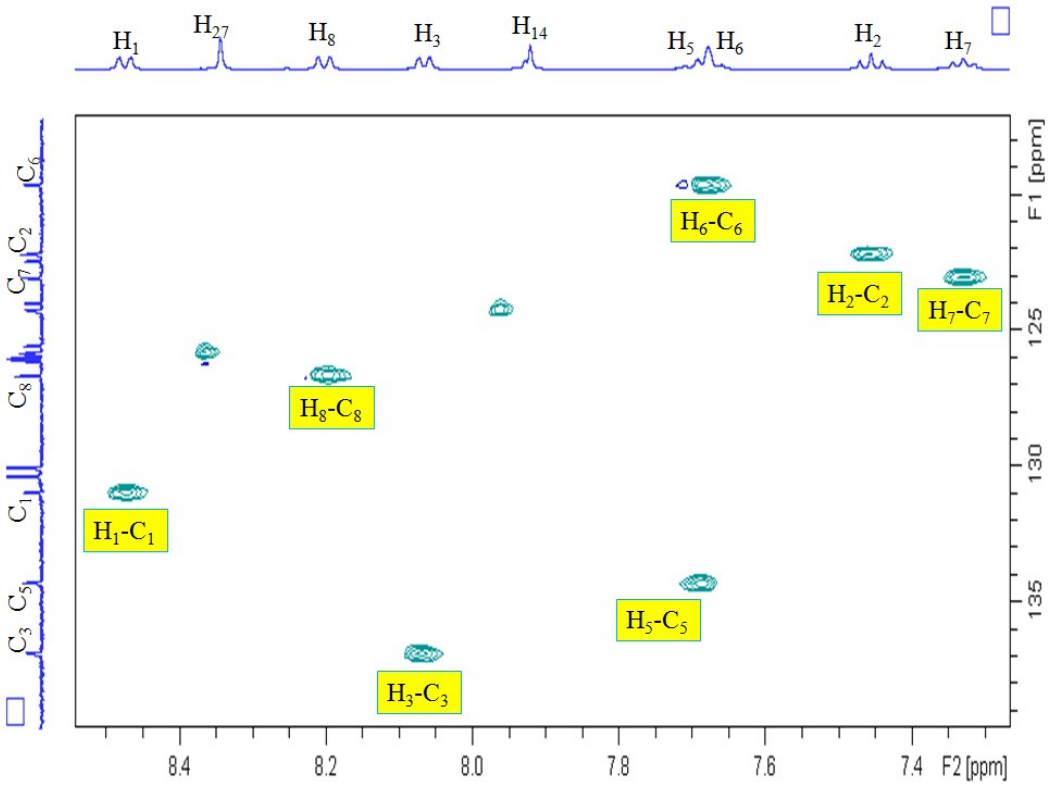

Figure S43. A part of ^{1}H-^{13}C HSQC NMR spectrum of compound **1** (DMSO-H_2O-DMSO-d_6 8:1:1 v/v).

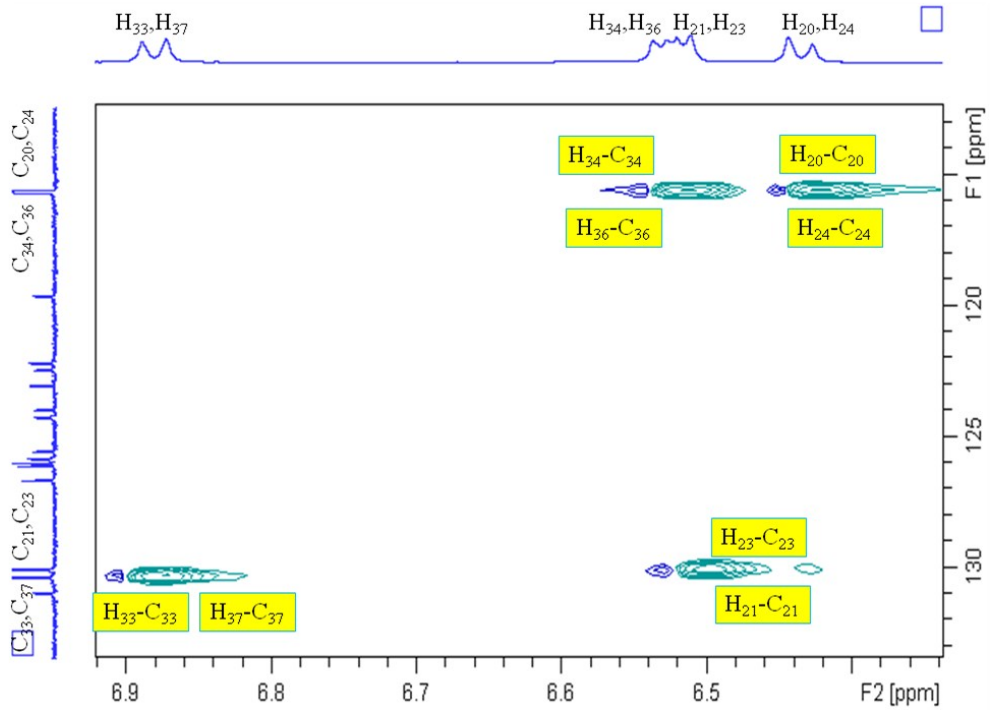

Figure S44. A part of ^{1}H-^{13}C HSQC NMR spectrum of compound **1** (DMSO-H_2O-DMSO-d_6 8:1:1 v/v).

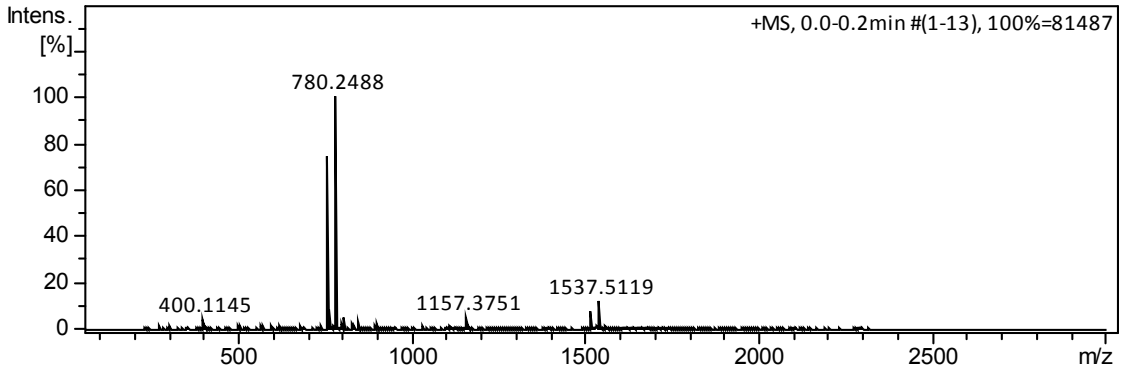

Figure S45. High Resolution Mass Spectrum of compound **1** (calcd *m/z* 758.2569 $[M+H]^+$).

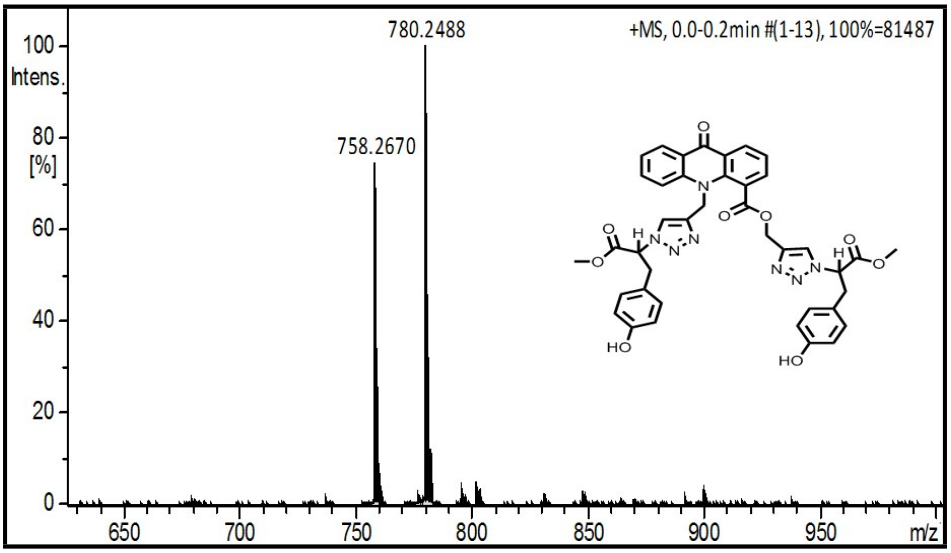

Figure S46. High Resolution Mass Spectrum of compound **1** (calcd *m/z* 758.2569 $[M+H]^+$).

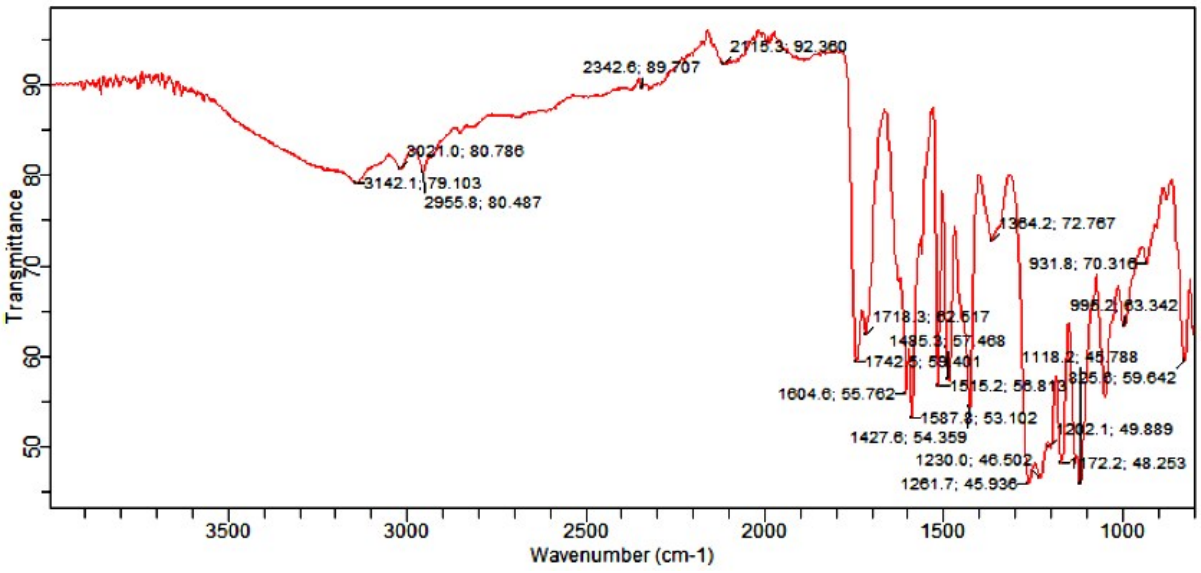

Figure S47. IR spectrum of compound **1**.

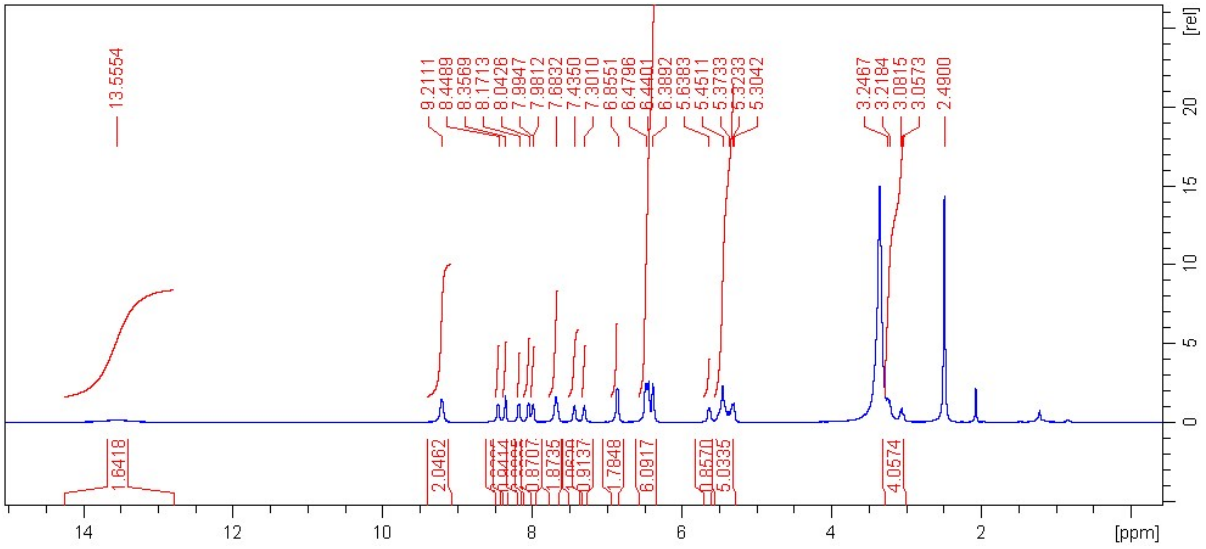

Figure S48. [1]H NMR assignments to compound **6** (DMSO-d_6).

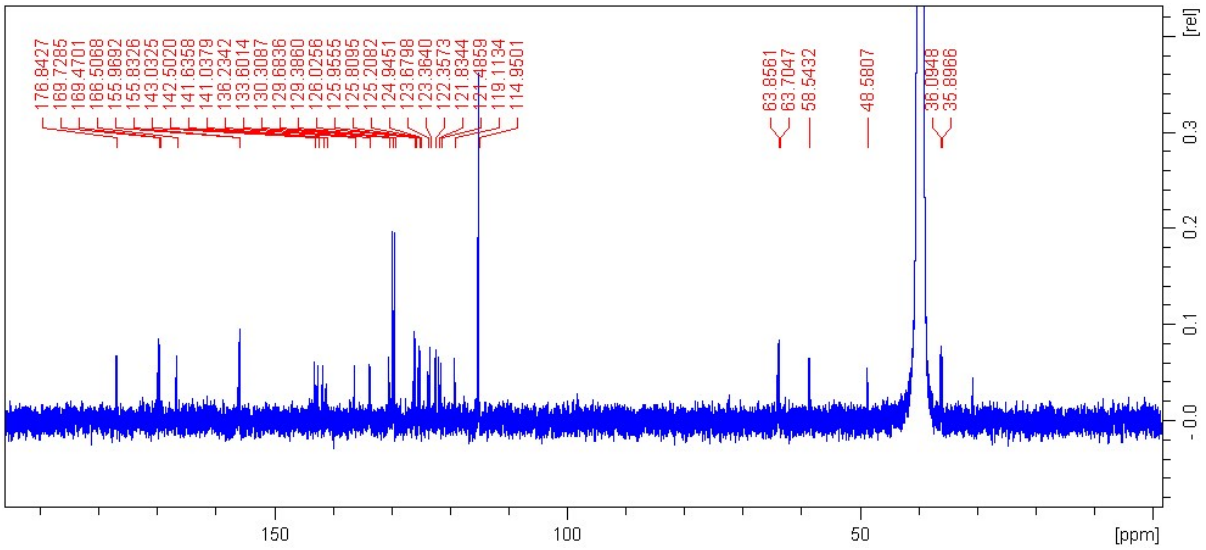

Figure S49. [13]C NMR assignments to compound **6** (DMSO-d_6).

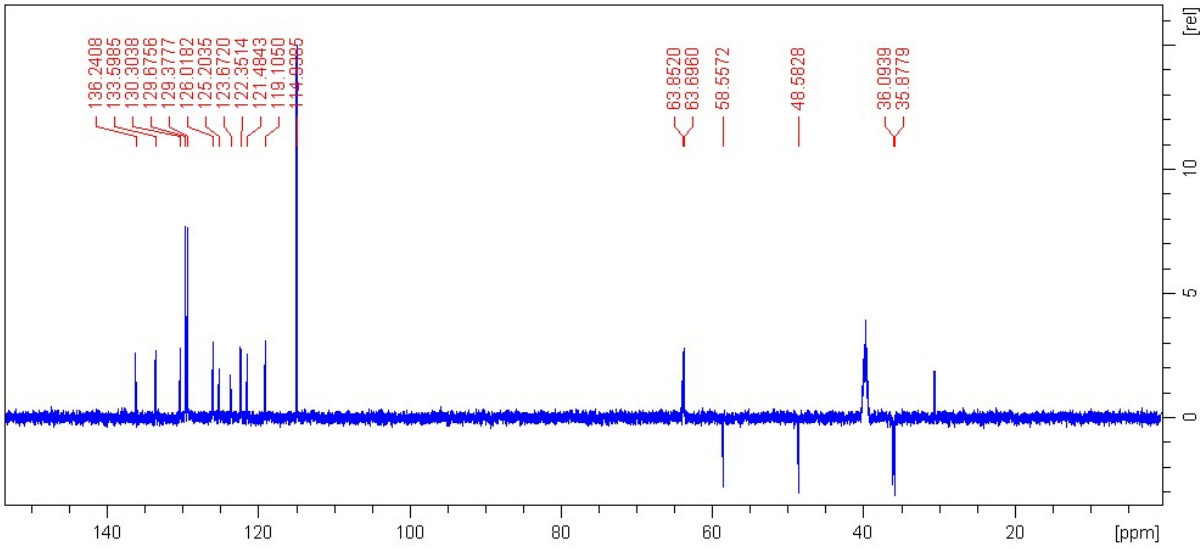

Figure S50. DEPT-135 NMR assignments to compound **6** (DMSO-d_6).

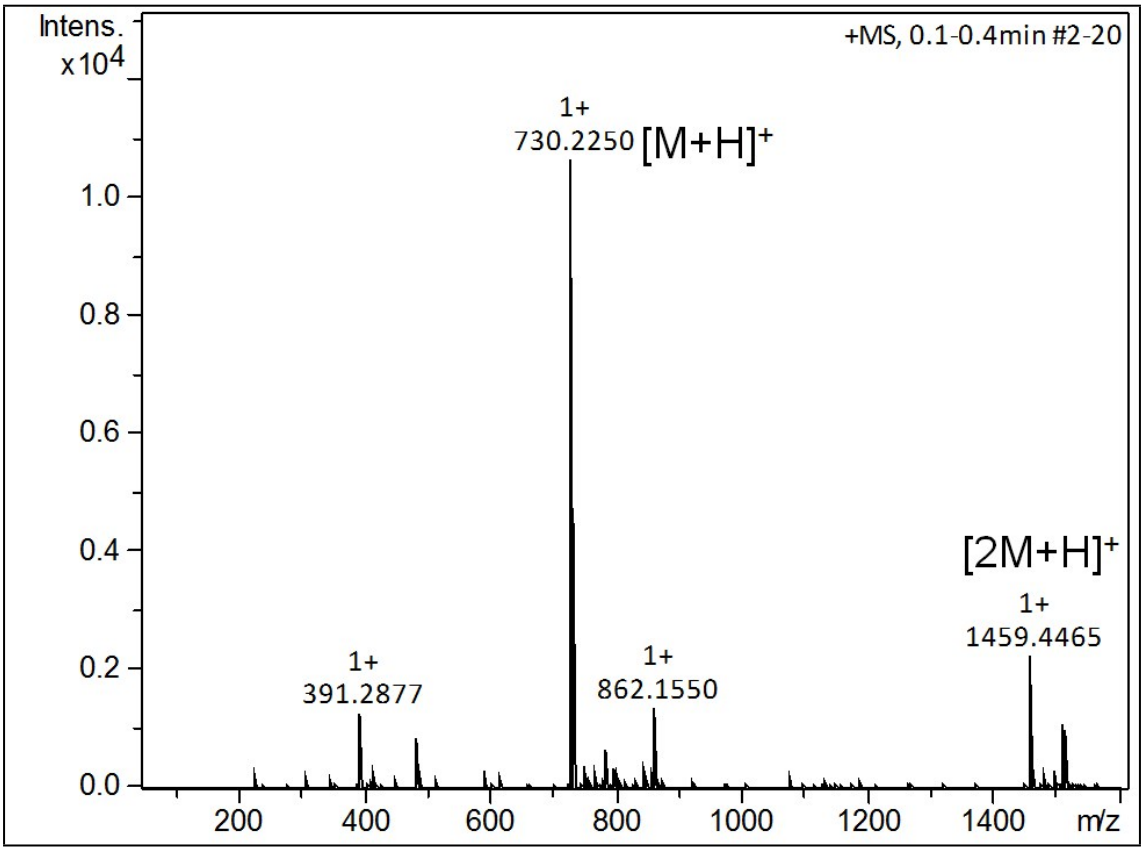

Figure S51. HRMS of compound **6** showing mass peak at *m/z* 730.2250 (calcd For $C_{38}H_{31}N_7O_9$, *m/z* 730.2256 [M+H]).

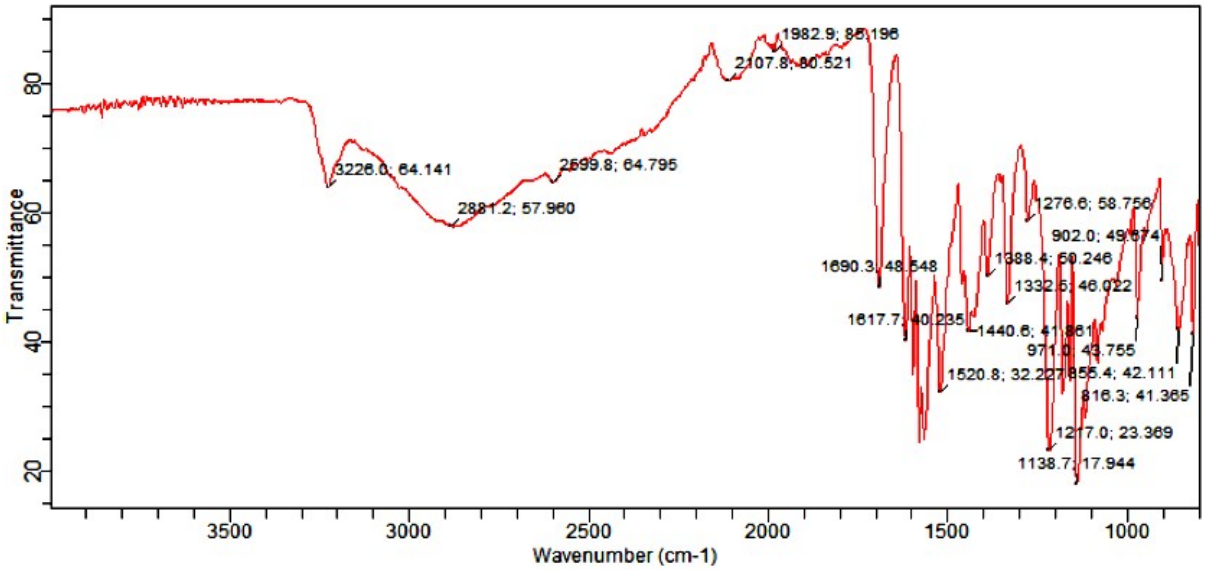

Figure S52. IR spectrum of compound **2**: $\bar{\upsilon}$ (cm^{-1}): 3226 (NH), 2881 (OH), 1690 (CO).

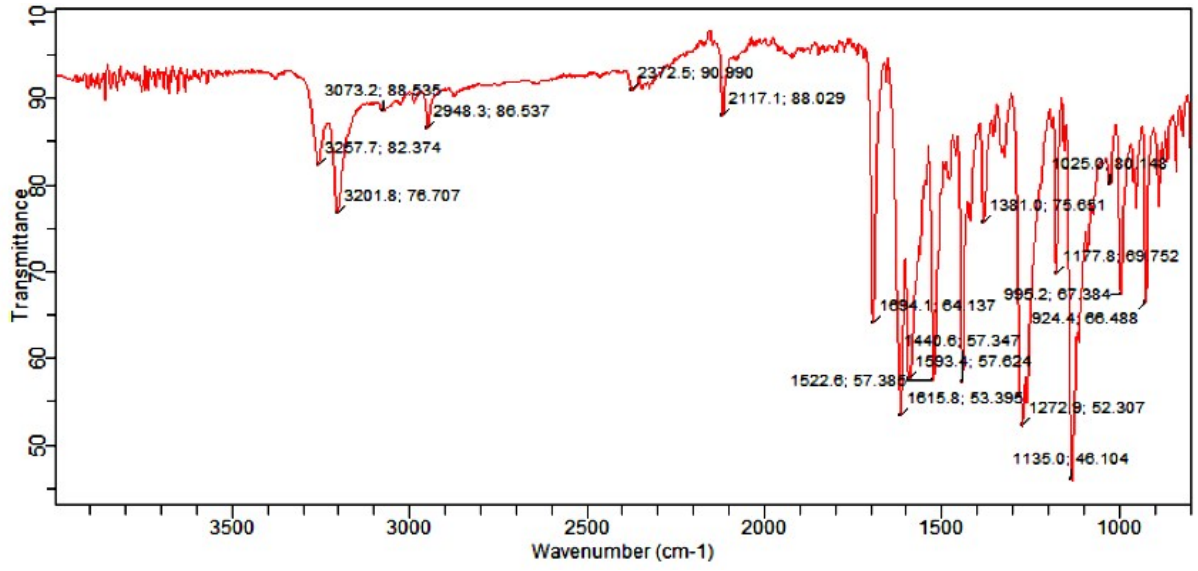

Figure S53. IR spectrum of compound **3**: $\bar{\upsilon}$ (cm^{-1}): 3257 (NH), 3201 (C≡H), 1694 (CO).

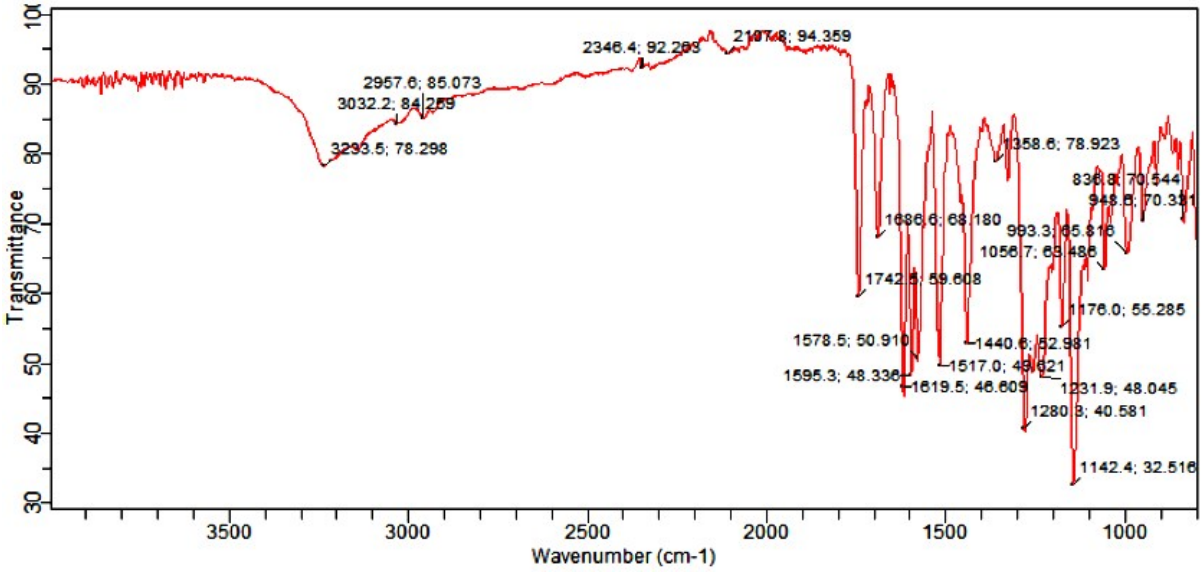

Figure S54. IR spectrum of compound **5**: $\bar{\upsilon}$ (cm^{-1}): 3293 (OH), 1742 (CO).

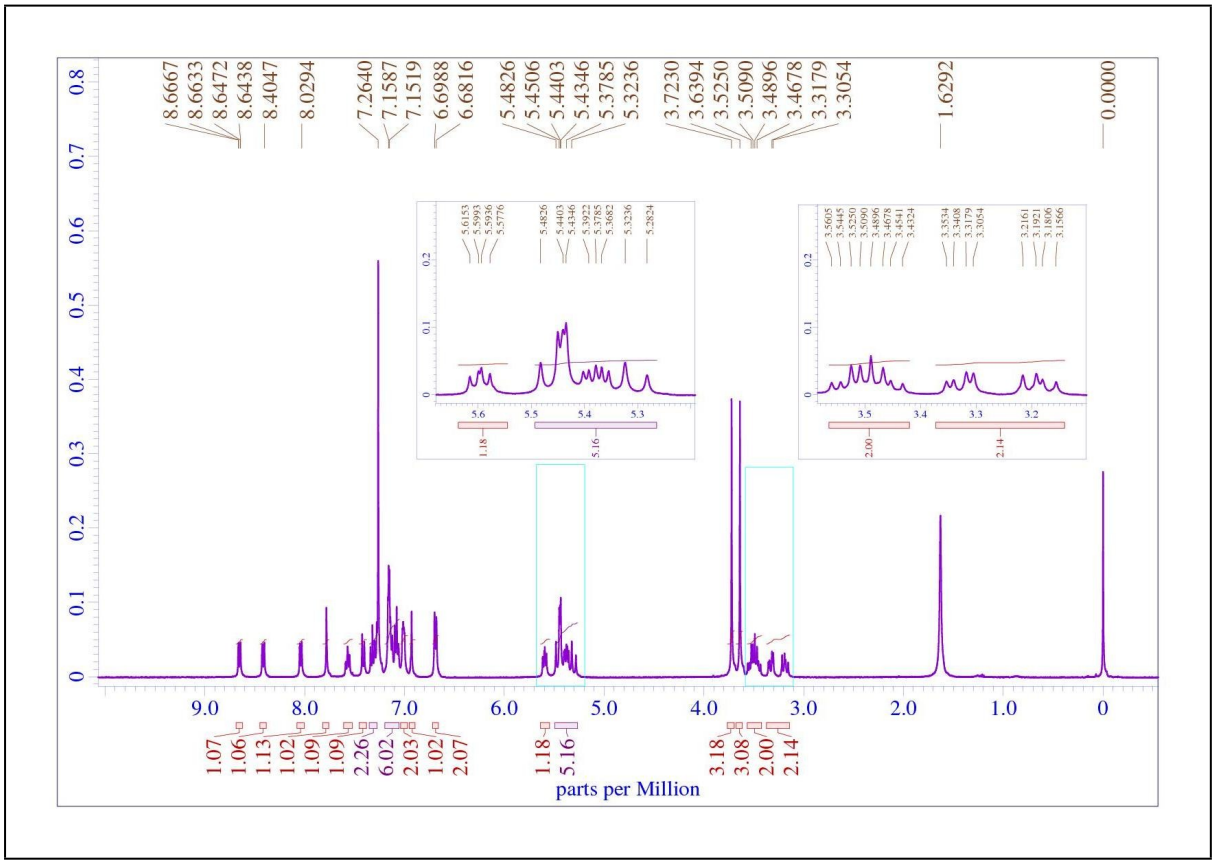

Figure S55. ^{1}H NMR of compound **8** ($CDCl_3$ as solvent).

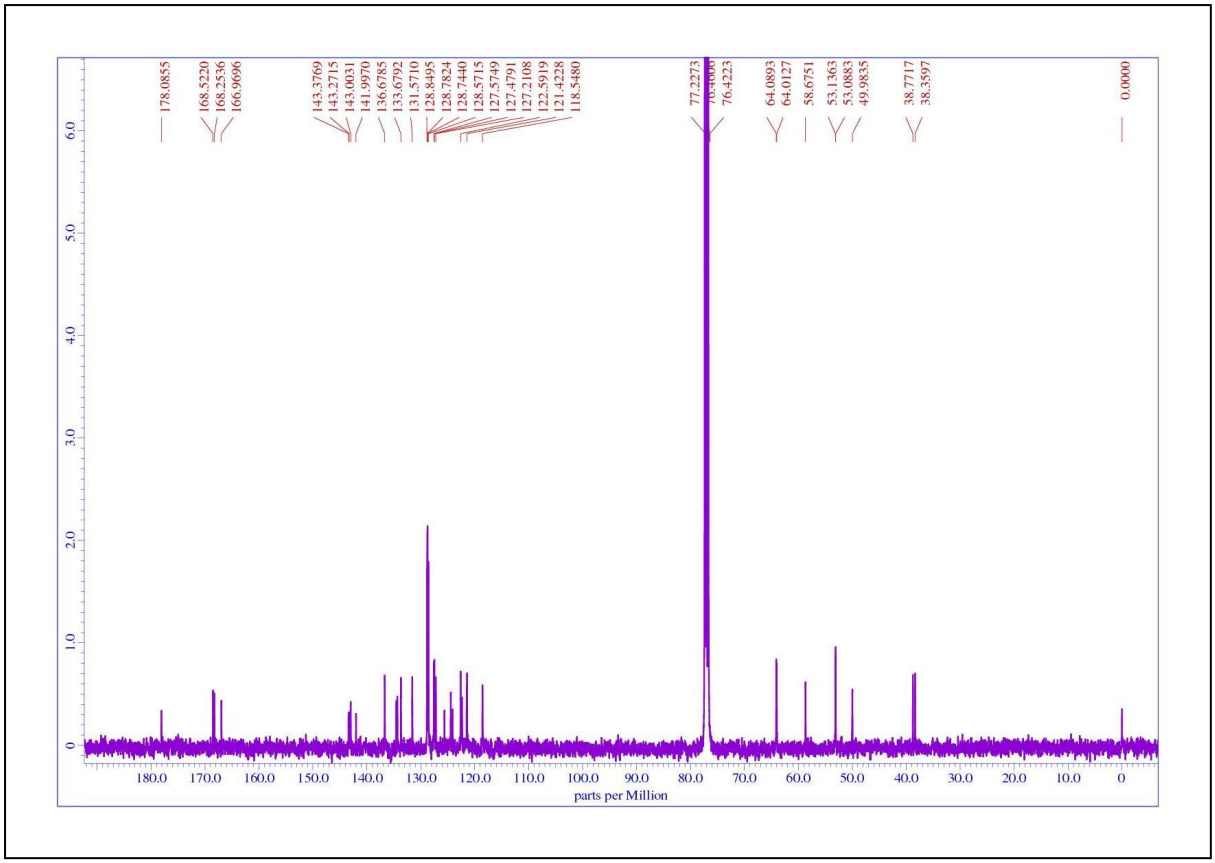

Figure S56. ^{13}C-NMR of compound **8** ($CDCl_3$ as solvent).

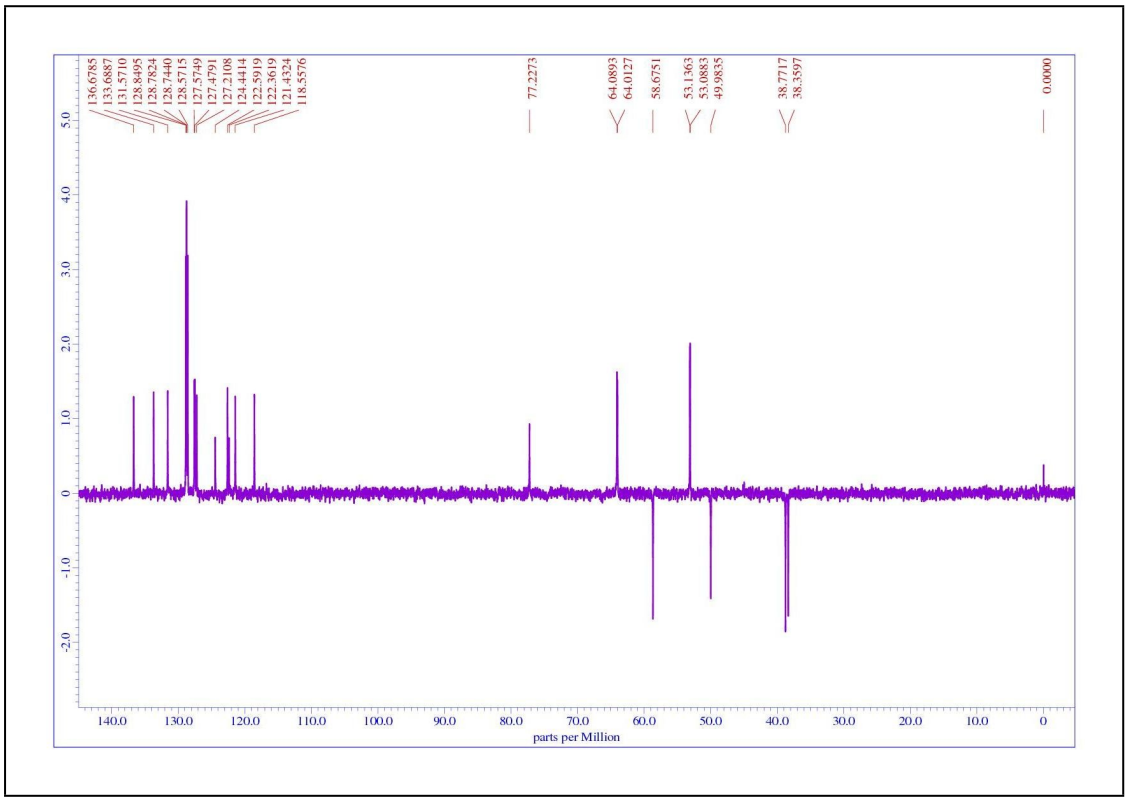

Figure S57. Dept-135 NMR of compound **8** ($CDCl_3$ as solvent).

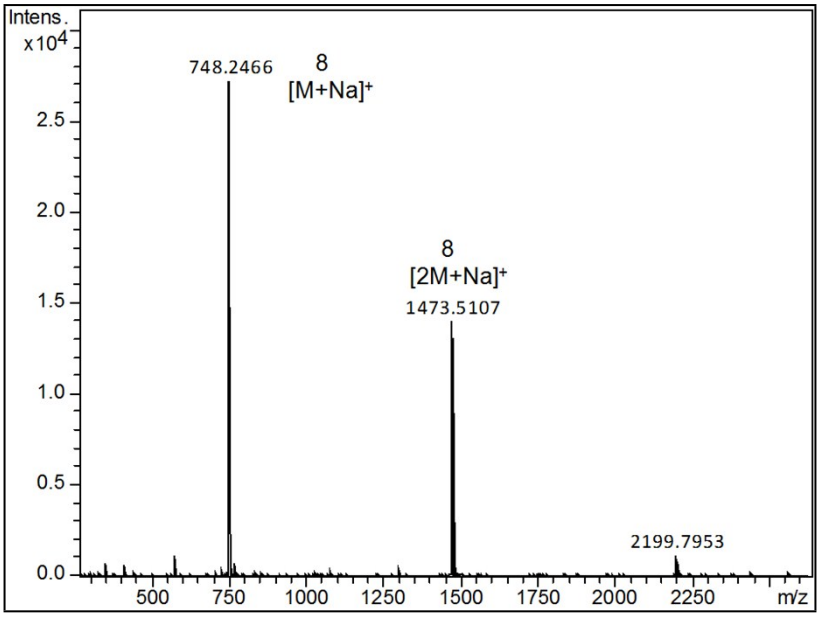

Figure S58. Mass spectrum of compound **8** shows mass peak at m/z 748.2466 $[M+Na]^+$, 1473.5107 $[2M+Na]^+$ (calc. m/z 748.2490 $[M+Na]^+$, 1473.5088 $[2M+Na]^+$).

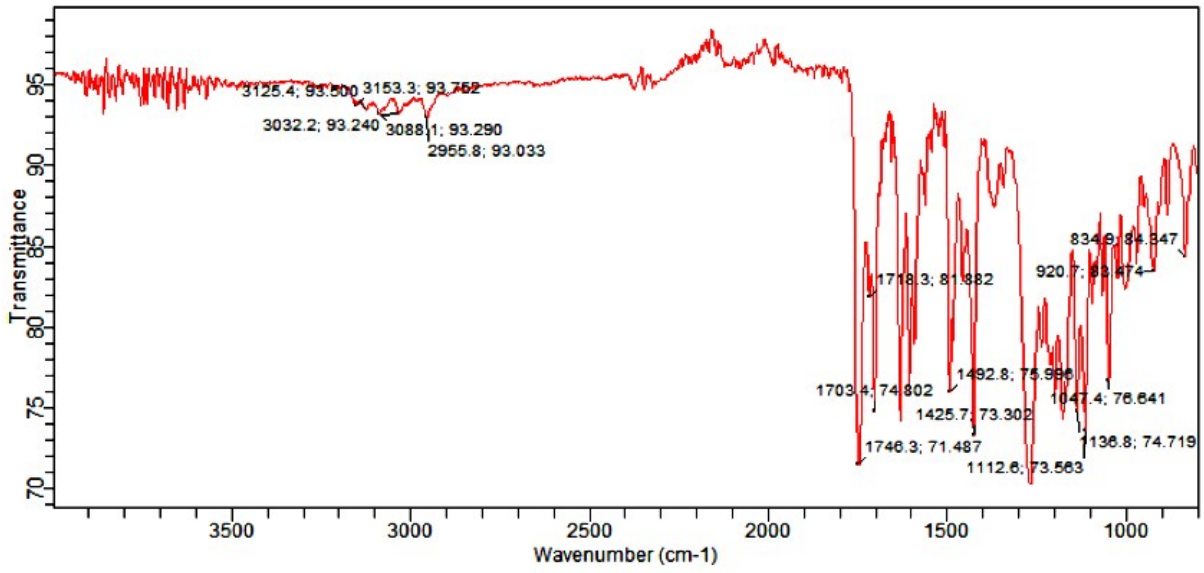

Figure S59. IR spectrum of compound **8**: $\bar{\upsilon}$ (cm^{-1}): 1746 (CO).

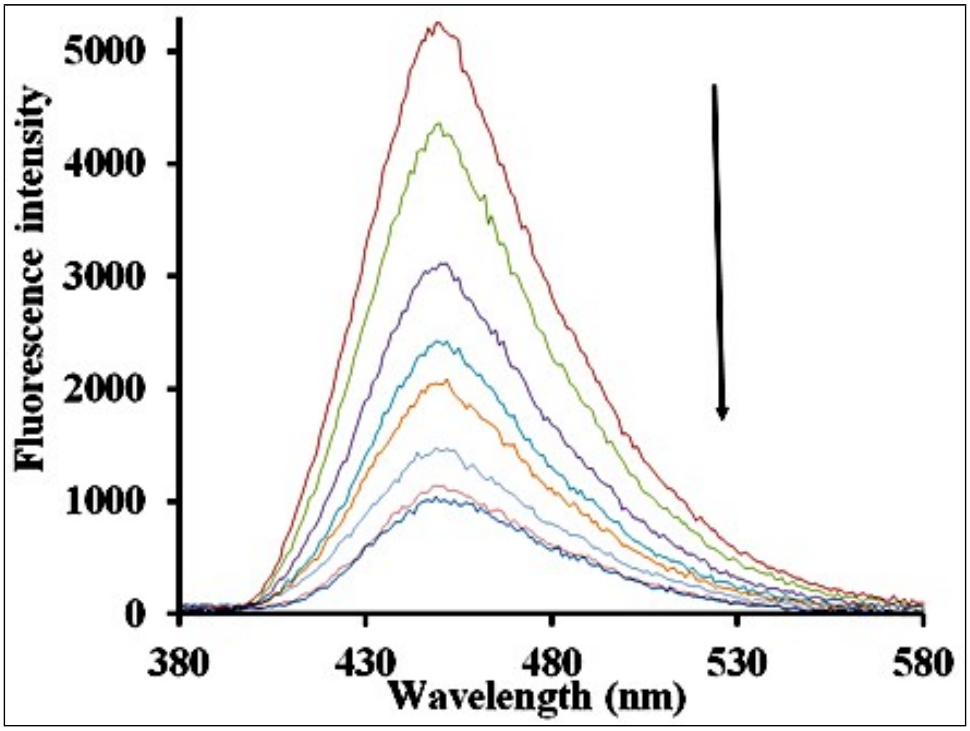

Figure S60A. Decrease in the fluorescence emission of compound **1** (5×10^{-6} M DMSO:H_2O, 3:7 v/v) at 452 nm on incremental addition of ATP. λ_{ex} 260 nm.

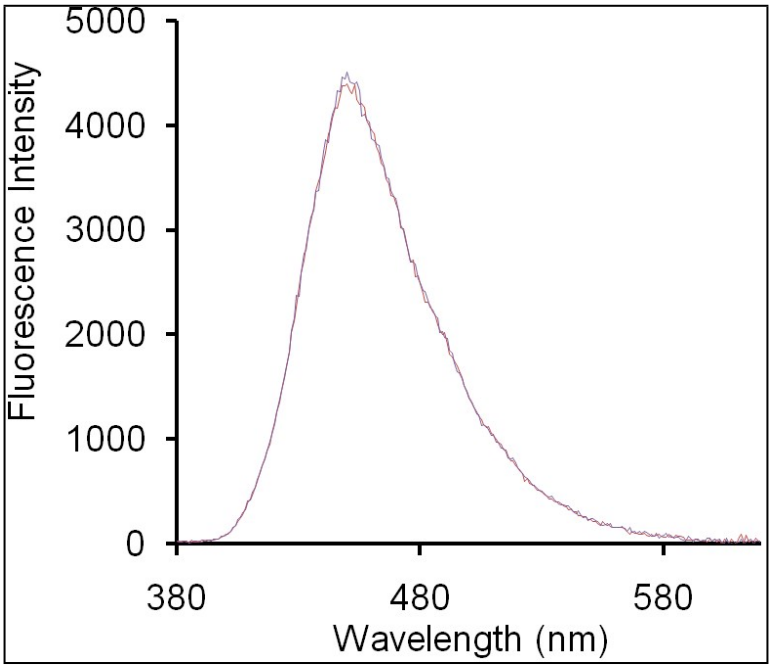

Figure S60B. Fluorescence spectra of compound **1** (blue trace) and after addition of water (red trace) equivalent to the volume of ATP solution added in Figure S59. This experiment ruled out the possibility of dilution factor responsible for the decrease in fluorescence intensity.

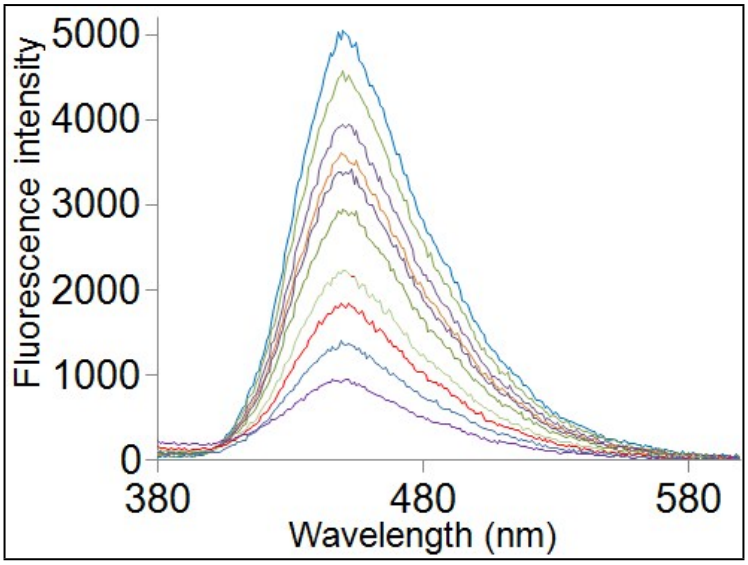

Figure S61. Decrease in the fluorescence emission of compound **1** (5×10^{-6} M DMSO:H_2O, 3:7 v/v) at 452 nm on incremental addition of GTP. λ_{ex} 260 nm.

Selectivity of compound 1 for ATP over ADP

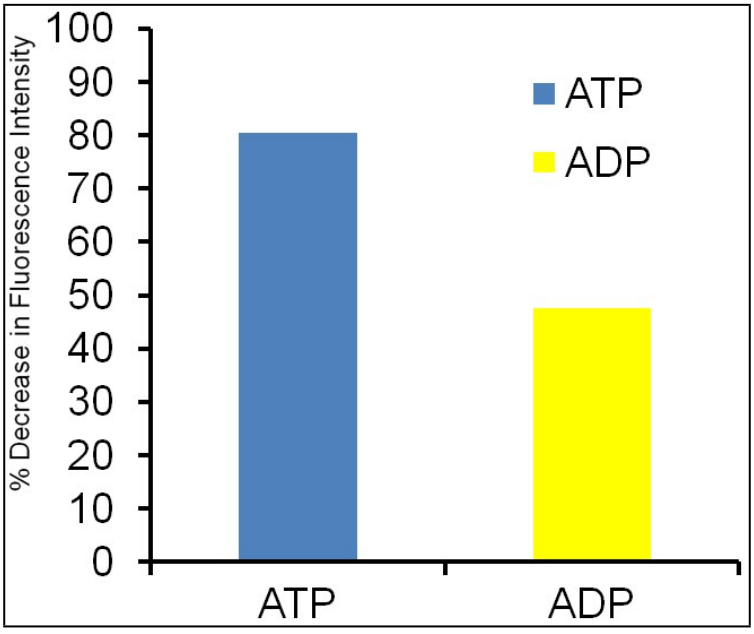

Figure S62. Bar graph showing % decrease in the fluorescence intensity of compound **1** on addition of 40 equiv ATP and ADP indicating that the compound is more responsive to ATP than ADP. From the percentage decrease in the fluorescence intensity in the presence of ATP (80%) and ADP (40%), the selectivity for ATP over ADP was calculated (80 x 100 / 40 = 200). Although the biological concentration of ATP is almost hundred fold of ADP[1] still we found that compound **1** is more selective for ATP over ADP and AMP

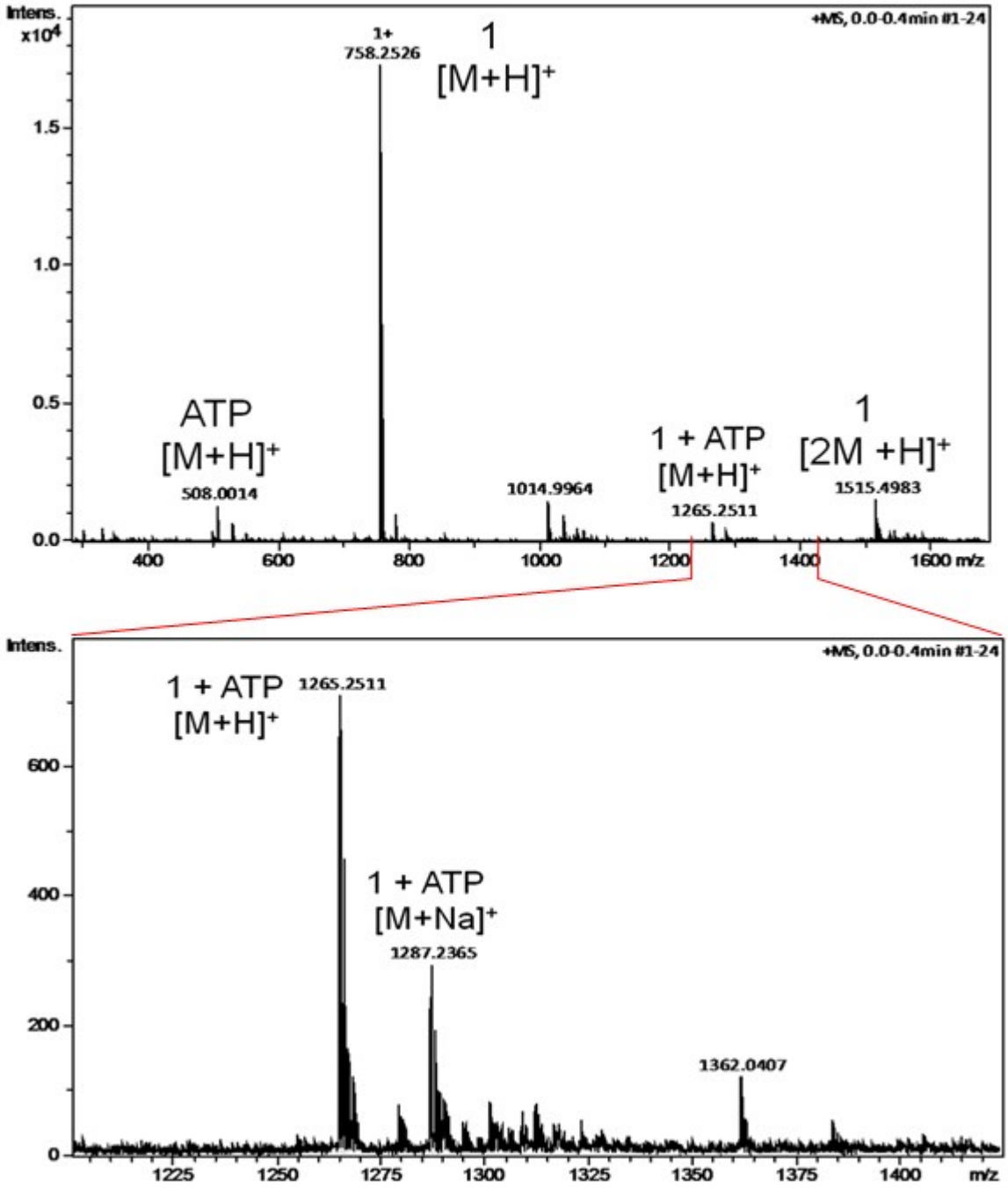

Figure S63. HRMS of compound **1** in the presence of ATP, ADP and AMP. Solution of **1** with equimolar ratio of ATP, ADP and AMP showed mass peak corresponding to *m/z* of the **1** – ATP complex only indicating the competitive binding of **1** with ATP.

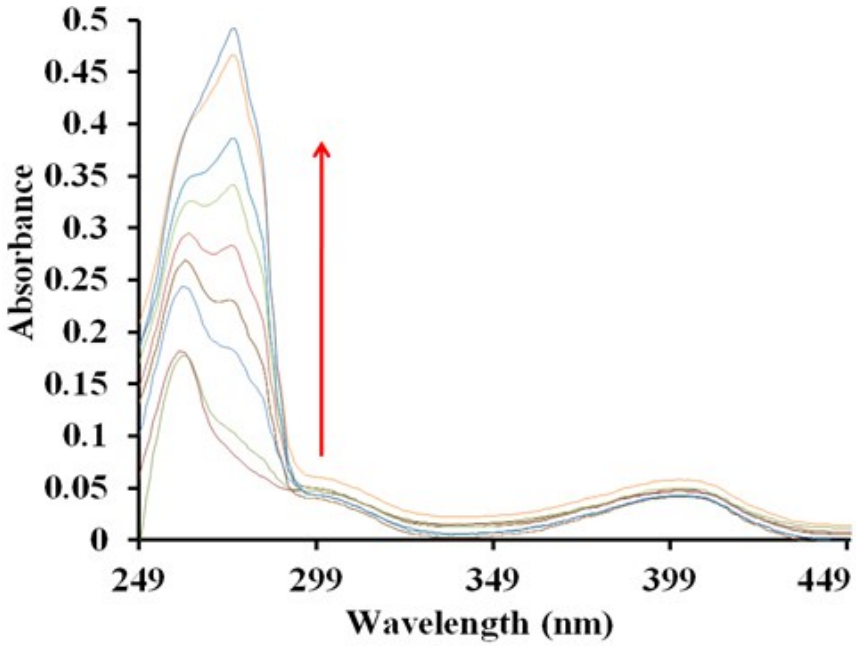

Figure S64. UV-visible spectrum of titration of compound **1** (5×10^{-6} M DMSO:H_2O, 1:9 v/v) with L-Tyr.

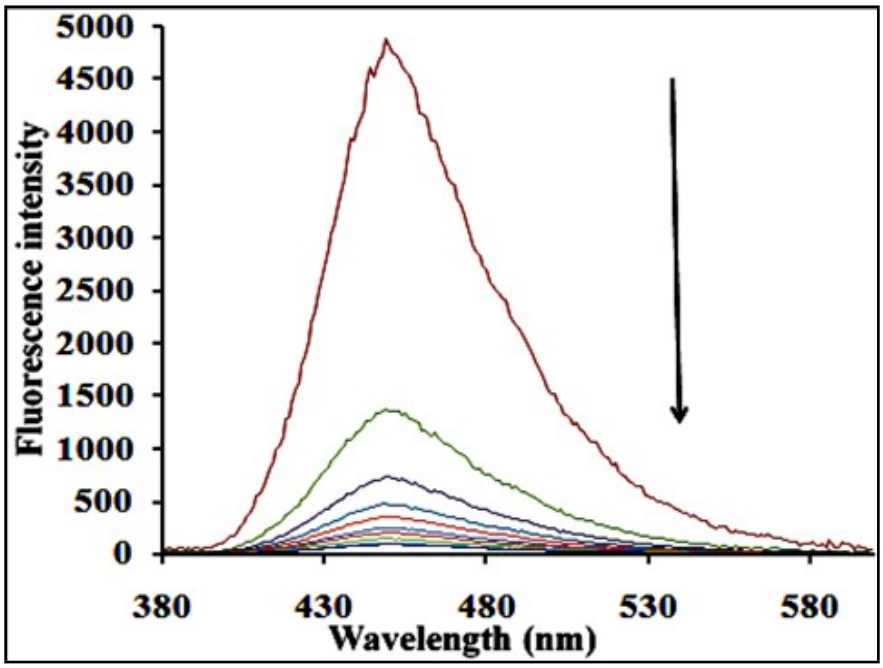

Figure S65. Decrease in the fluorescence emission of compound **1** (5×10^{-6} M DMSO:H_2O, 3:7 v/v) at 452 nm on incremental addition of L-Tyr (4 equiv). λ_{ex} 260 nm.

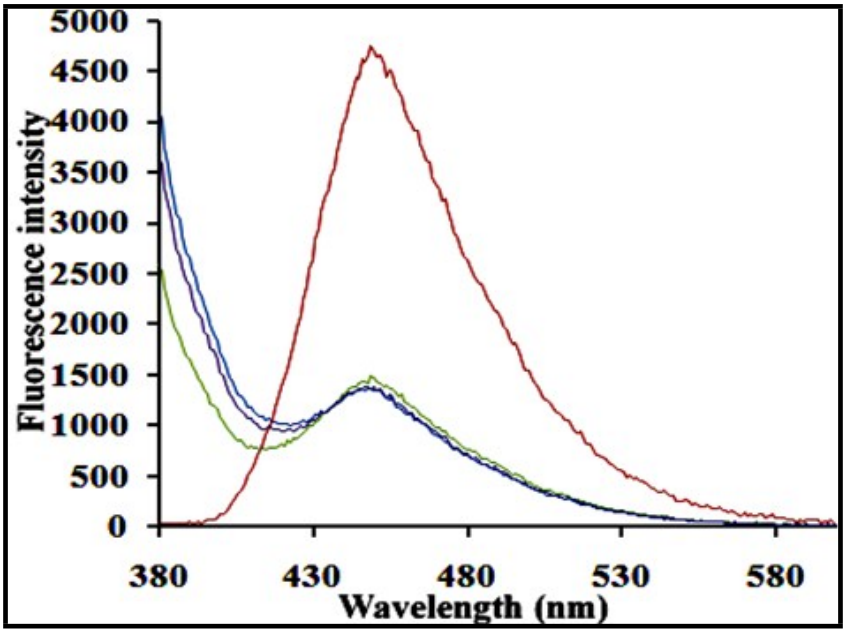

Figure S66. Fluorescence emission spectra of titration of compound **1** (5×10^{-6} M DMSO:H_2O, 3:7 v/v) against L-tryptophan at excitation wavelength of 260 nm. L-tryptophan was added up to 6 equivalents that resulted in the decrease of fluorescence emission band at 452 nm.

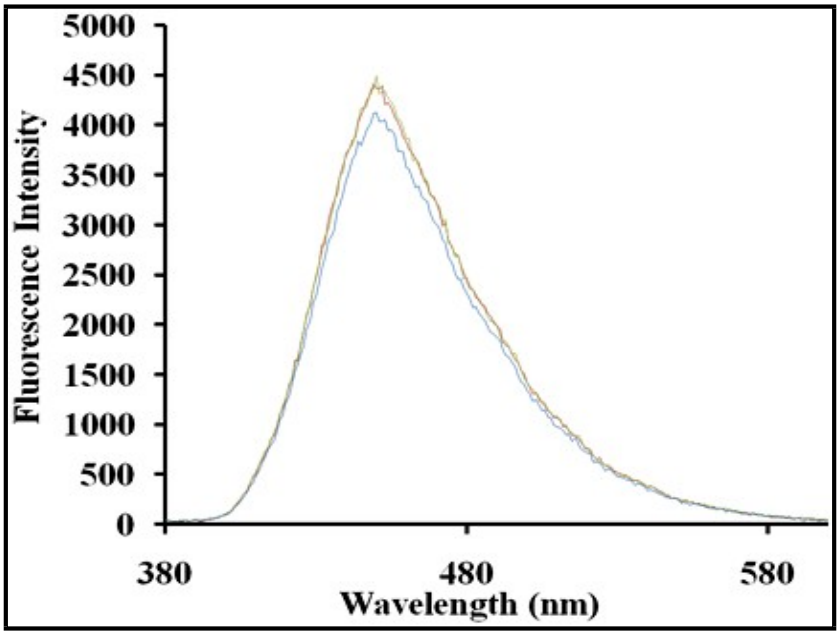

Figure S67. Fluorescence emission spectra of compound **1** (5×10^{-6} M) in DMSO-H_2O (3:7 v/v) on addition of 100 equivalent of L-histidine at excitation wavelength of 260 nm.

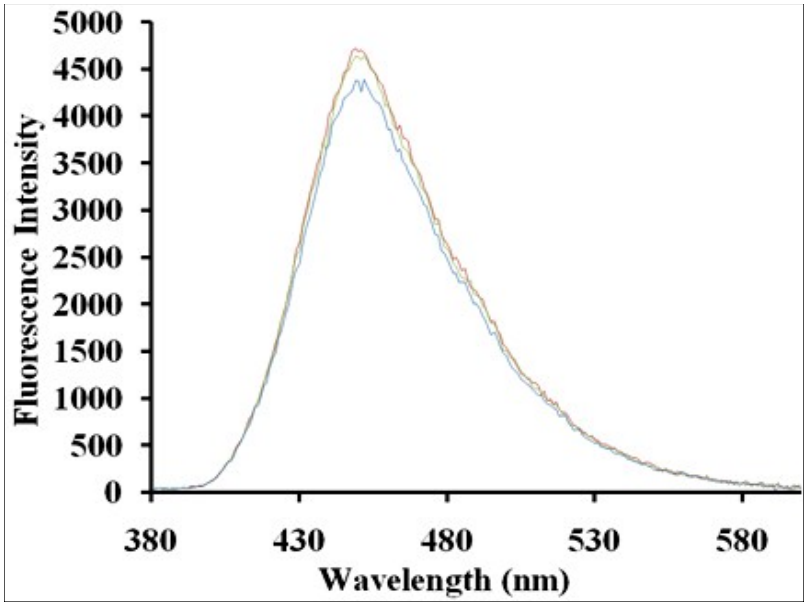

Figure S68. Fluorescence emission spectra of compound **1** (5×10^{-6} M) in DMSO-H_2O (3:7 v/v) on addition of 100 equivalent of L-valine at excitation wavelength of 260 nm.

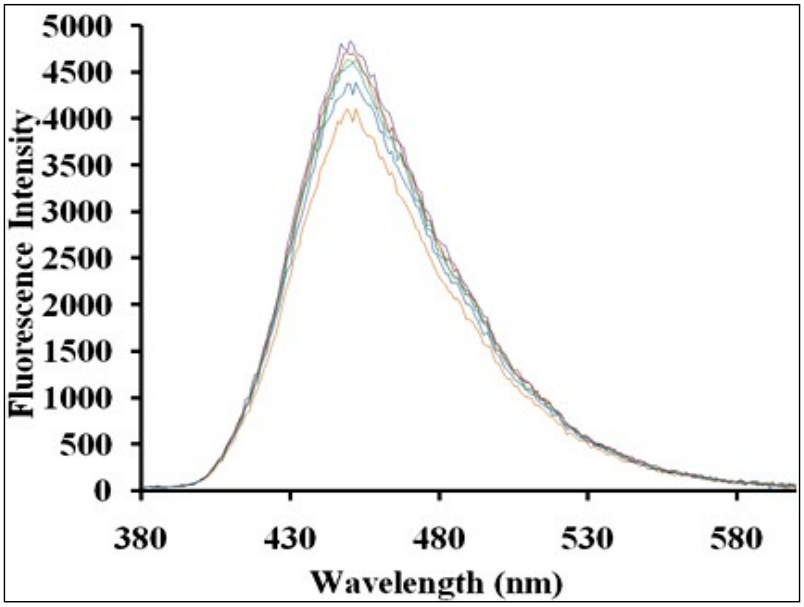

Figure S69. Fluorescence emission spectra of compound **1** (5×10^{-6} M) in DMSO-H_2O (3:7 v/v) on addition of 100 equivalent of L-proline at excitation wavelength of 260 nm.

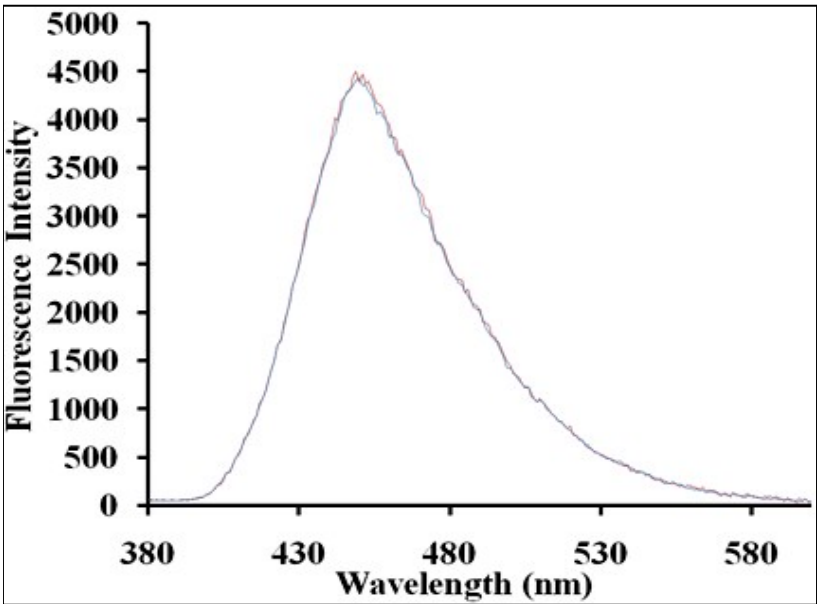

Figure S70. Fluorescence emission spectra of compound **1** (5×10^{-6} M) in DMSO-H_2O (3:7 v/v) on addition of 100 equivalent of L-isoleucine at excitation wavelength of 260 nm.

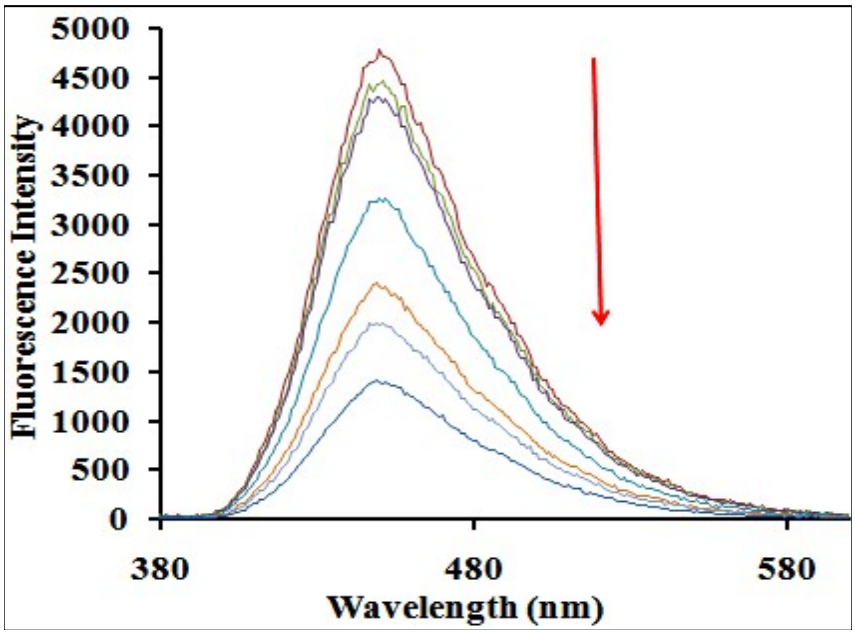

Figure S71. Fluorescence emission spectra of titration of compound **1** (5×10^{-6} M) in DMSO-H_2O (3:7 v/v) on addition of L-phenylalanine up to 115 equivalent decreases the intensity of emission band at 452 nm at excitation wavelength of 260 nm.

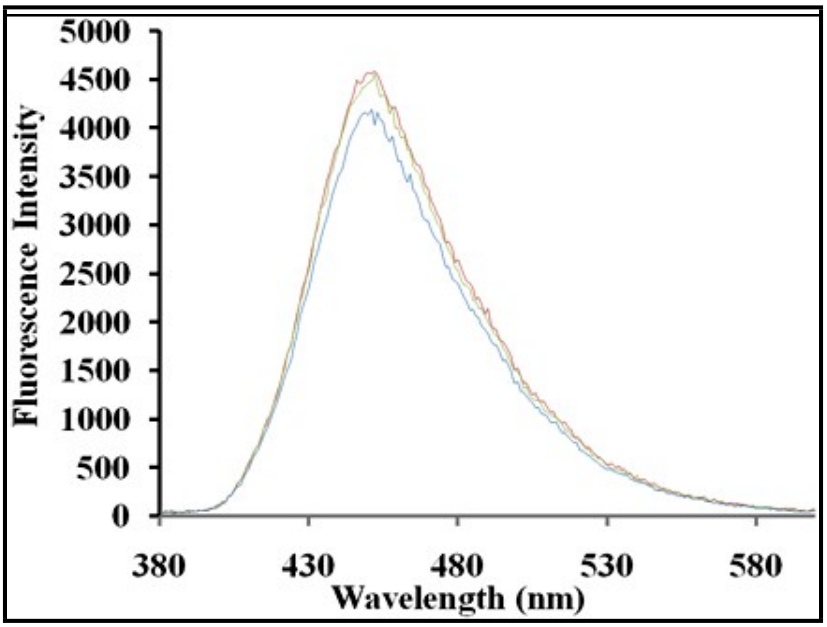

Figure S72. Fluorescence emission spectra of compound **1** (5×10^{-6} M) in DMSO-H_2O (3:7 v/v) on addition of 100 equivalent of L-alanine at excitation wavelength of 260 nm.

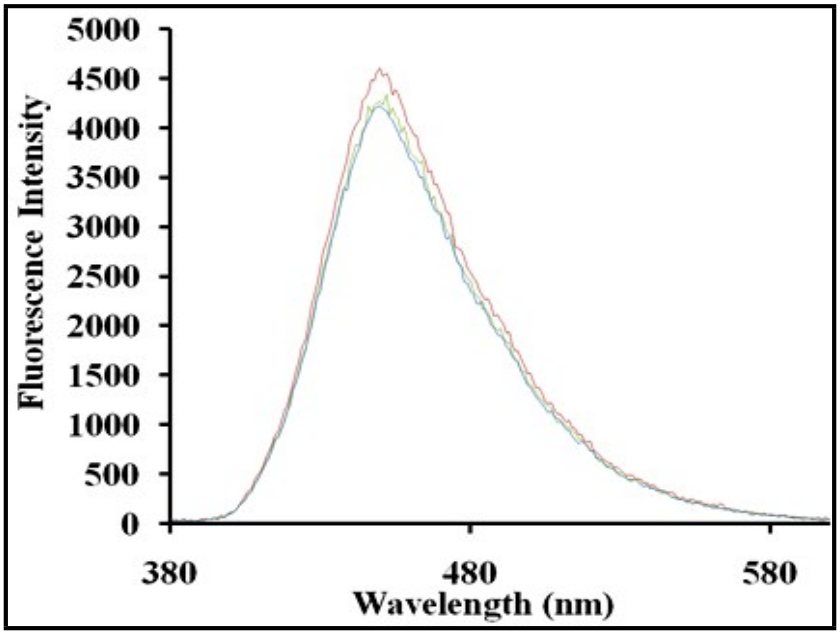

Figure S73. Fluorescence emission spectra of compound **1** (5×10^{-6} M) in DMSO-H_2O (3:7 v/v) on addition of 100 equivalent of L-cystiene at excitation wavelength of 260 nm.

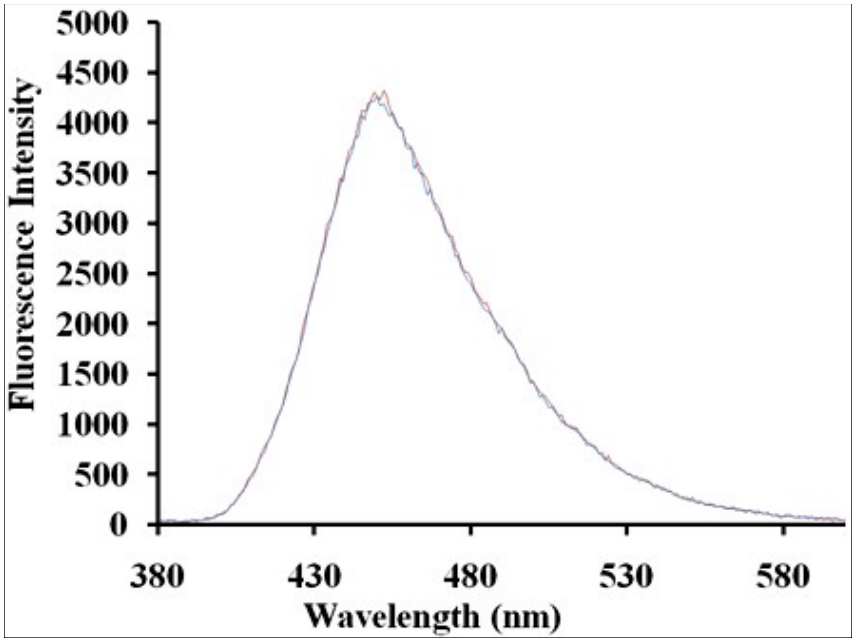

Figure S74. Fluorescence emission spectra of compound **1** (5×10^{-6} M) in DMSO-H_2O (3:7 v/v) on addition of 100 equivalent of L-lysine at excitation wavelength of 260 nm.

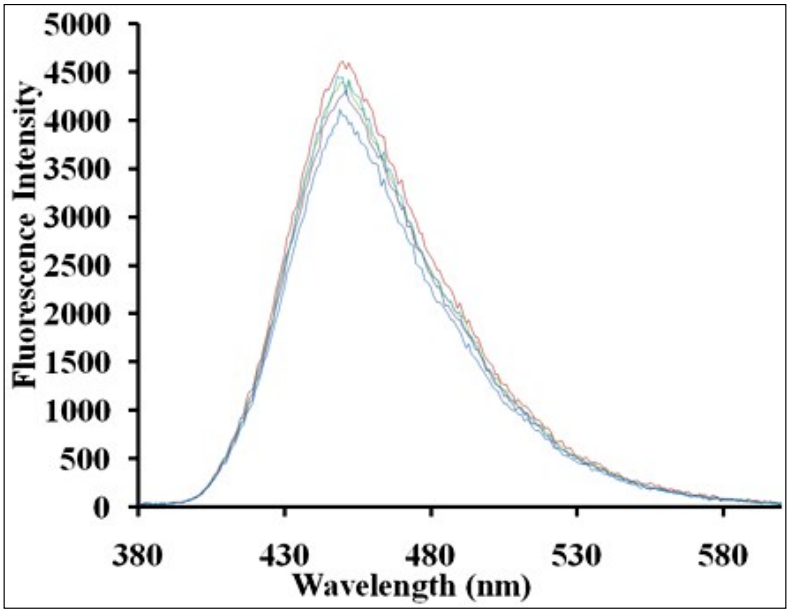

Figure S75. Fluorescence emission spectra of compound **1** (5×10^{-6} M) in DMSO-H_2O (3:7 v/v) on addition of L-serine up to 100 equivalent at excitation wavelength of 260 nm.

Selectivity of compound 1 for L-Tyr over L-Trp and L-Phe

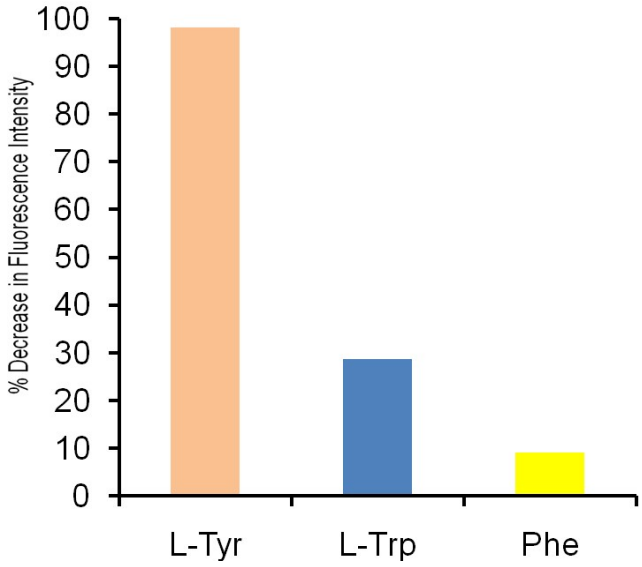

Figure S76. Bar graph showing % decrease in the fluorescence intensity of compound **1** on addition of 4 equivalents L-Tyr, L-Trp and L-Phe. Similar to the calculation of selectivity for ATP over ADOP, here also the selectivity for L-Tyr over L-Trp and L-Phe was calculated from the percentage decrease in the fluorescence intensity of the compound in presence of respective amino acids.

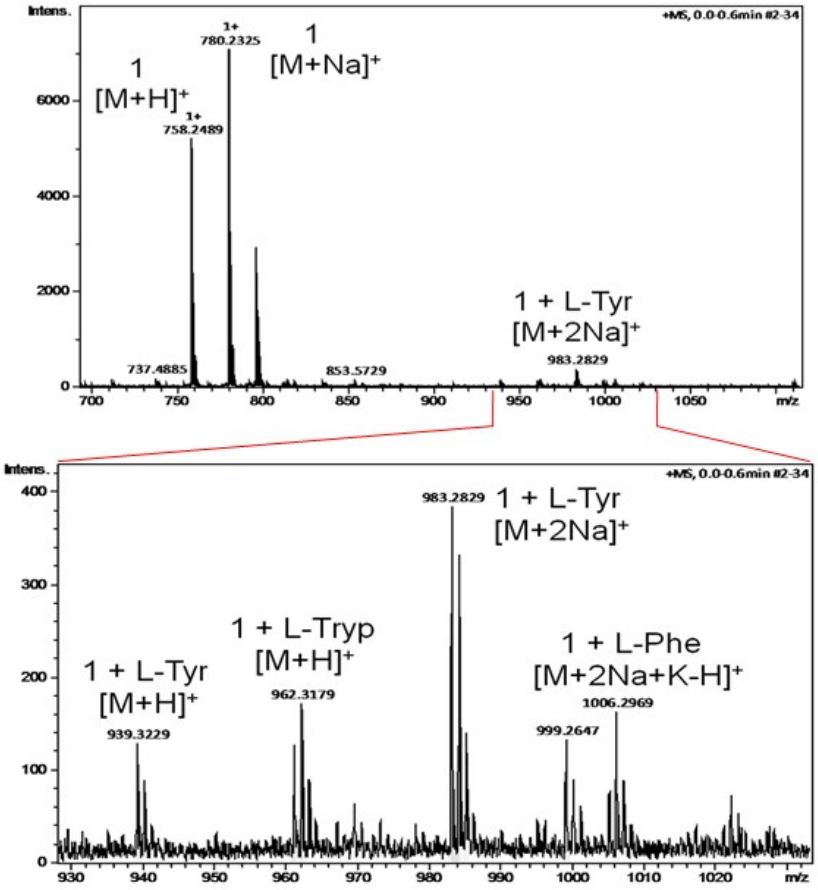

Figure S77. HRMS of compound **1** in presence of L-Tyr, L-Phe and L-Trp.

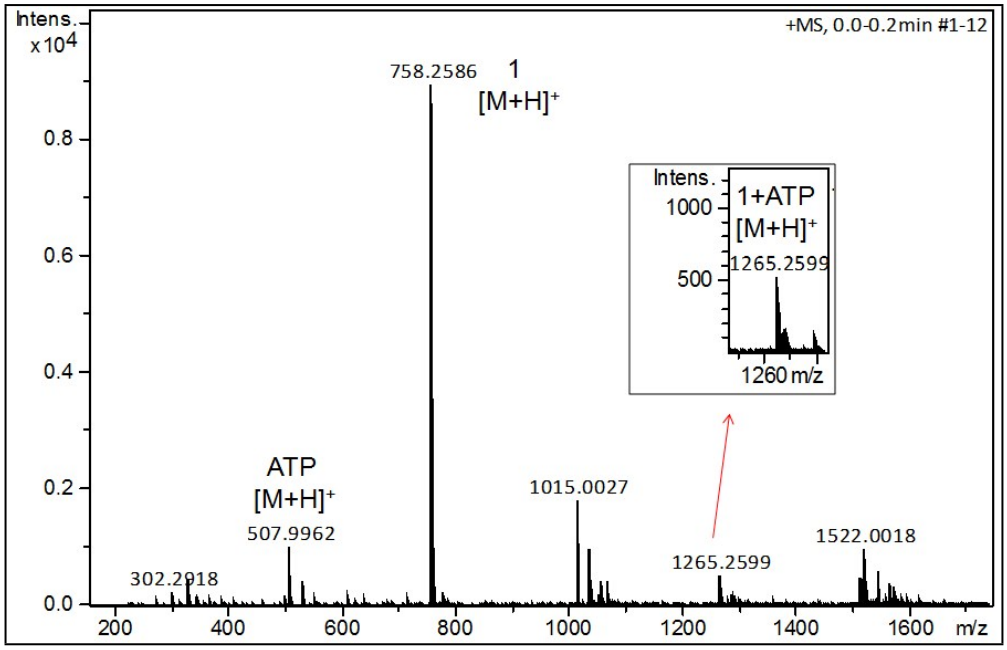

Figure S78. Mass spectra of solution of compound **1** (5×10^{-6} M in DMSO-H_2O 3:7) and ATP (5 μM). Compound **1** forms 1:1 complex with ATP. Mass calculated for $C_{40}H_{35}N_7O_9$+$C_{10}H_{16}N_5O_{13}P_3$ 1265.2526 $[M+H]^+$, found 1265.2599.

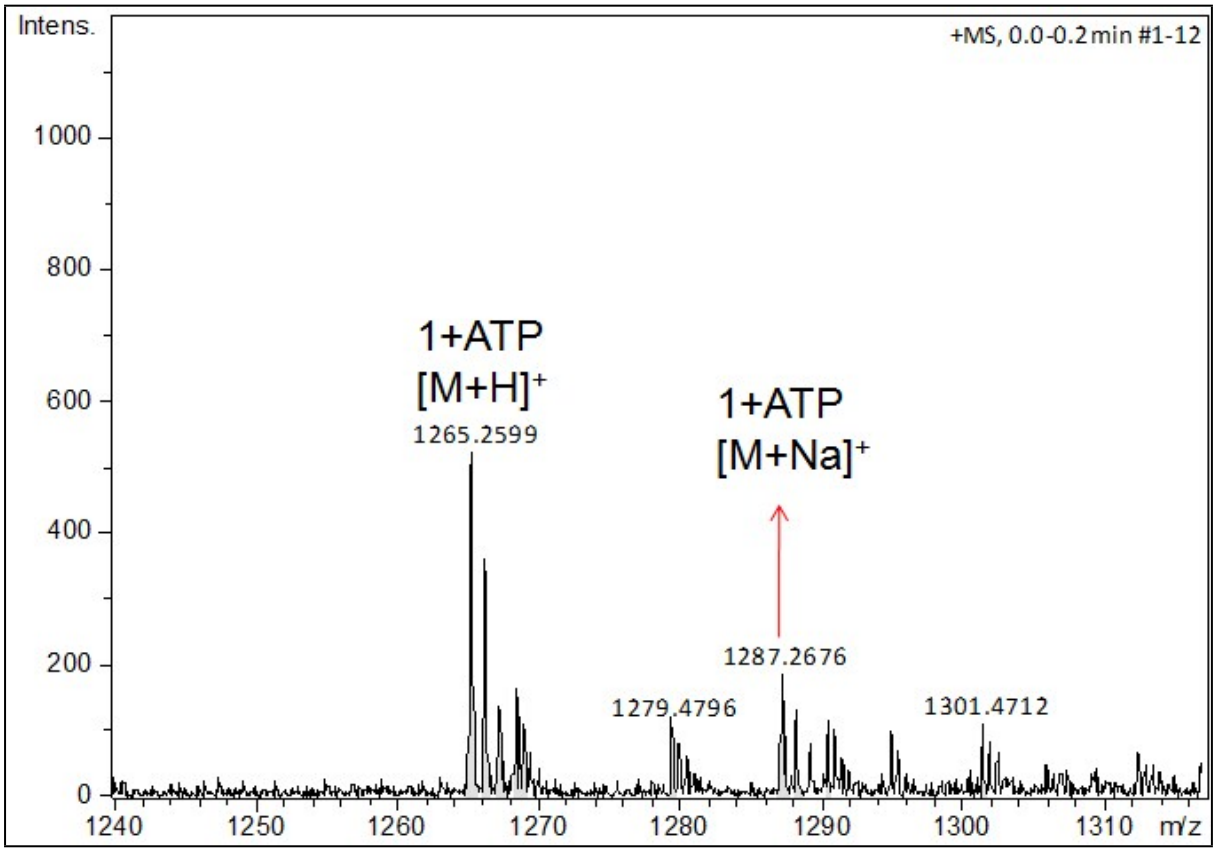

Figure S79. A part of Figure S78 is expanded.

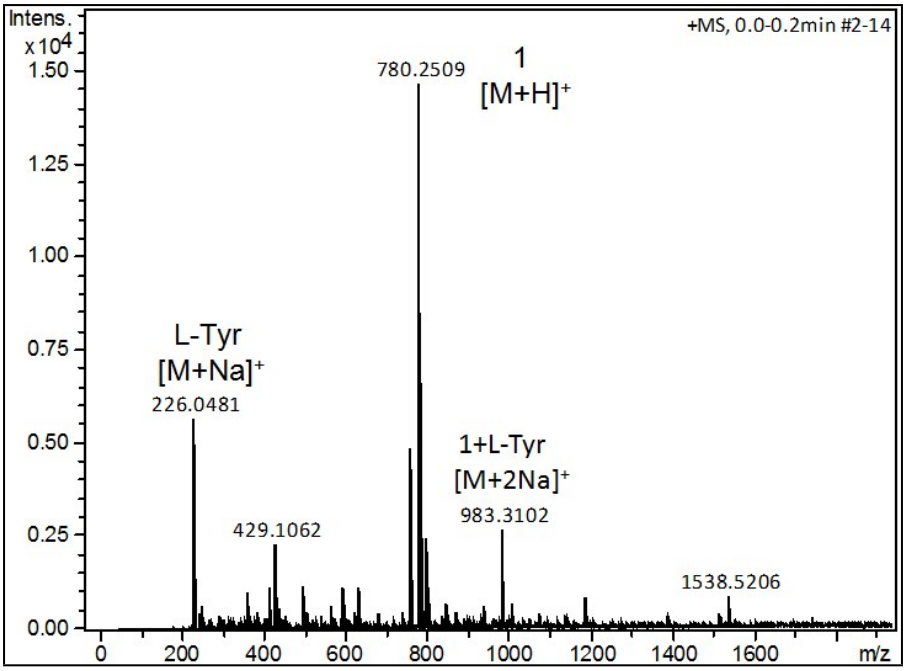

Figure S80. Mass spectrum of solution of solution of compound **1** (5×10^{-6} M) and L-Tyr (5 μM) in DMSO-H_2O (3:7 v/v). Compound **1** forms 1:1 and 1:2 complex with L-Tyr. Mass calcd for $C_{40}H_{35}N_7O_9.C_9H_{11}NO_3$ (**1** + Tyr) 939.3307 $[M+H]^+$, found 939.3338. Mass calcd for $C_{40}H_{35}N_7O_9.C_9H_{10}NO_3$ (**1** + Tyr) 983.2946 $[M+2Na]^+$, found 983.3102.

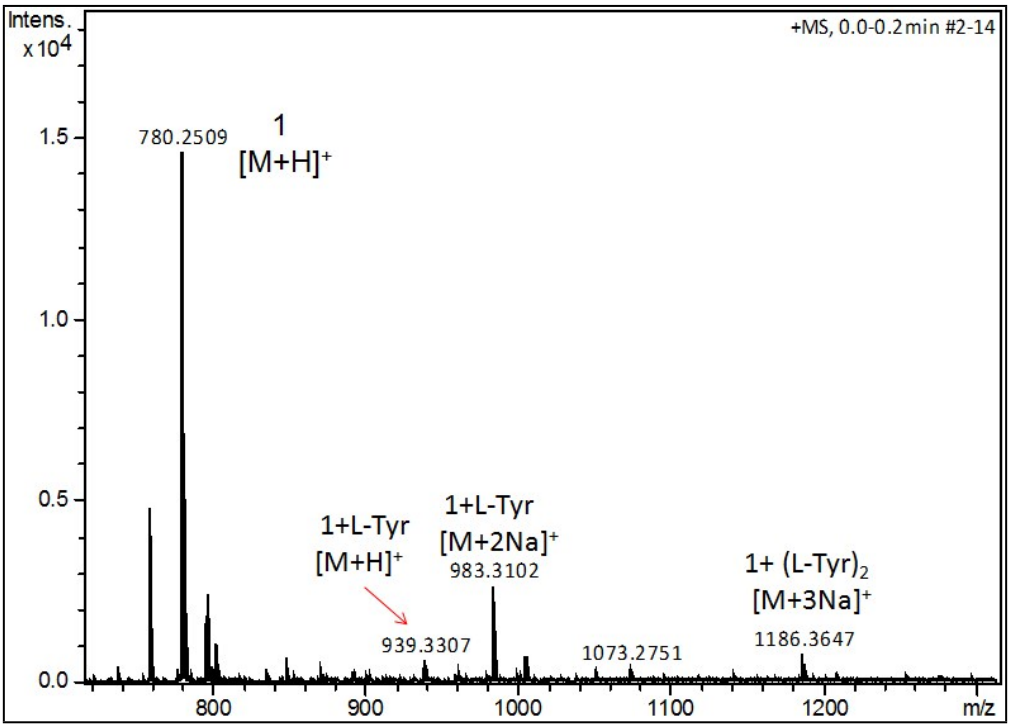

Figure S81. Expansion of a part of mass spectrum in Figure S80.

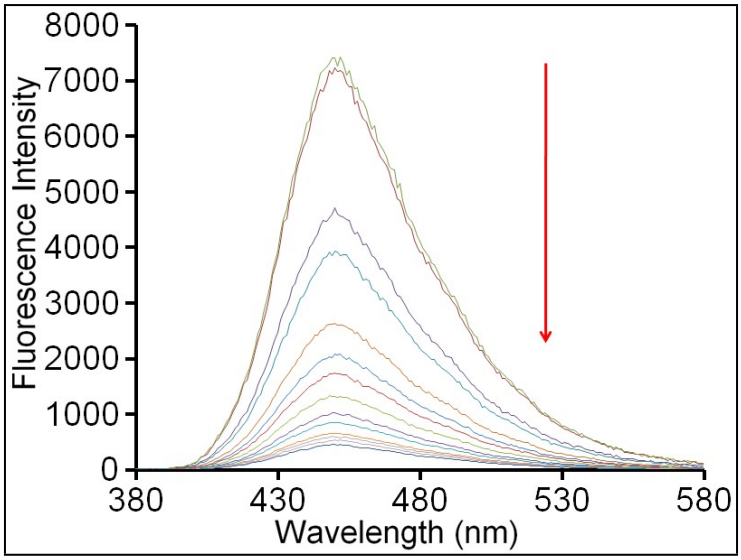

Figure S82. Fluorescence emission spectra of titration of compound **7** (5 μM in DMSO:water 3:7) with D-Tyr at excitation wavelength of 260 nm. 2 equivalents of D-Tyr were added successively up to 20 equivalents and decrease in the fluorescence emission intensity of band at 452 nm was observed.

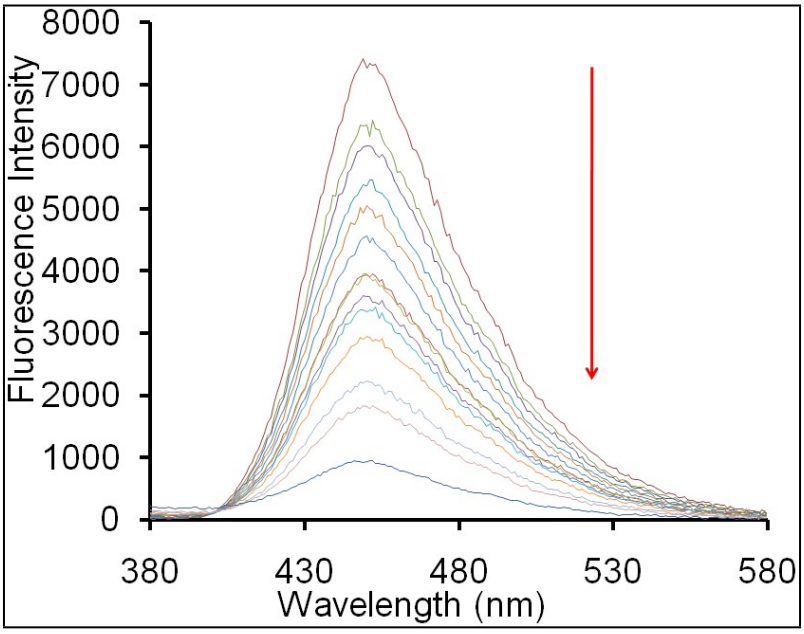

Figure S83. Fluorescence emission spectra of titration of compound **7** (5 μM in DMSO:water 3:7) with ATP at excitation wavelength of 260 nm. 4 equivalents of ATP was added successively up to 36 equivalents and decrease in the fluorescence emission intensity of band 452 nm was observed.

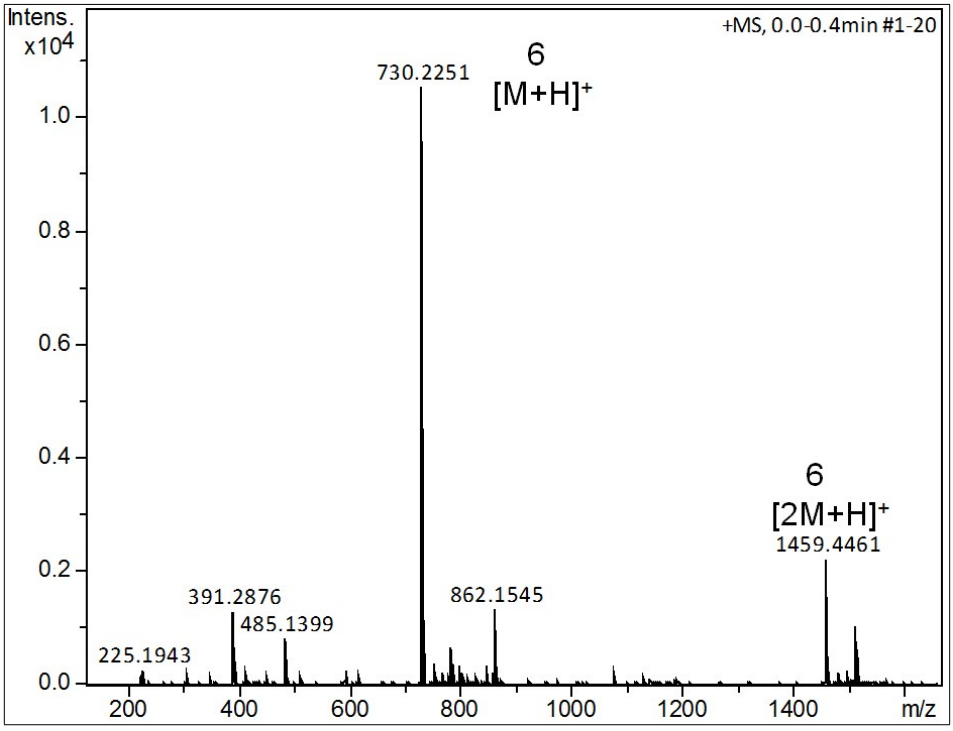

Figure S84a. HRMS of compound **1** after 3h treatment with LiOH. The peak at *m/z* 730.2251 corresponds to *m/z* of **6** (calcd *m/z* 730.2256 $[M+H]^+$).

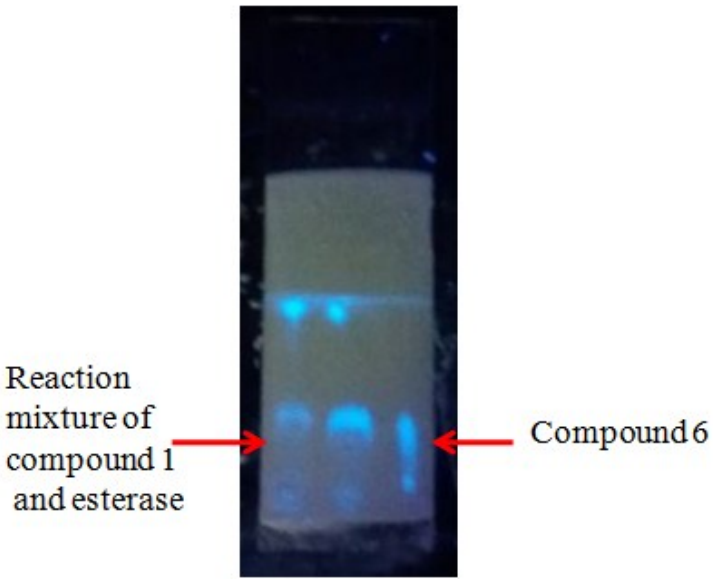

Figure S84b. Compound **1** (3 mg, 3.96 mmol) was dissolved in 3 mL acetone. Esterase (extracted from pig liver) was taken in 1.5 mL of 1 μM HEPES buffer (pH 7.4) and it was added to the solution of compound **1**. The mixture was stirred at 28–30 °C for 72h. The TLC of this mixture (left spot) shows the formation of compound **6** only (right spot) (central spot is overlapping of reaction mixture with compound **6**). In TLC of the reaction mixture, the spot at the top corresponds to compound **1**.

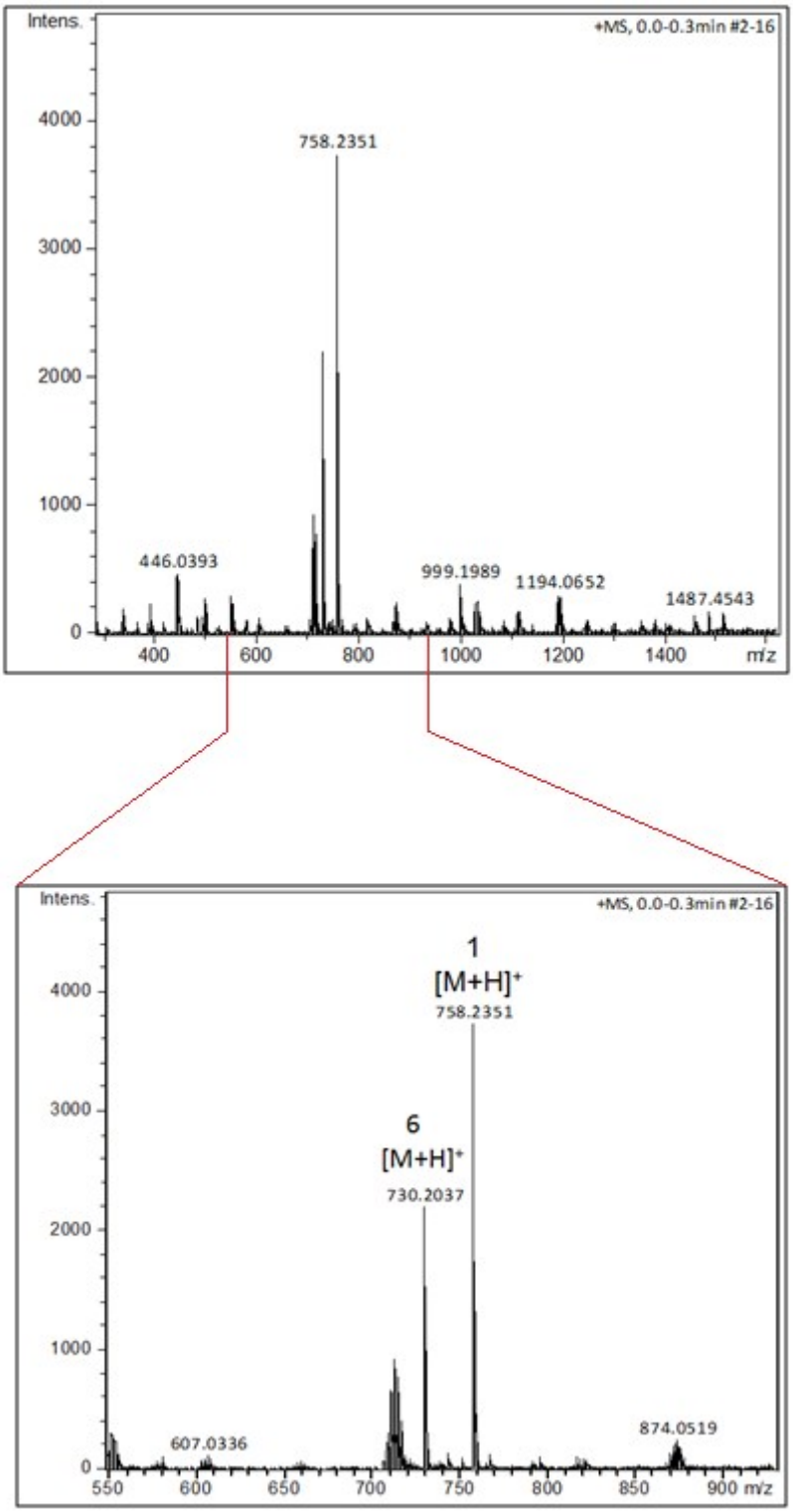

Figure S84c. Mass spectrum of the reaction mixture of Figure S84b after 72h. Peak at *m/z* 758 corresponds to the mass of compound **1** whereas peak at *m/z* 730 indicates the hydrolysis of terminal ester groups of **1** and formation of compound **6** (calcd m/z 730.2256 $[M+H]^+$). No formation of products corresponding to the breakdown of internal ester bond were observed.

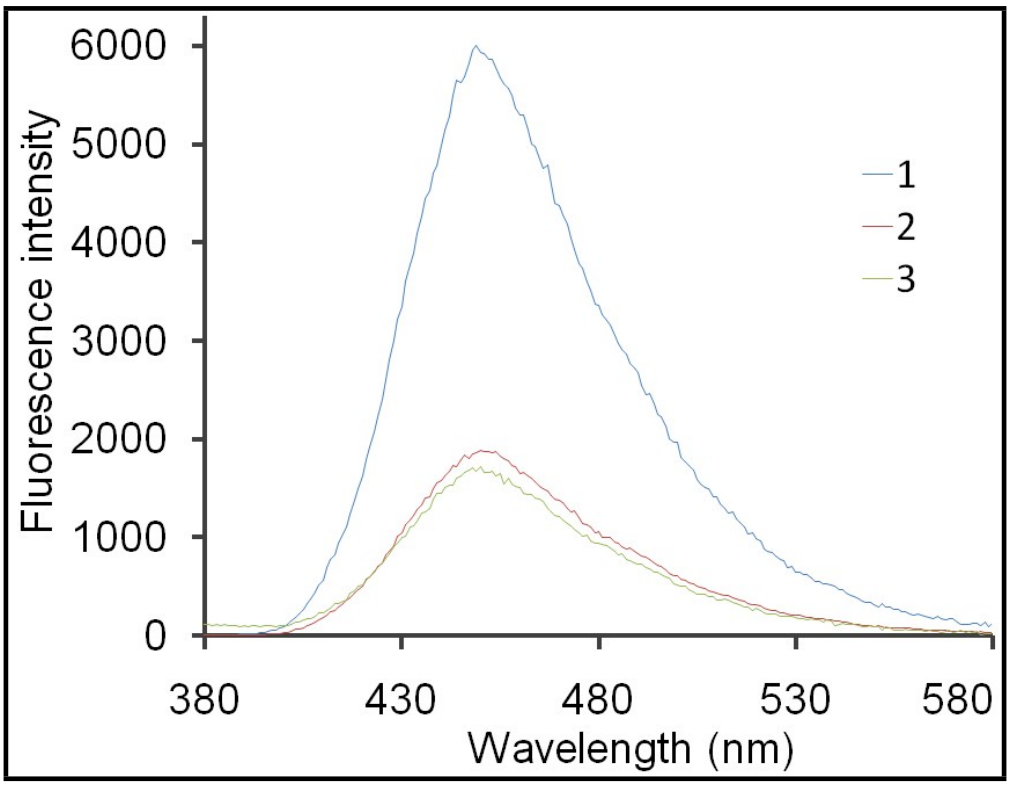

Figure S85. Fluorescence spectra of compound **6** (5 μM in DMSO-H_2O, 3:7) (trace 1) on addition of 4 equiv L-Tyr (trace 2) and 50 equiv ATP (trace 3).

Calculation of Binding constant (K_a) for compound 1 – ATP and compound 1 – L-Tyr complexes

Change in fluorescence intensity of the compound on stepwise addition of ATP and L-Tyr was observed. Benesi-Hildebrand equation was used for calculation of binding constant from Fluorescence emission spectra for respective titrations.

$1/(I_f-I_{obs}) = 1/ (I_f-I_{fc}) + (1/K(I_f-I_{fc}))\ 1/[Ligand]$

Where

I_f = Fluorescence Intensity of free Host.

I_{obs} = Fluorescence intensity of host at intermediate concentration of ligand.

I_{fc} = Fluorescence intensity of host at saturation.

[Ligand] = concentration of ligand.

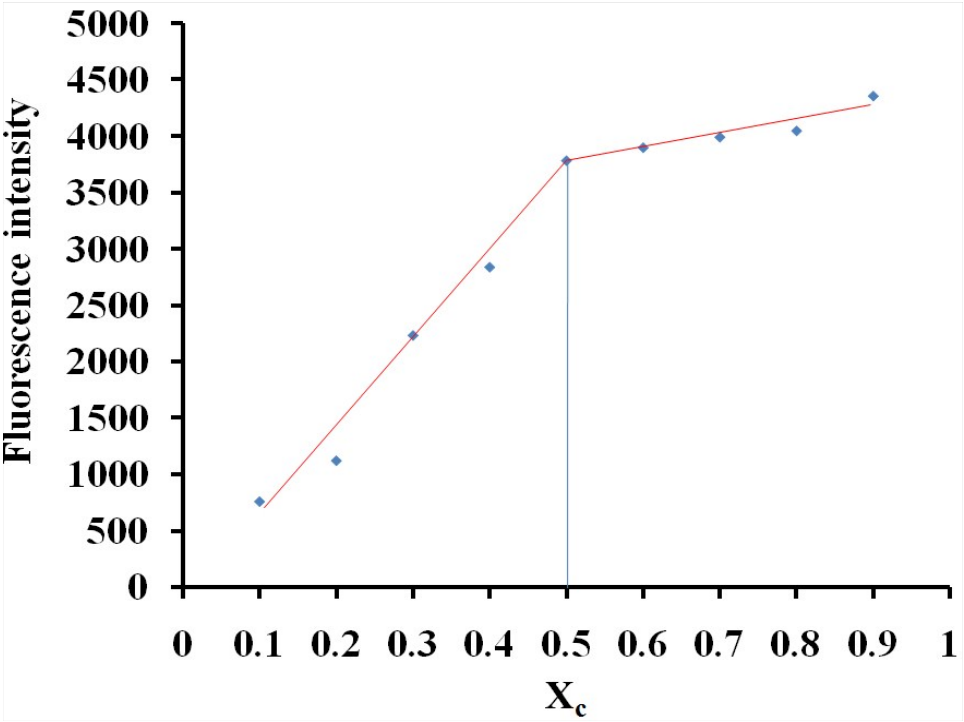

Figure S86. Job plot of compound **1** with ATP showing 1:1 stoichiometry. X_C = mole fraction of compound **1**.

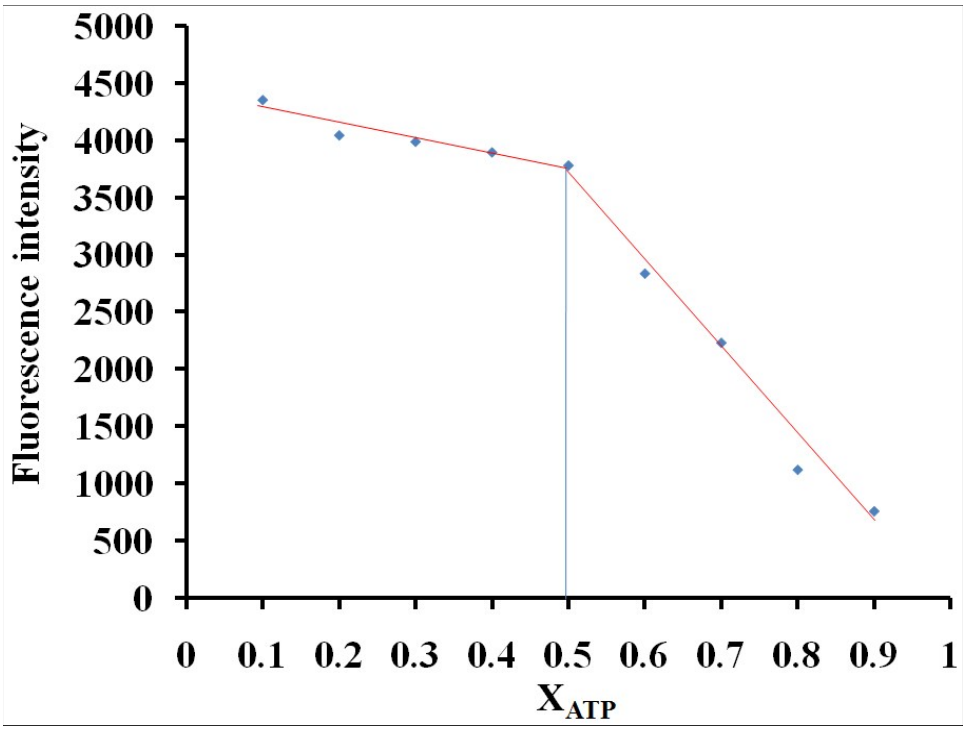

Figure S87. Job plot of compound **1** with ATP showing 1:1 stoichiometry. X_{ATP} = mole fraction of ATP

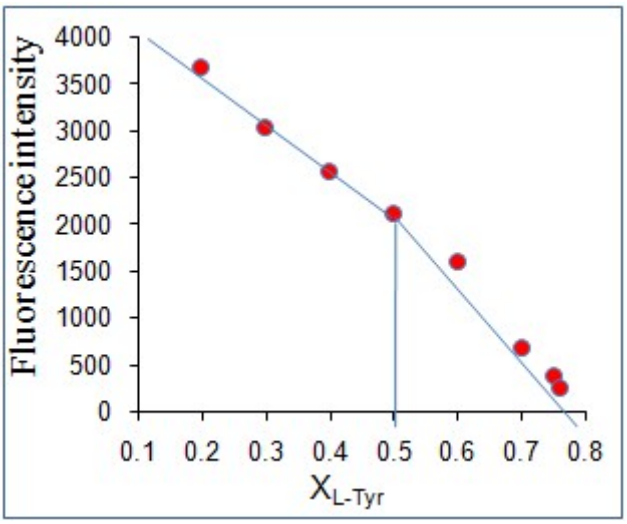

Figure S88. Job plot of compound **1** with L-Tyr showing 1:1 stoichiometry. $X_{L\text{-}Tyr}$ = Mole fraction of L-Tyr.

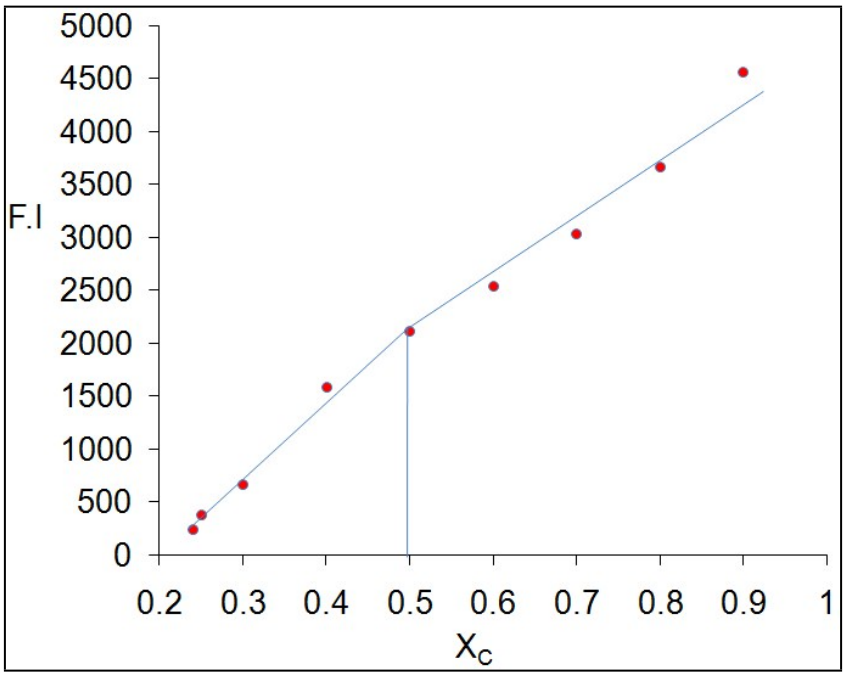

Figure S89. Job plot of compound **1** with L-Tyr showing 1:1 stoichiometry. X_C = Mole fraction of compound **1**.

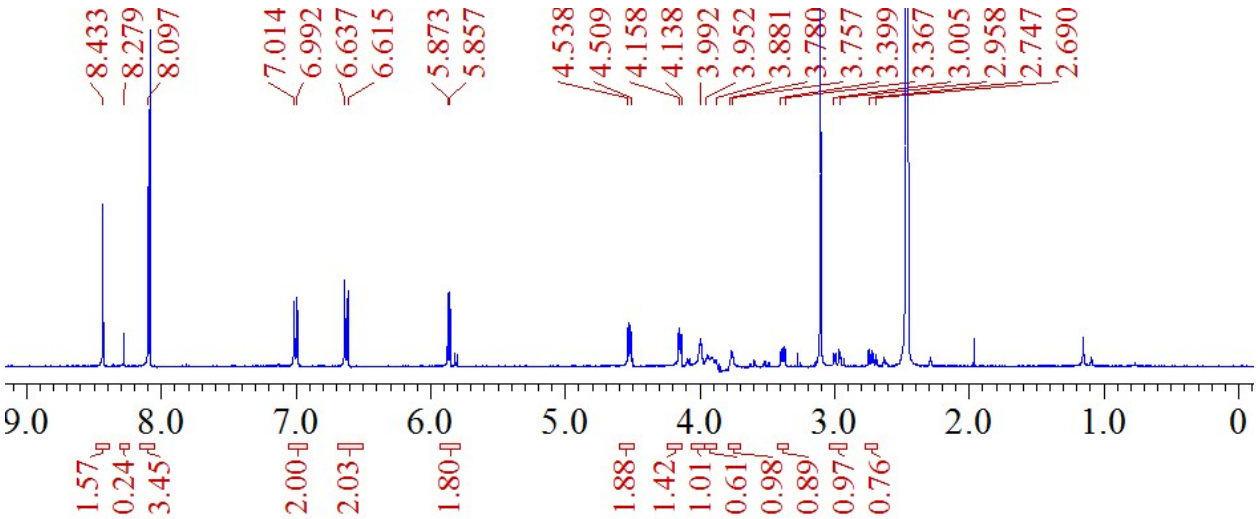

Figure S90A. ^{1}H NMR of tyrAd in DMSO-d_6 with 10% D_2O. D_2O was used due to solubility reasons.

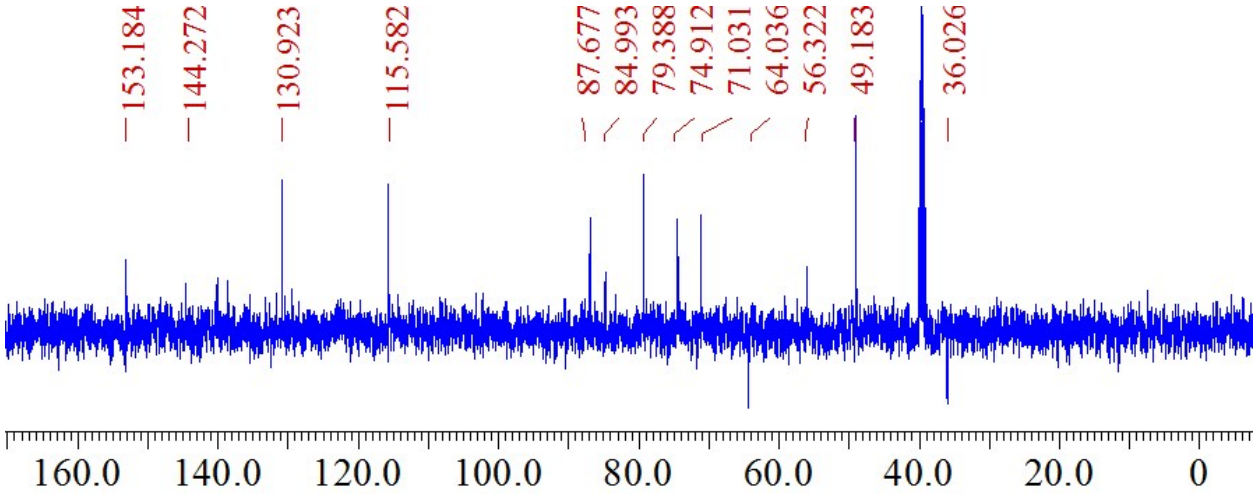

Figure S90B. DEPT-135 NMR spectrum of tyrAd.

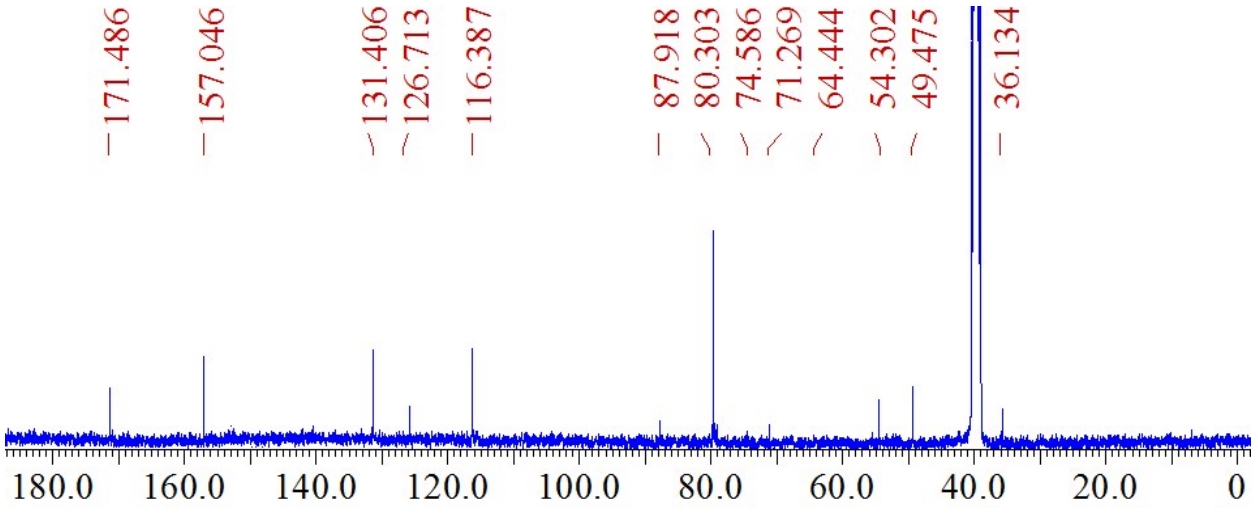

Figure S90C. ^{13}C NMR spectrum of tyrAd.

Mass Spectrometry. The mass spectra were recorded on Bruker MicroTOF QII mass spectrometer using different methods such as 'small', 'wide', 'large', 'intact protein' so that mass of all possible species is detected. Using KdScientific automated pump with flow rate of 180 µL/h, the solution of compound/reaction mixture diluted in acetonitrile-water-formic acid (7:2.9:0.1) was injected to the electrospray ionization source. Desolvation was performed with dry N_2 gas heated at 180 ^oC. Various parameters of the mass spectrometer were optimized for maximum ion abundance. Typically, the capillary voltage was 4500 V and vacuum was maintained at 3-4x10^{-7} mbar. By varying the collision RF and other ion transfer parameters, the mass spectra were recorded in different mass ranges so that mass peaks in the lower mass range as well as higher mass range are picked up.

For LC-MS, the Dionex Ultimate 3000 system was linked to mass spectrometer. 2 µL of the sample was loaded to C-18 column (Acclaim® 120 C18 5 µm 120 Å (4.6 x 250 mm) and acetonitrile-water (2:8 – 1:0) was used as eluent in gradient/isocratic method. The flow rate was kept 0.2 mL and absorbance was set at 260 nm.

The concentration of tyrAd formed in the reaction mixture as a function of time/concentration of ATP was monitored by integrating (area under curve AUC) its peak in the LC-MS using HyStar and Quant analysis software. TyrAd was quantified using the standard curve (plot of conc vs area for the known concentrations of tyrAd) in QuantAnalysis software of Bruker Daltonic (Figure S91). Since the formation of tyrAd in the enzymatic reaction was fast, more polar eluent was used to speed up the elution of tyrAd so that the interval between two LC runs is not very large. LC-MS were also recorded by varying the concentration of ATP in the solution of compound **1**/TyrTS mediated reactions. The kinetic parameters were calculated from the change in integration (AUC)/concentration of tyrAd as a function of [ATP] formed under the intermediacy of **1**/TyrTS and plotting against [1/ATP].

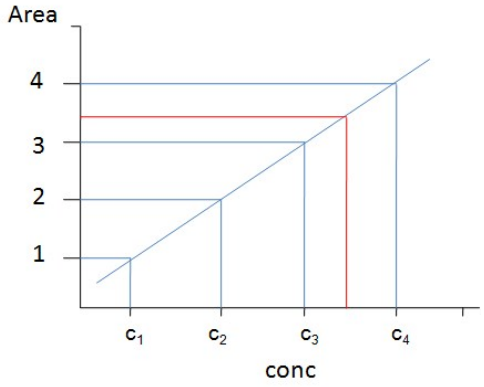

Figure S91. Plot of standard curve of tyrAd between its concentrations and corresponding peak intensity (AUC) and findig the concentration of tyrAd in the reaction mixture (red line).

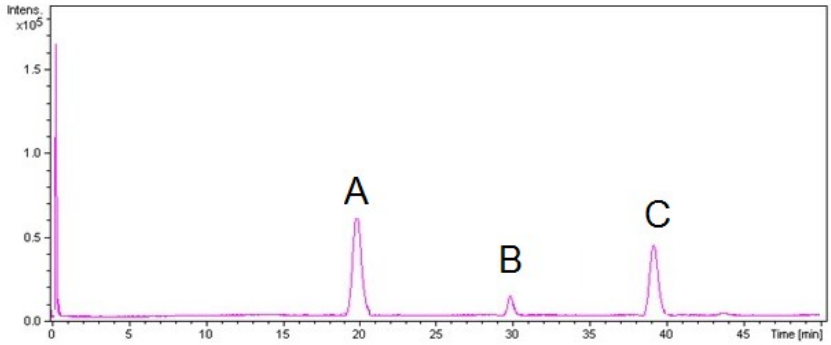

Figure S92. LC chromatogram of solution of compound **1** (5×10^{-6} M) with L-Tyr (5 μM), ATP (5 μM) and magnesium acetate (80 μM) in DMSO-H_2O (3:7 v/v) incubated at 37 ^oC for 5 min. The peaks in the chromatogram correspond to the mass of: (A) compound **1**, (B) ATP and (C) tyr. Reaction mass was eluted in ACN - H_2O.

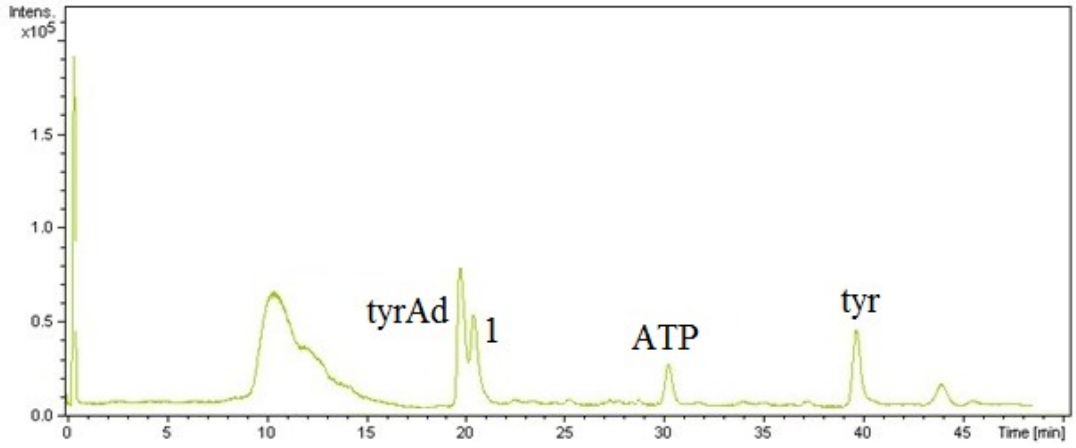

Figure S93. LC chromatogram of the solution of Figure S91 after 50 min of the reaction.

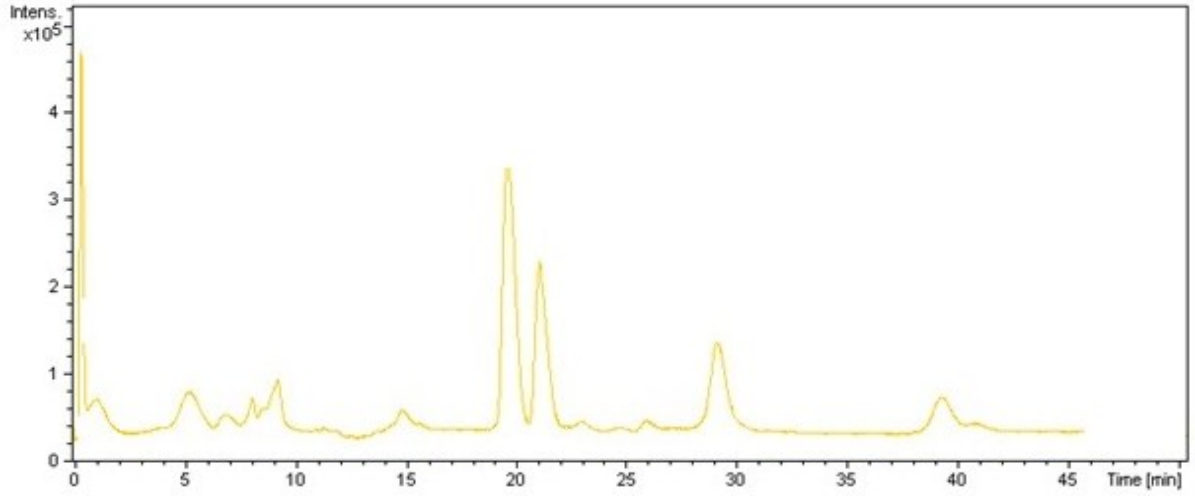

Figure S94. LC chromatogram of the solution of Figure S91 after 100 min of the reaction.

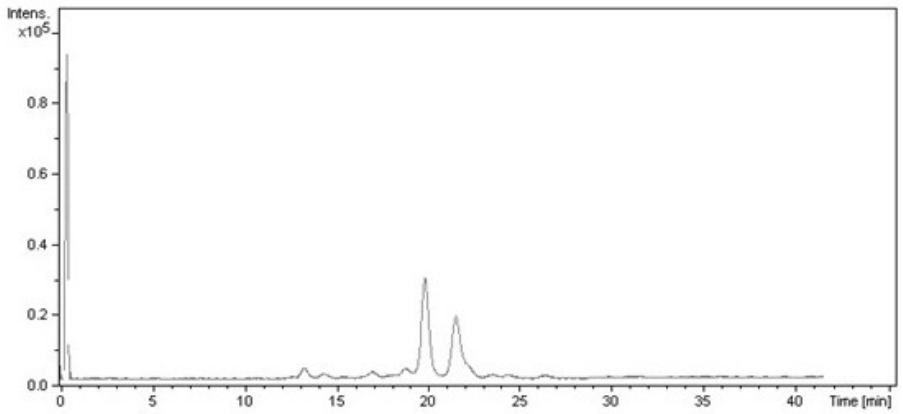

Figure S95. LC chromatogram of the solution of Figure S91 after 140 min of the reaction.

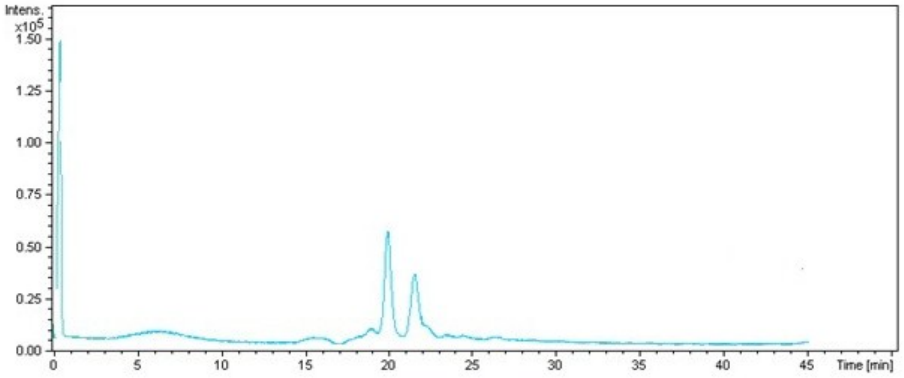

Figure S96. LC chromatogram of the solution of Figure S91 after 180 min of the reaction.

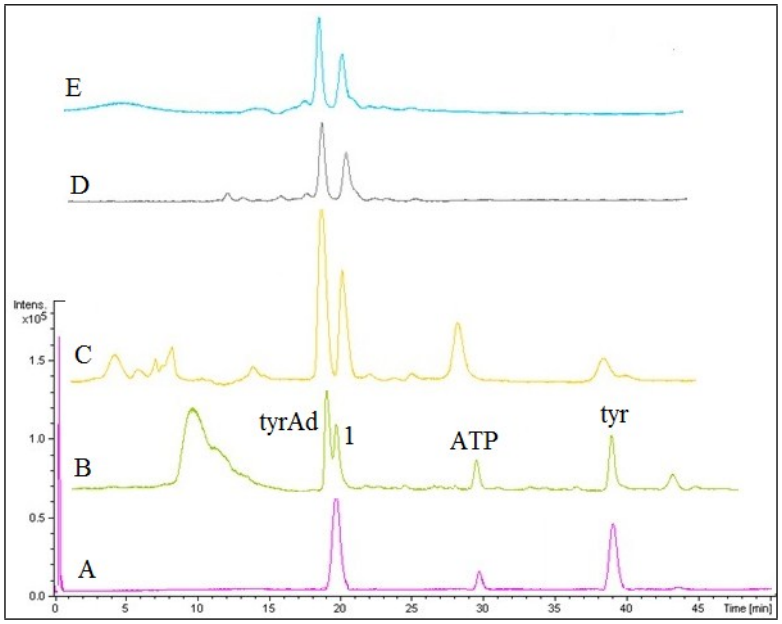

Figure S97. Overlay of LC chromatograms of solution of compound **1** (5×10^{-6} M) with L-Tyr (5 μM), ATP (5 μM) and magnesium acetate (80 μM) in DMSO-H_2O (3:7 v/v) recorded at different time intervals: (A) 10 min, (B) 50 min, (C) 100 min, (D) 140 min, (E) 180 min. In all the chromatograms, the peak near zero is due to internal calibrant.

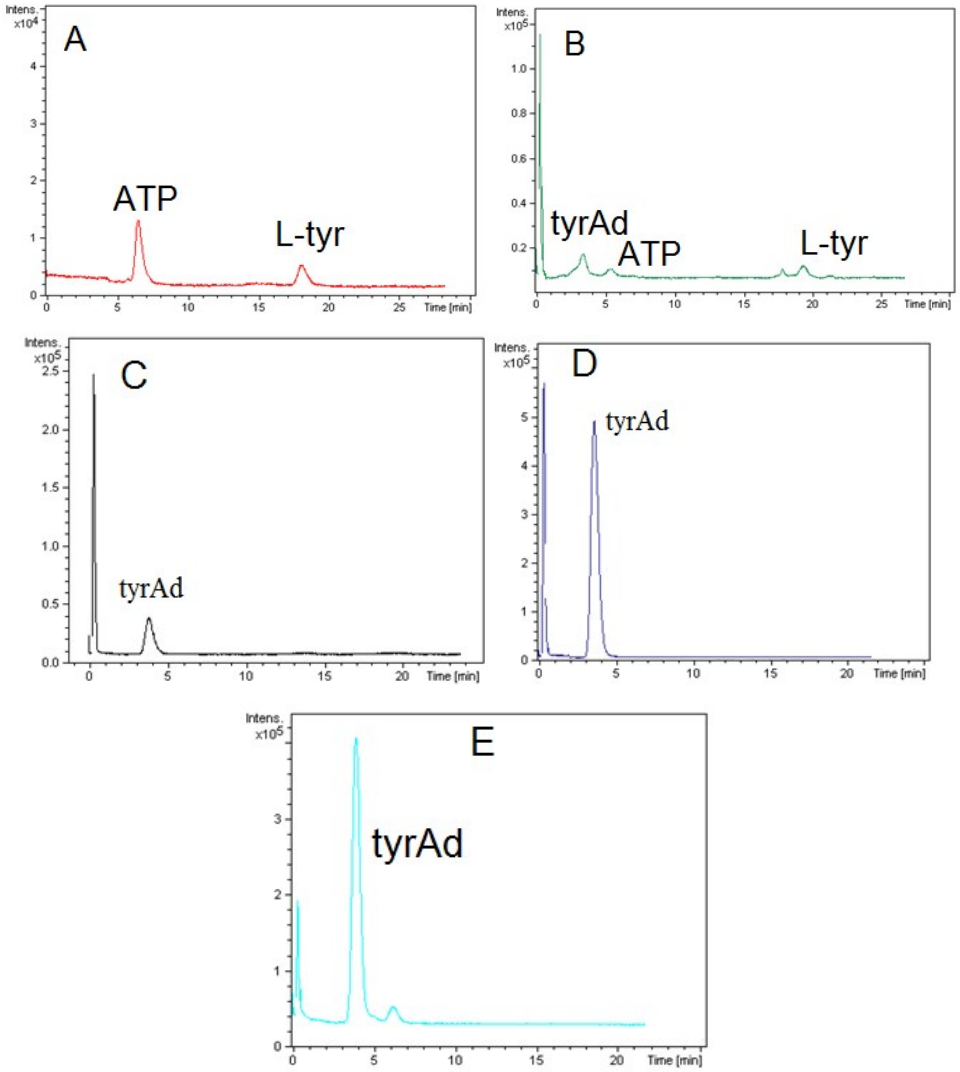

Figure S98. LC chromatograms of solution of 490 µM ATP, 400 µM L-Tyrosine and 20 µL of appropriately diluted tyrosyl tRNA synthetase in 2 mL of buffer (3 µM HEPES, 50 mM $MgCl_2$, 80 mM KCl) in ultrapure water at different time intervals: (A) 10 min, (B) 30 min, (C) 50 min, (D) 70 min, (E) 90 min. Eluent was H_2O- ACN, 90:10 in isocratic mode so that interference of the enzyme peak is avoided. Enzyme was eluted at 30 min when H_2O – ACN was used as eluent in the ratio 4:6.

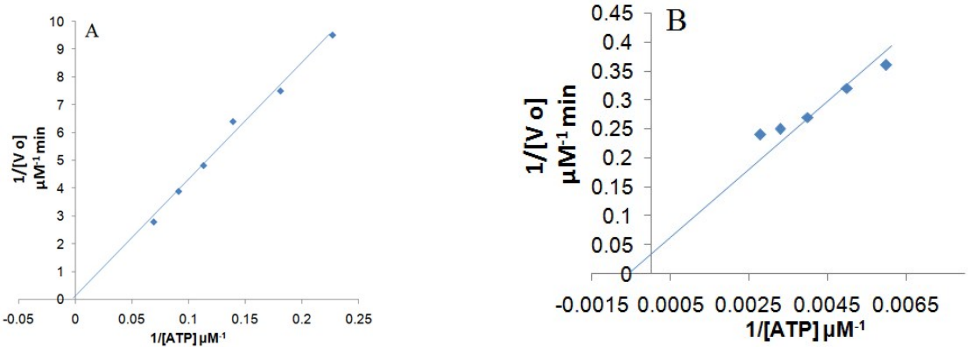

Figure S99. Kinetic parameters of: (A) Tyrosyl-tRNA synthetase catalyzed formation of tyrosyl-adenylate, (B) compound **1** catalyzed formation of tyrosyl-adenylate.

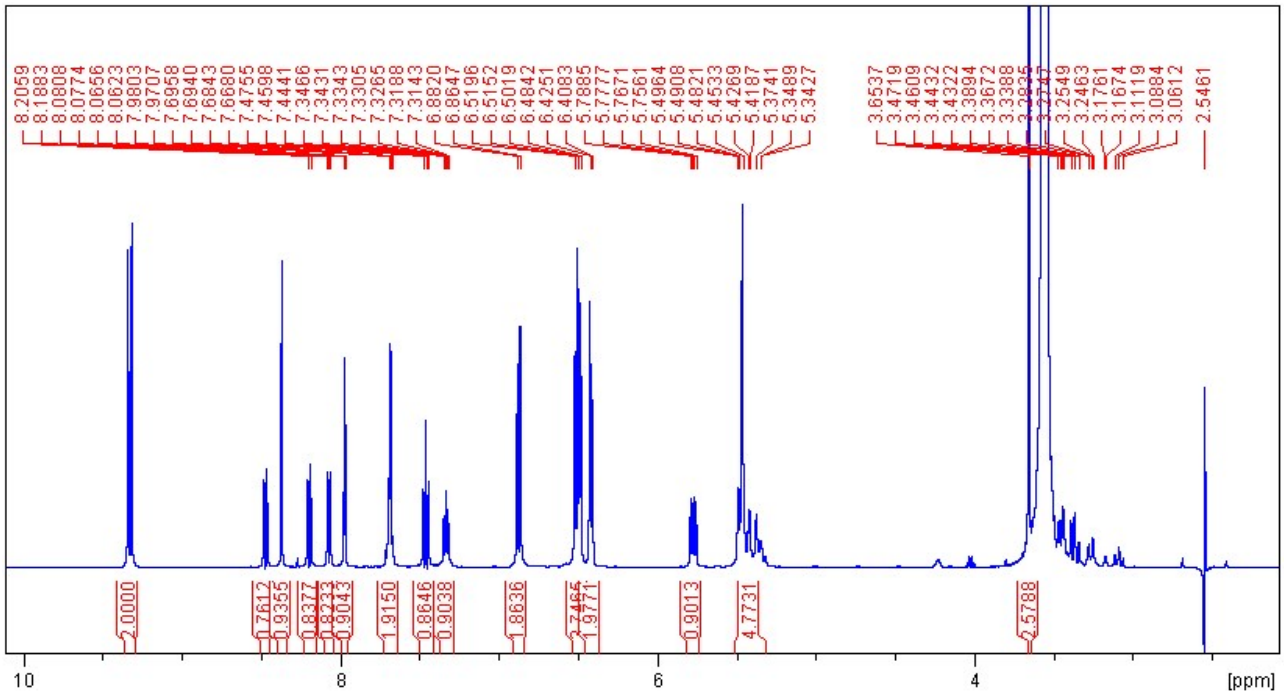

Figure S100. ^{1}H NMR spectrum of compound **1** (DMSO – H_2O – DMSO-d_6 8:1:1 v/v).

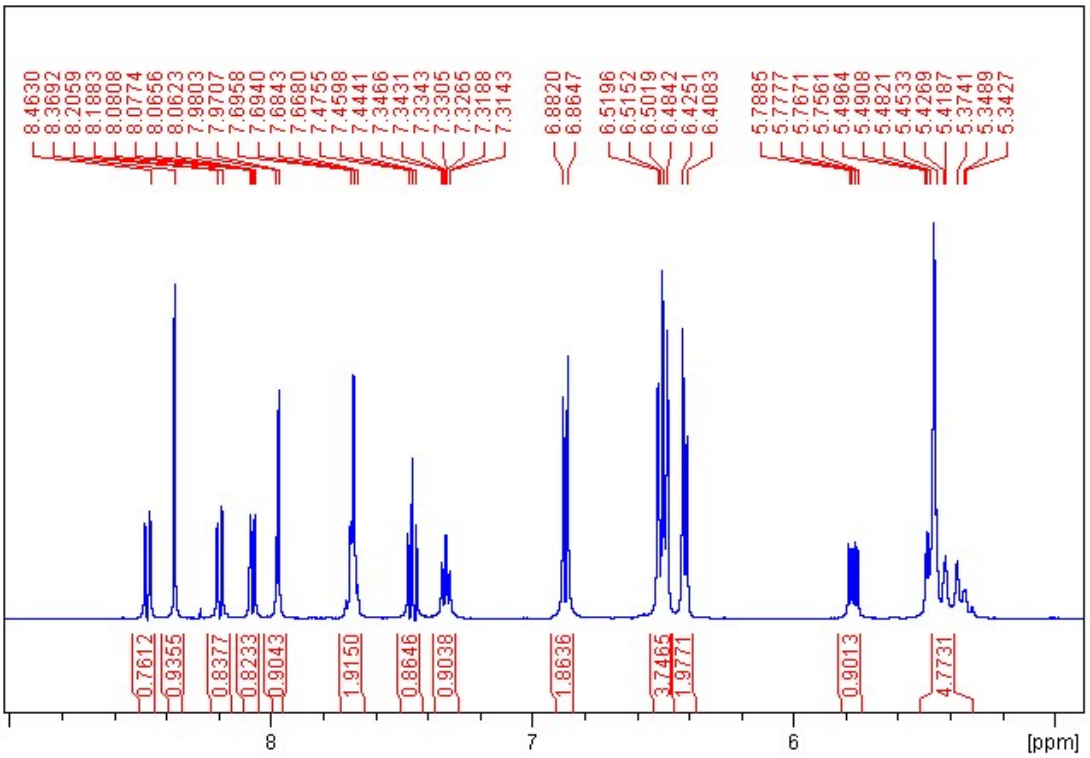

Figure S101. A part of ^{1}H NMR spectrum of compound **1** (DMSO – H_2O – DMSO-d_6 8:1:1 v/v).

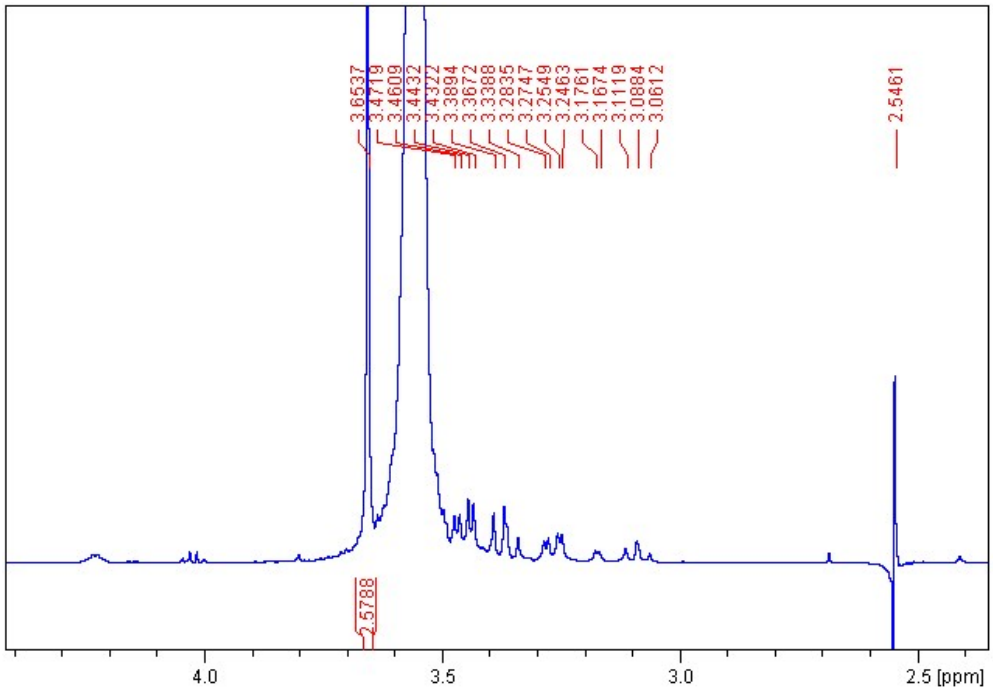

Figure S102. A part of ^{1}H NMR spectrum of compound **1** (DMSO – H_2O – DMSO-d_6 8:1:1 v/v).

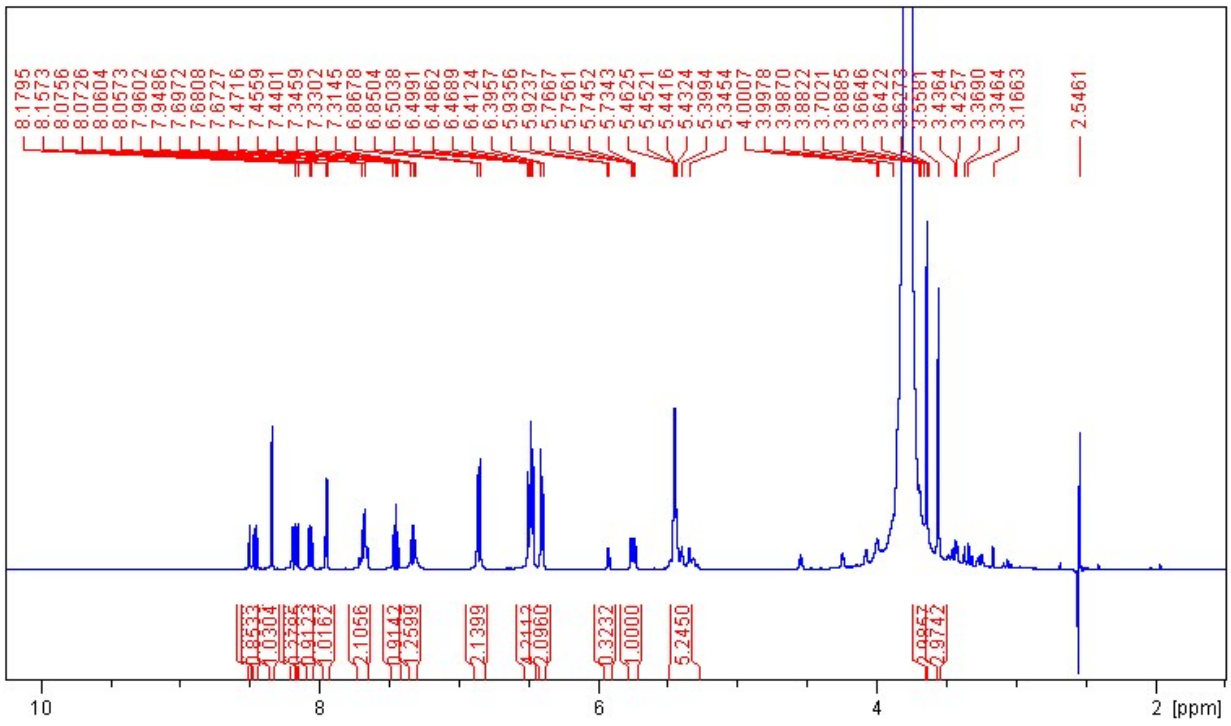

Figure S103. ^{1}H NMR spectrum of solution of compound **1** (10 mM) and ATP (10 mM) in DMSO – H_2O – DMSO-d_6 (8:1:1 v/v). Spectra were recorded at 25 – 40 °C and same chemcial shift was observed up to 40 °C.

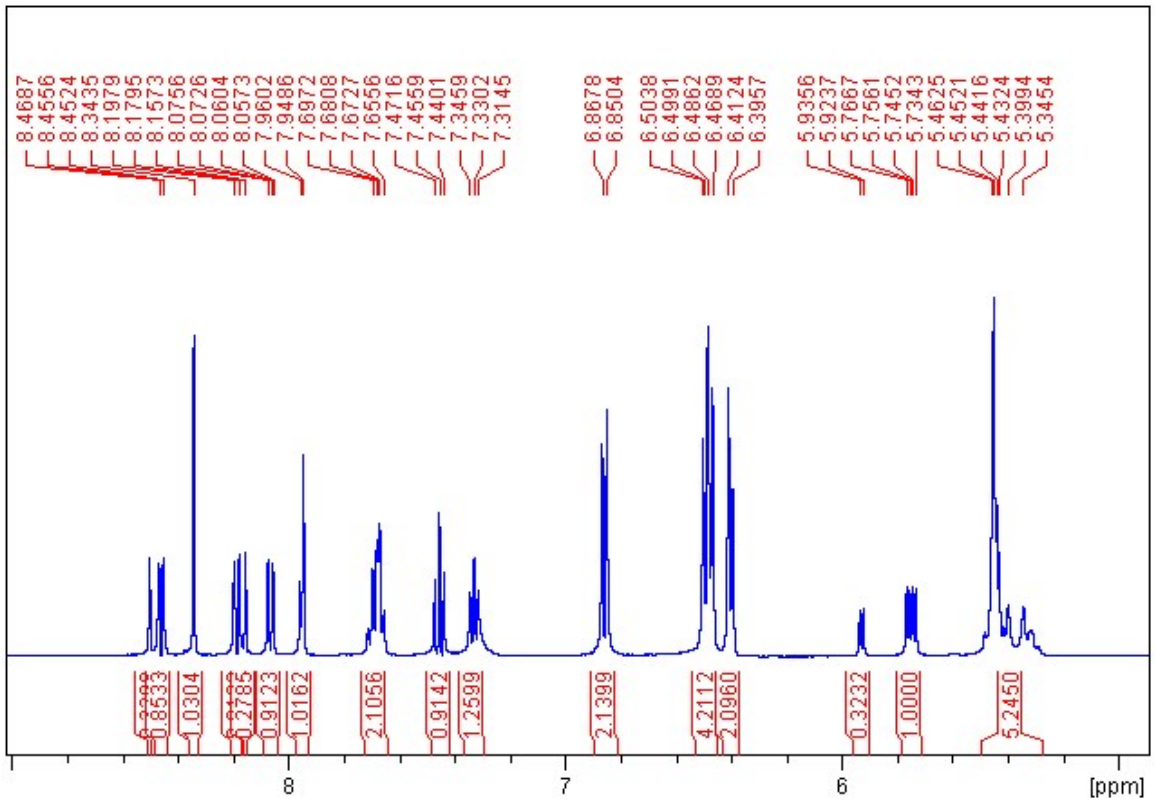

Figure S104. A part of ^{1}H NMR spectrum of solution of compound **1** and ATP (DMSO – H_2O – DMSO-d_6 8:1:1 v/v).

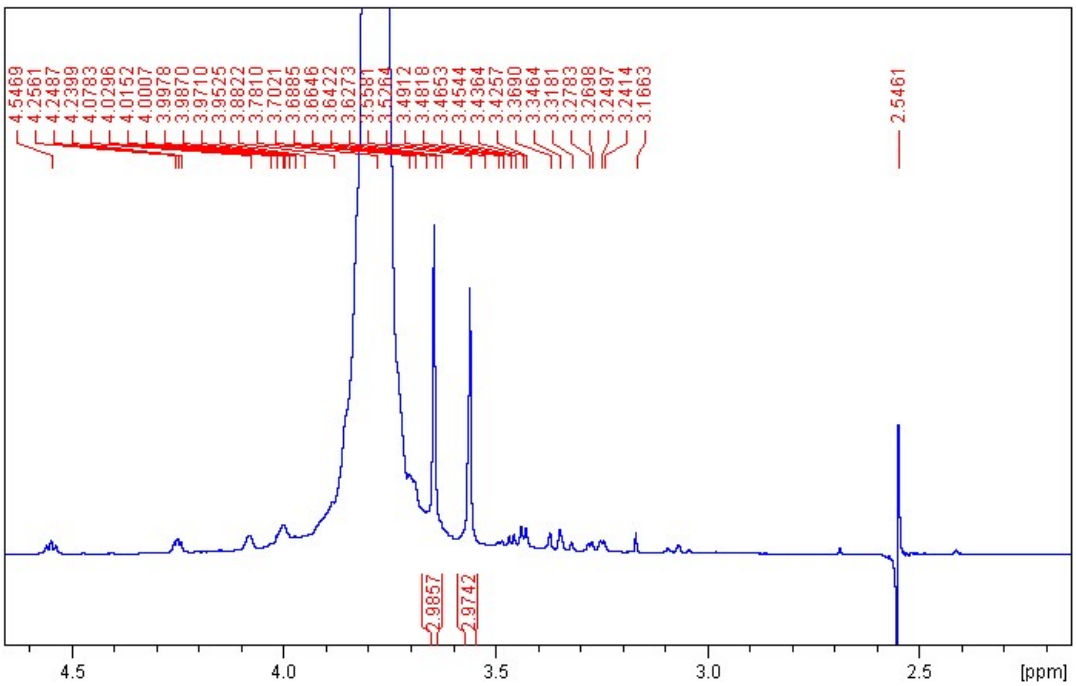

Figure S105. A part of ^{1}H NMR spectrum of solution of compound **1** and ATP (DMSO – H_2O – DMSO-d_6 8:1:1 v/v).

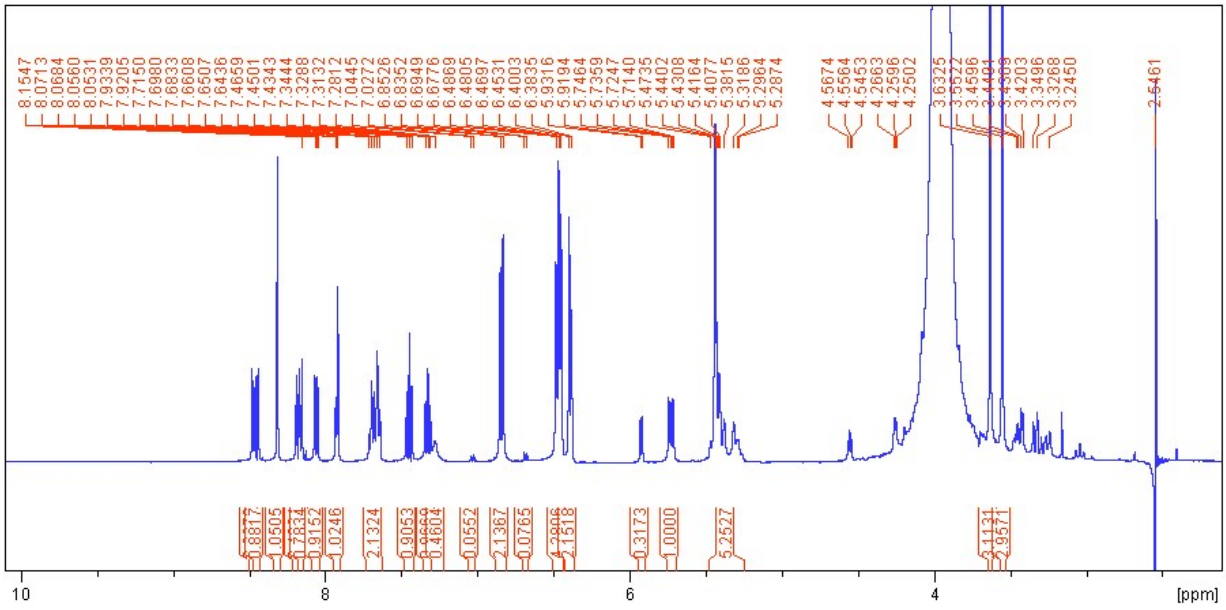

Figure S106. ^{1}H NMR spectrum of solution of compound **1** (10 mM), ATP (10 mM) and L-Tyr (0.84 mM) in DMSO – H_2O – DMSO-d_6 (8:1:1 v/v). Spectra were recorded at 25 – 40 ^{o}C and same chemcial shift was observed up to 40 ^{o}C.

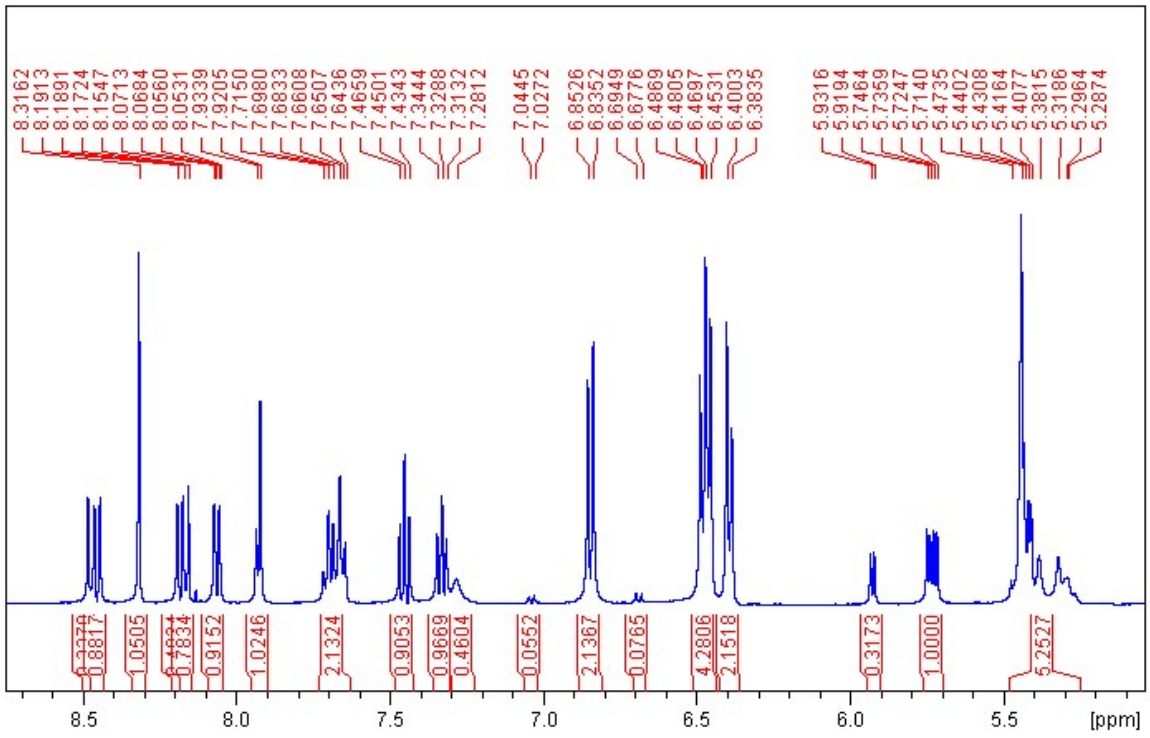

Figure S107. A part of ^{1}H NMR spectrum of solution of compound **1**, ATP and L-Tyr (DMSO – H_2O – DMSO-d_6 8:1:1 v/v).

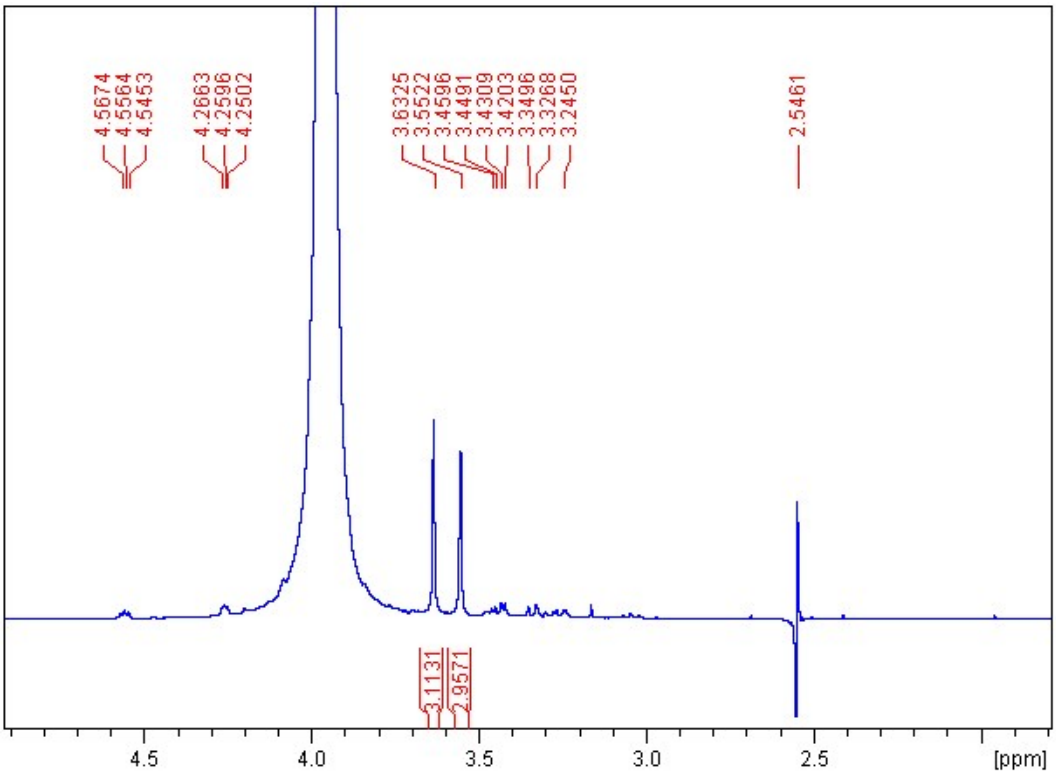

Figure S108. A part of ^{1}H NMR spectrum of solution of compound **1**, ATP and L-Tyr (DMSO – H_2O – DMSO-d_6 8:1:1 v/v).

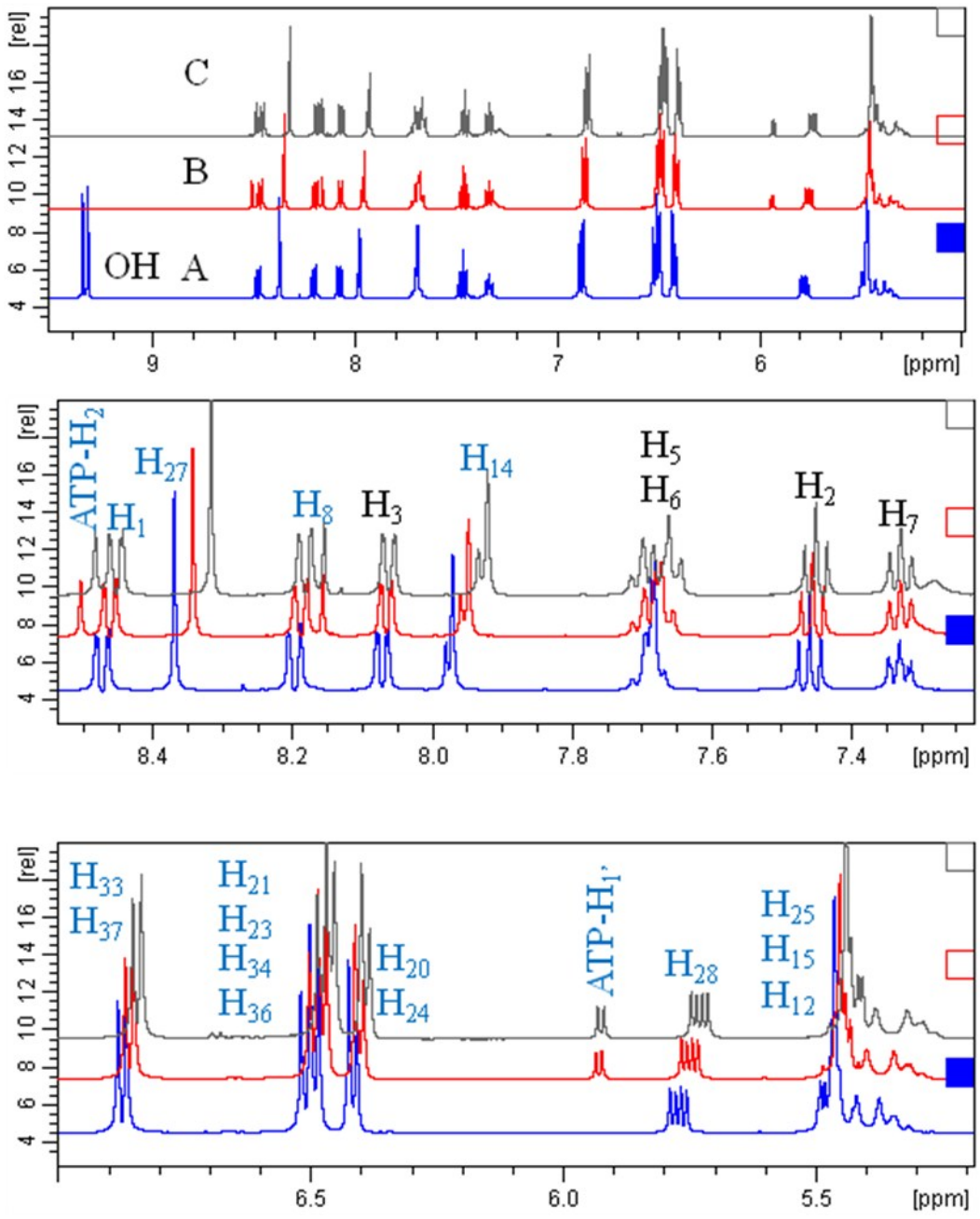

Figure S109. Change in the chemical shift of compound **1** (Blue trace) on addition of ATP (red trace) and subsequent addition of L-Tyr (black trace).

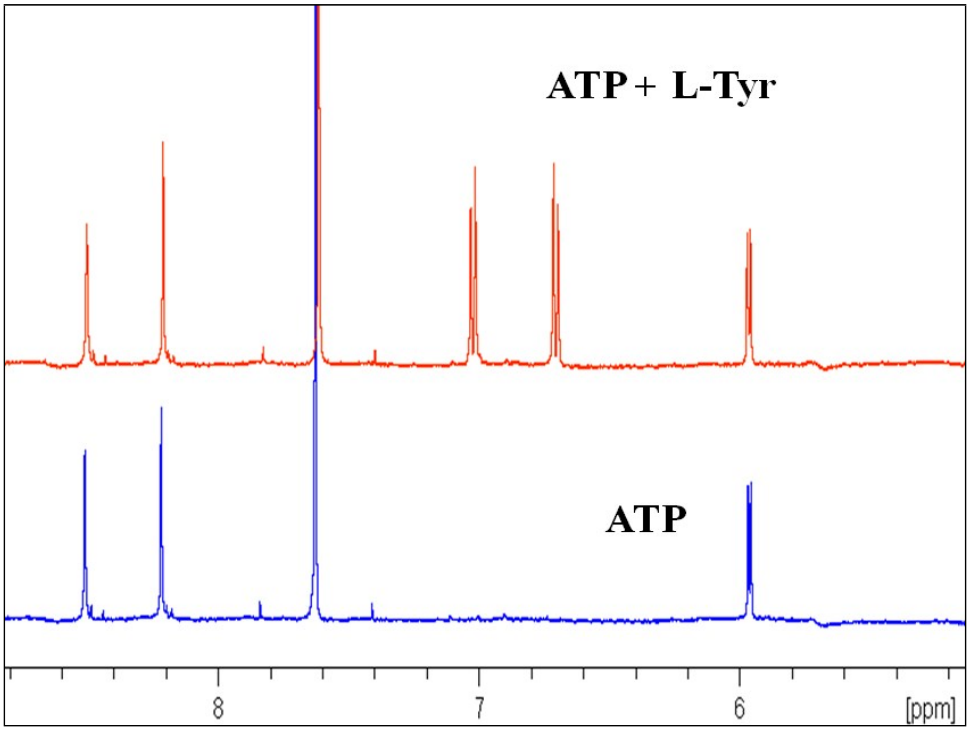

Figure S110. ^{1}H NMR of ATP (lower trace) and ATP + L-Tyr (upper trace). Both ATP and L-Tyr were 10^{-3} M each.

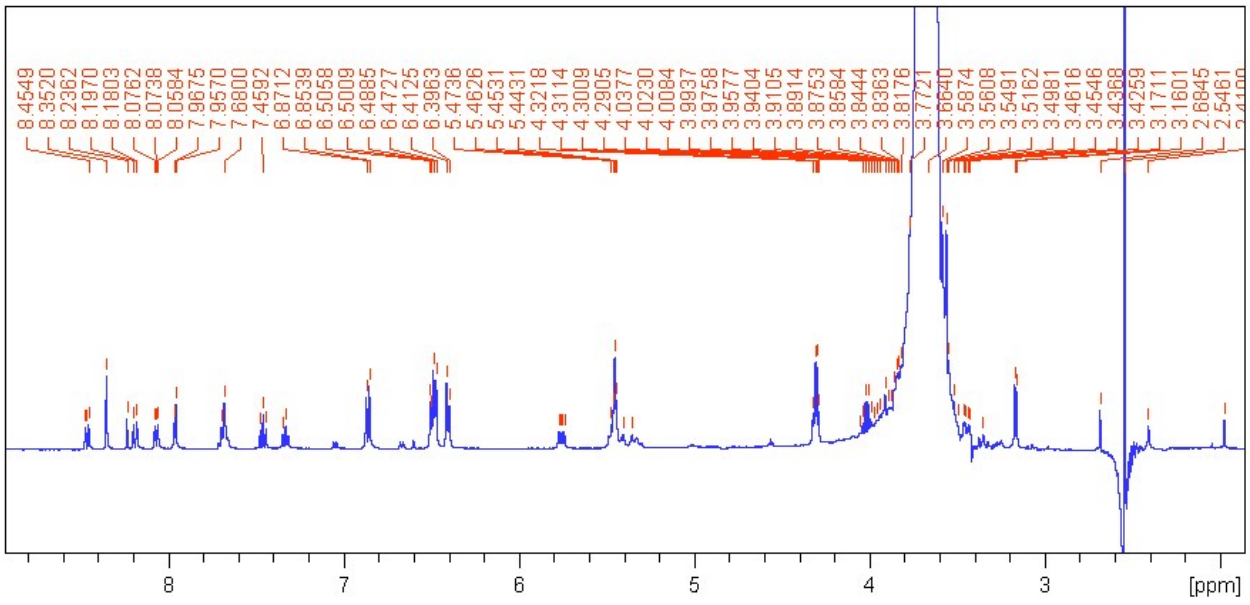

Figure S111. ^{1}H NMR spectrum of compound **1** (DMSO-H_2O-DMSO-d_6, 8:1:1 v/v).

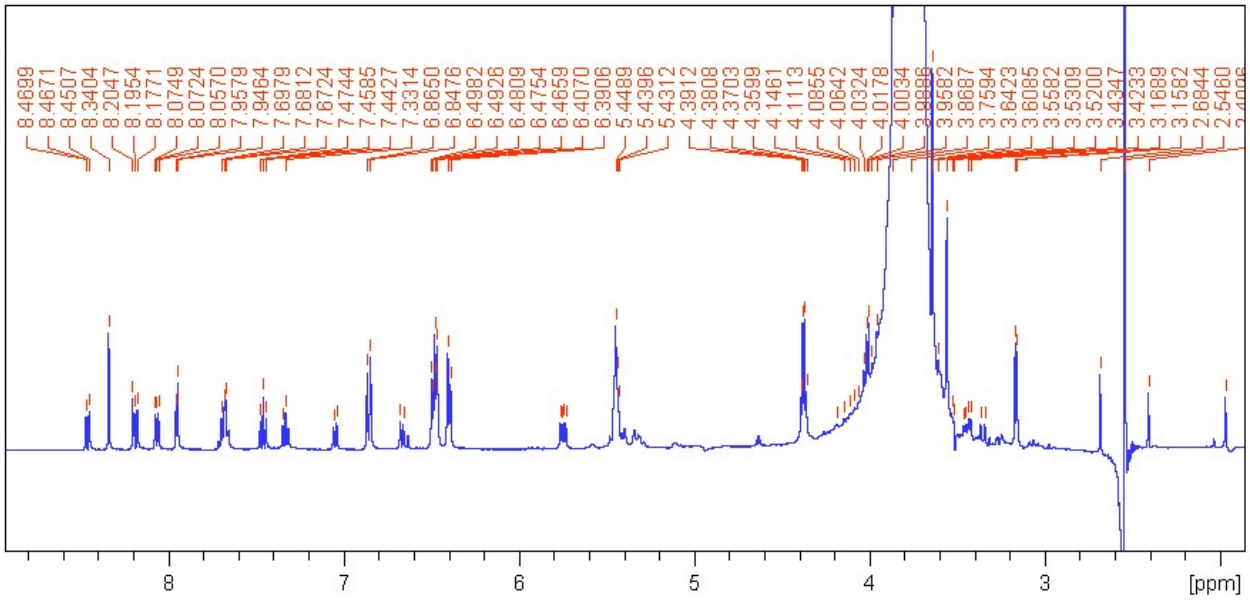

Figure S112. ^{1}H NMR spectrum of compound **1** + L-Tyr (DMSO-H_2O-DMSO-d_6, 8:1:1 v/v).

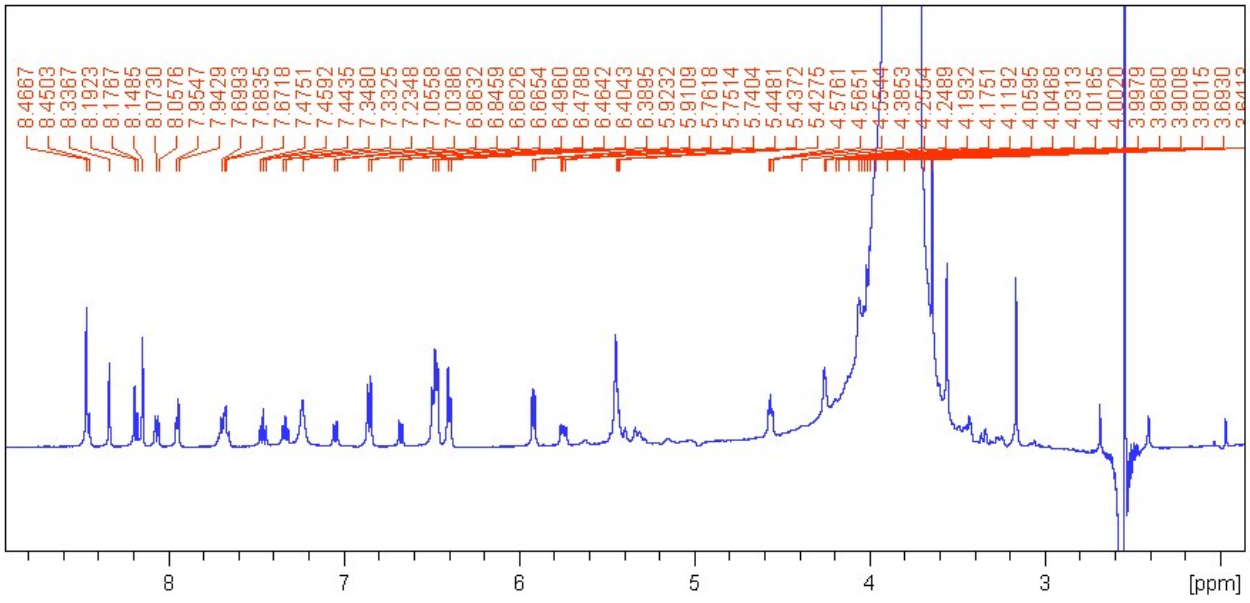

Figure S113. ^{1}H NMR spectrum of compound **1** + L-Tyr + ATP (DMSO-H_2O-DMSO-d_6, 8:1:1 v/v).

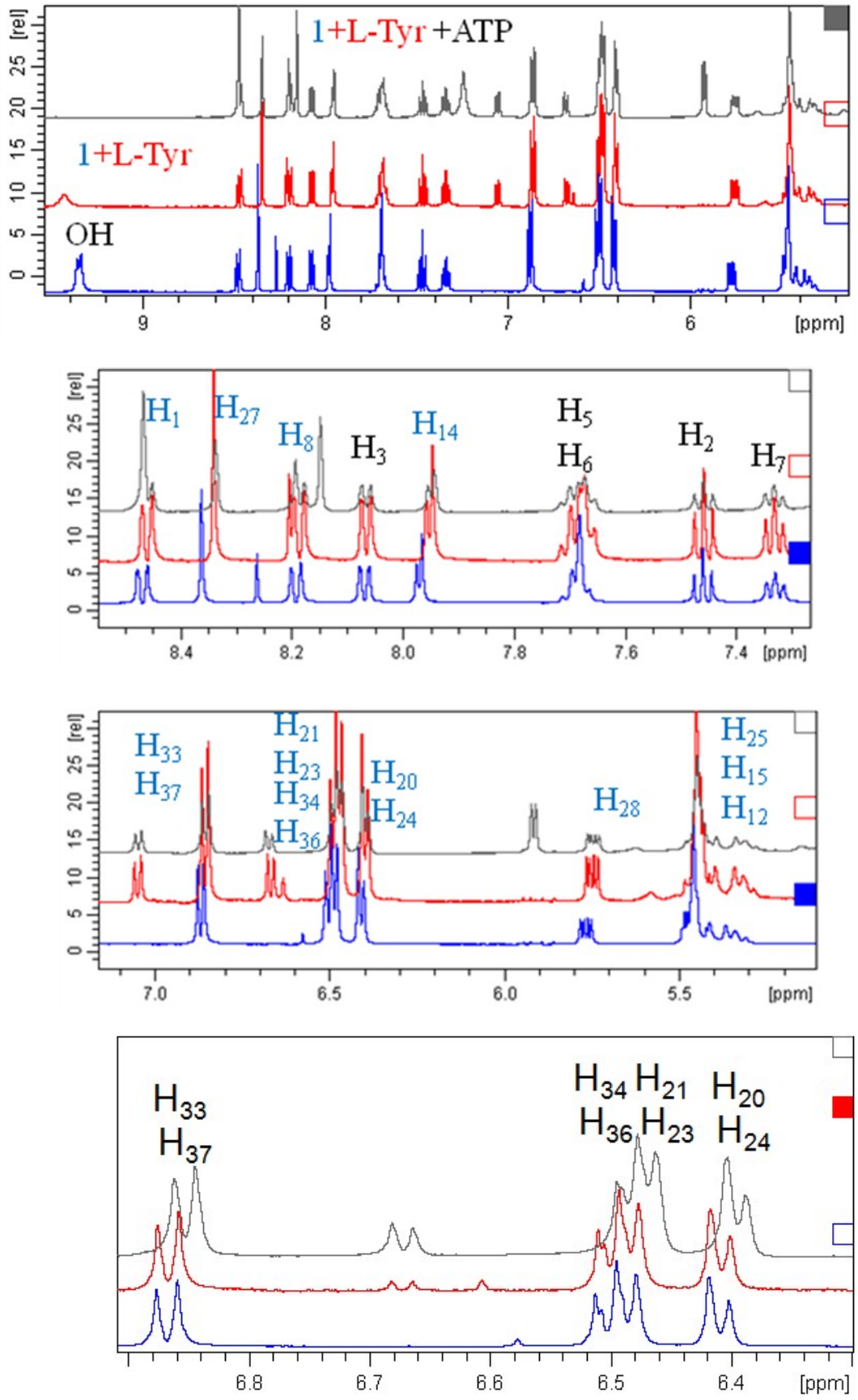

Figure S114. ^{1}H NMR spectrum of compound **1** (Blue trace), compound **1** + L-Tyr (Red trace) and compound **1** + L-tyr + ATP (Black trace).

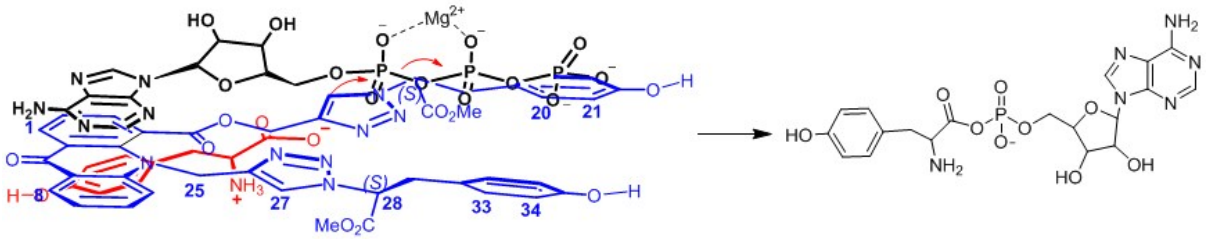

Figure S115. Proposed mechanism for compound **1** mediated formation of tyrosyl adenylate.

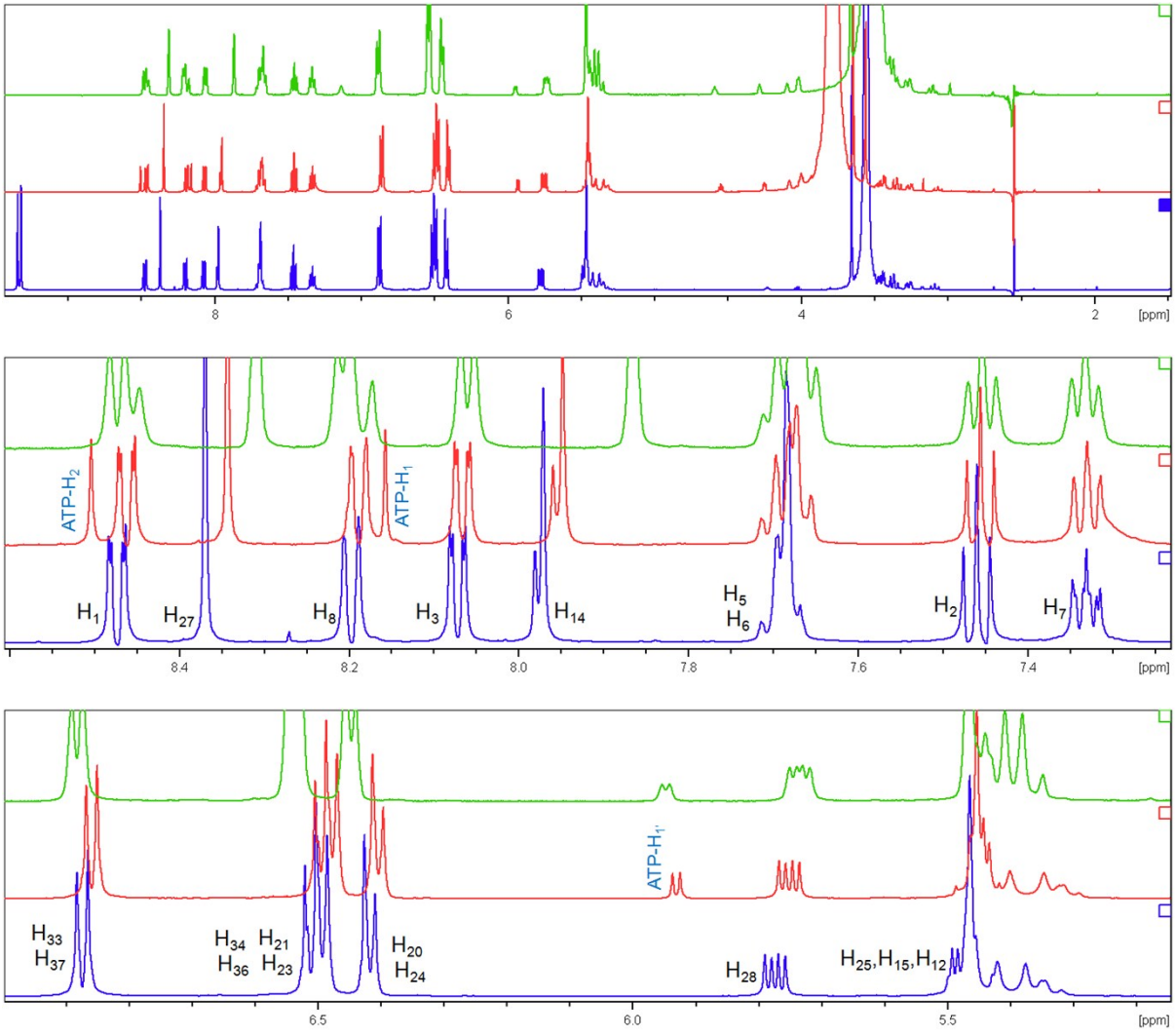

Figure S116. Comparison of the change in proton chemical shifts of compound **1** (blue trace) on addition of ATP and L-Tyr at different temperature: 25 °C (red trace) and 50 °C (green trace). At 50 °C, the aromatic protons did not show change in chemical shifts.

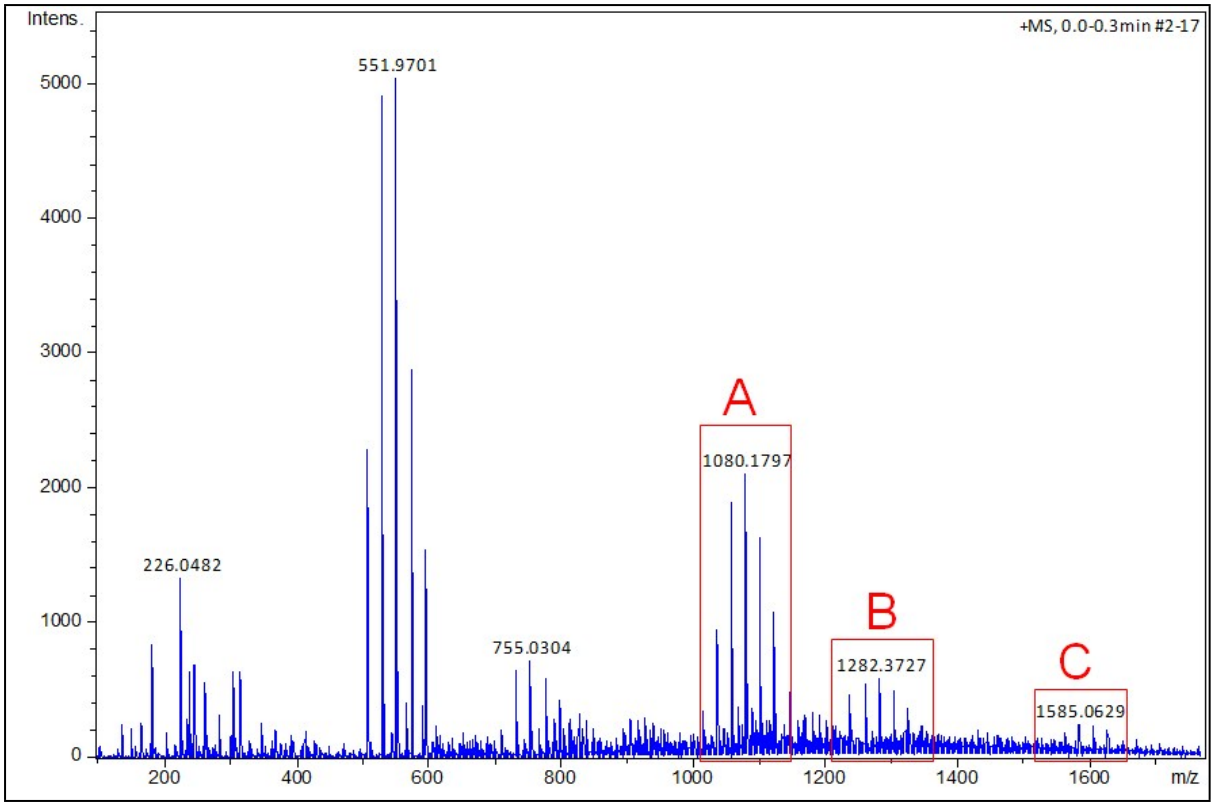

Figure S117. Mass spectrum of solution of 490 µM ATP, 400 µM L-Tyrosine and 20 µL of appropriately diluted tyrosyl tRNA synthetase in 2 mL of buffer (3 µM HEPES, 50 mM $MgCl_2$, 80 mM KCl) in ultrapure water.

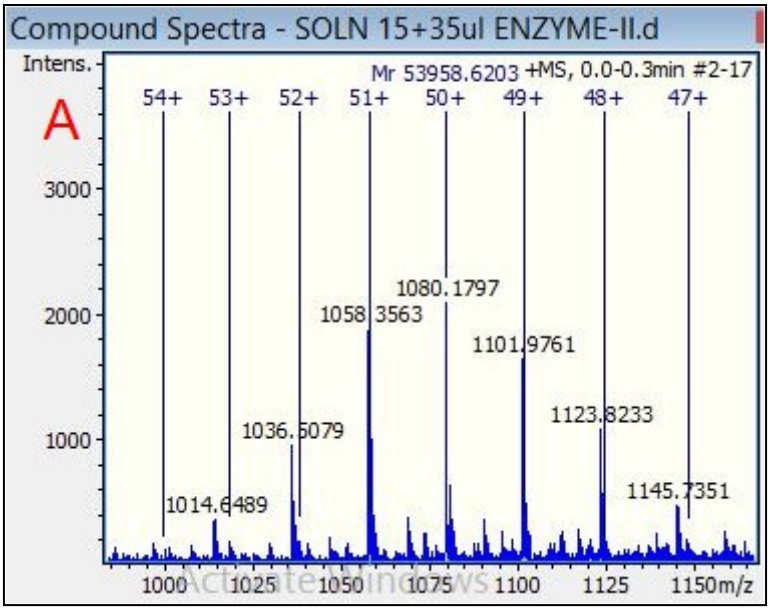

Figure S117A. Part A of Fig 117 is expanded.

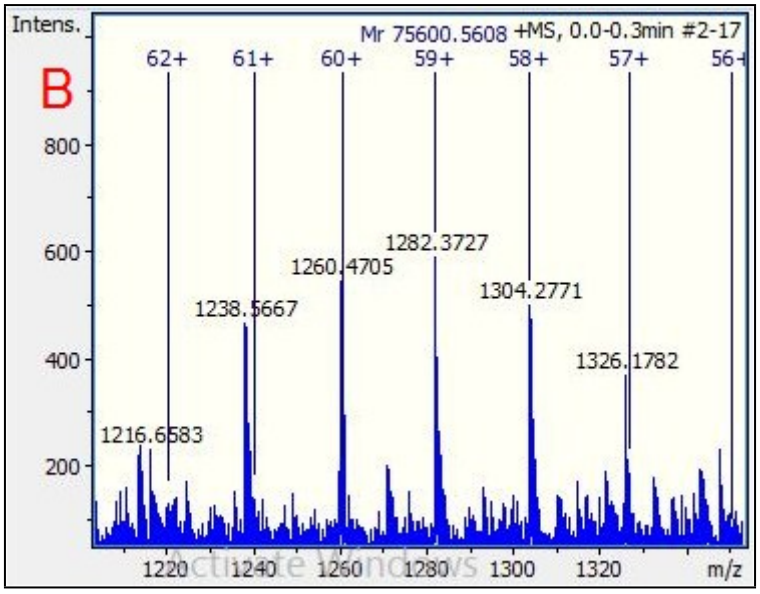

Figure S117B. Part b of Fig 117 is expanded.

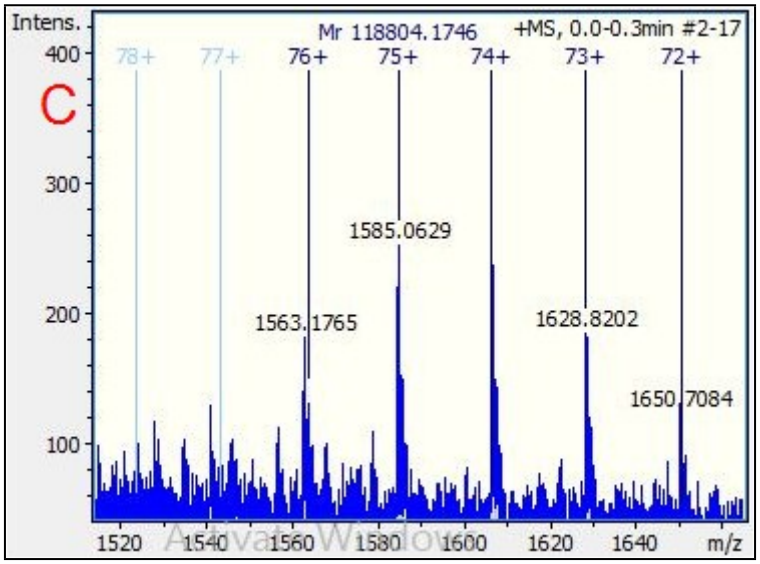

Figure S117C. Part C of Fig 117 is expanded.

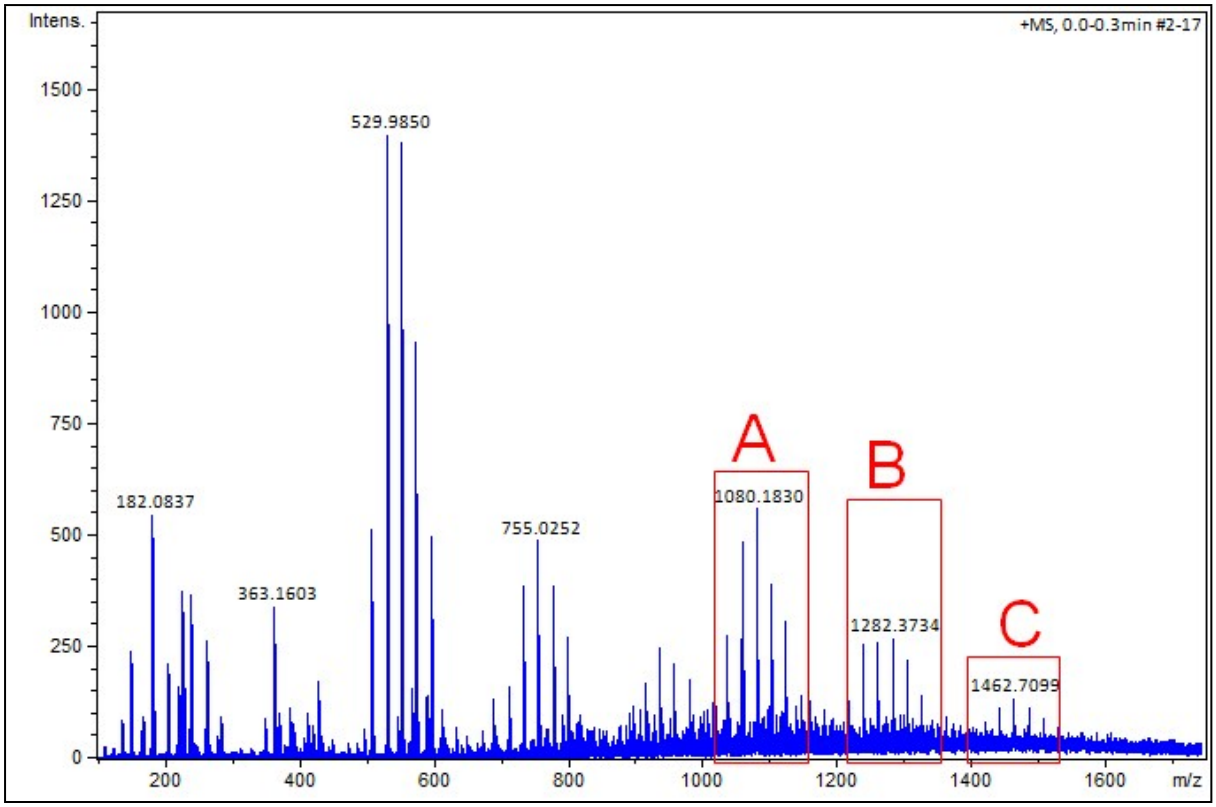

Figure S118. 20 µL of appropriately diluted tRNA solution was added to the above solution of Figure S117 and the mass spectrum was recorded.

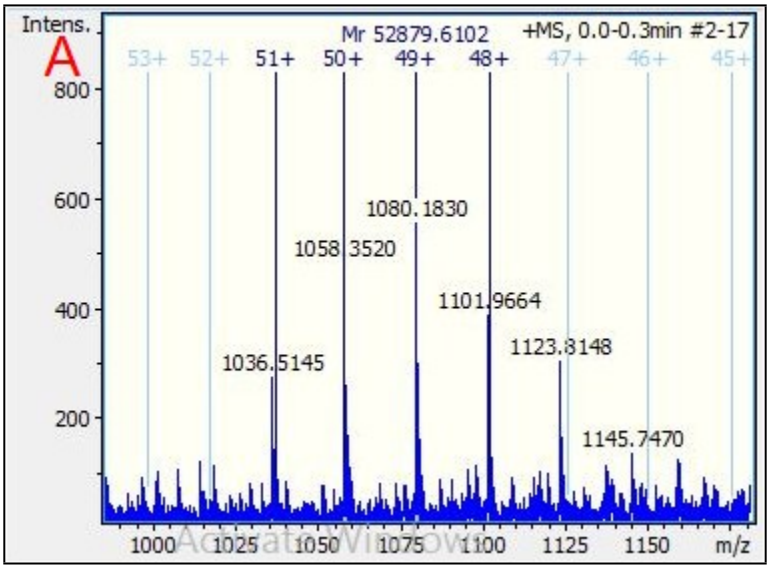

Figure S118A. Part A of Fig 118 is expanded.

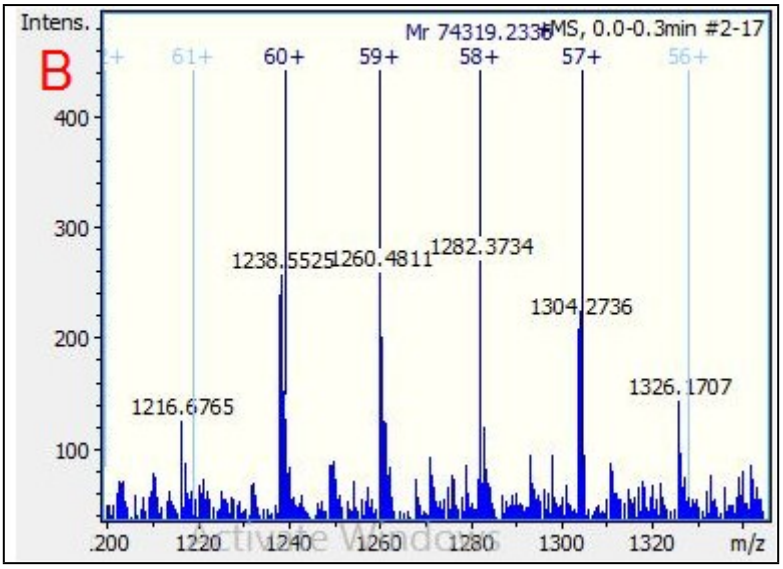

Figure S118B. Part B of Fig 118 is expanded.

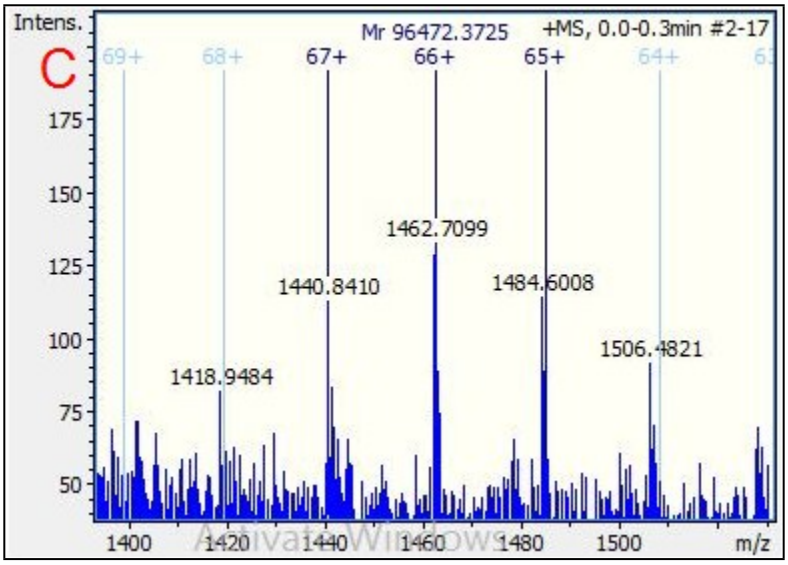

Figure S118C. Part C of Fig 118 is expanded.

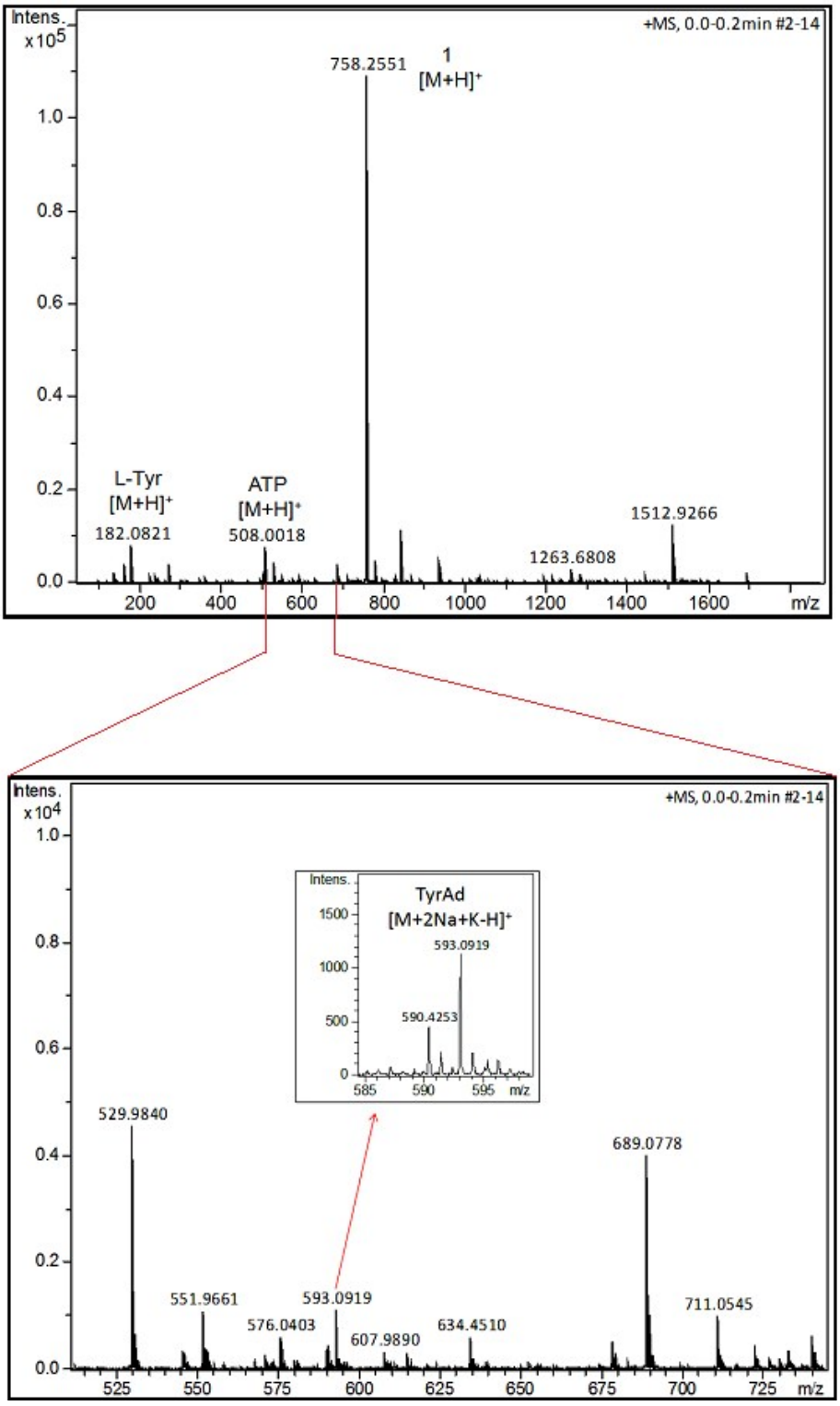

Figure S119. Mass spectrum of solution of 490 µM ATP, 400 µM L-tyrosine, 10 µM compound **1** and 20 µl of appropriately diluted (50 nM) tyrosyl tRNA synthetase in 2 ml of buffer (3 µM HEPES, 50 mM $MgCl_2$, 80 mM KCl) in ultrapure water. Mass peak of tyrosyl adenylate at *m/z* at 593.0917 $[M+2Na+K-H]^+$ (calcd *m/z* 593.0534) was observed.

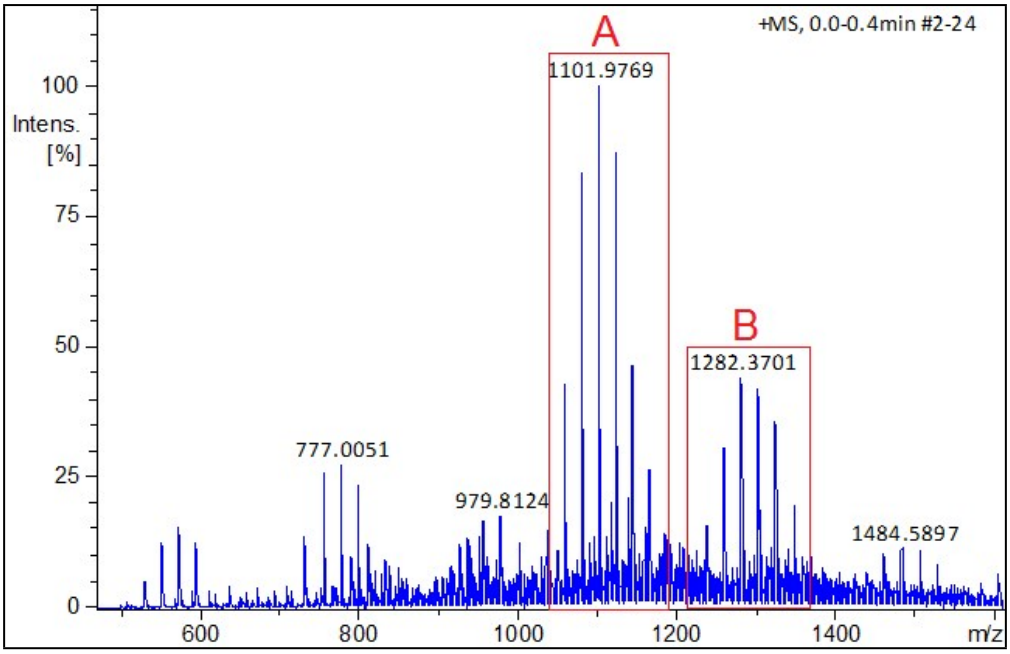

Figure S119A. Mass spectrum of solution of 490 µM ATP, 400 µM L-tyrosine, 10 µM compound **1** and 20 µl of appropriately diluted (50 nM) tyrosyl tRNA synthetase in 2 ml of buffer (3 µM HEPES, 50 mM $MgCl_2$, 80 mM KCl) in ultrapure water. Mass spectrum was recorded in 'intact protein' method to see the peaks of the enzyme.

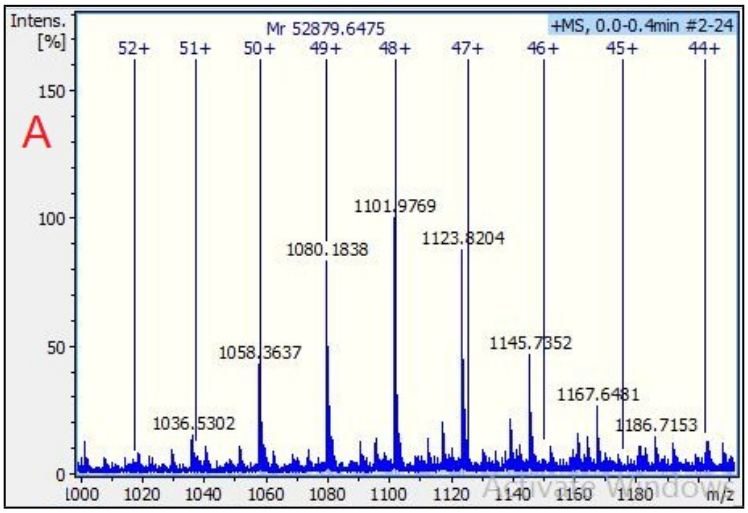

Figure S119B. Part A of mass spectrum of Figure S119A.

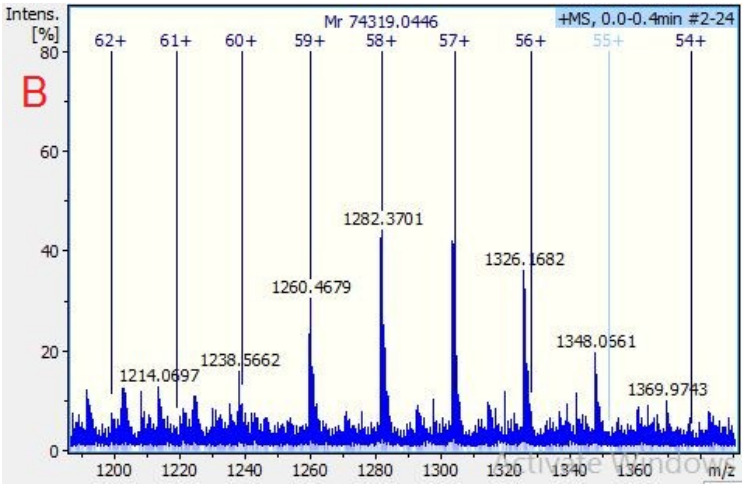

Figure 119C. Part B of mass spectrum of Figure S119A.

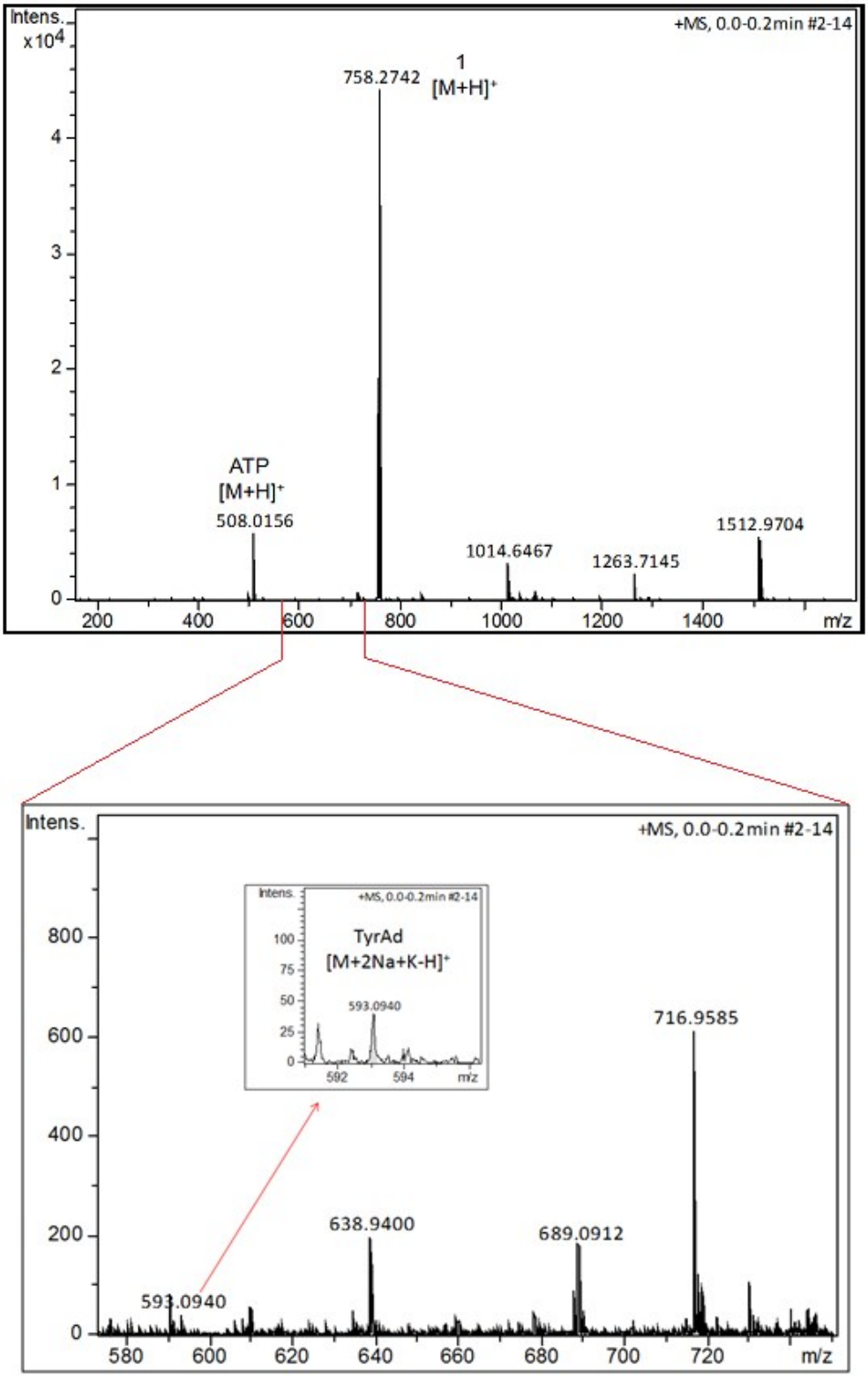

Figure S120. 20 µl of appropriately diluted tRNA solution was added to the solution of Figure S119 and the mass spectrum was recorded. Mass peak of tyrosyl adenylate at *m/z* 593.0926 $[M+2Na+K-H]^+$ (calcd *m/z* 593.0534).

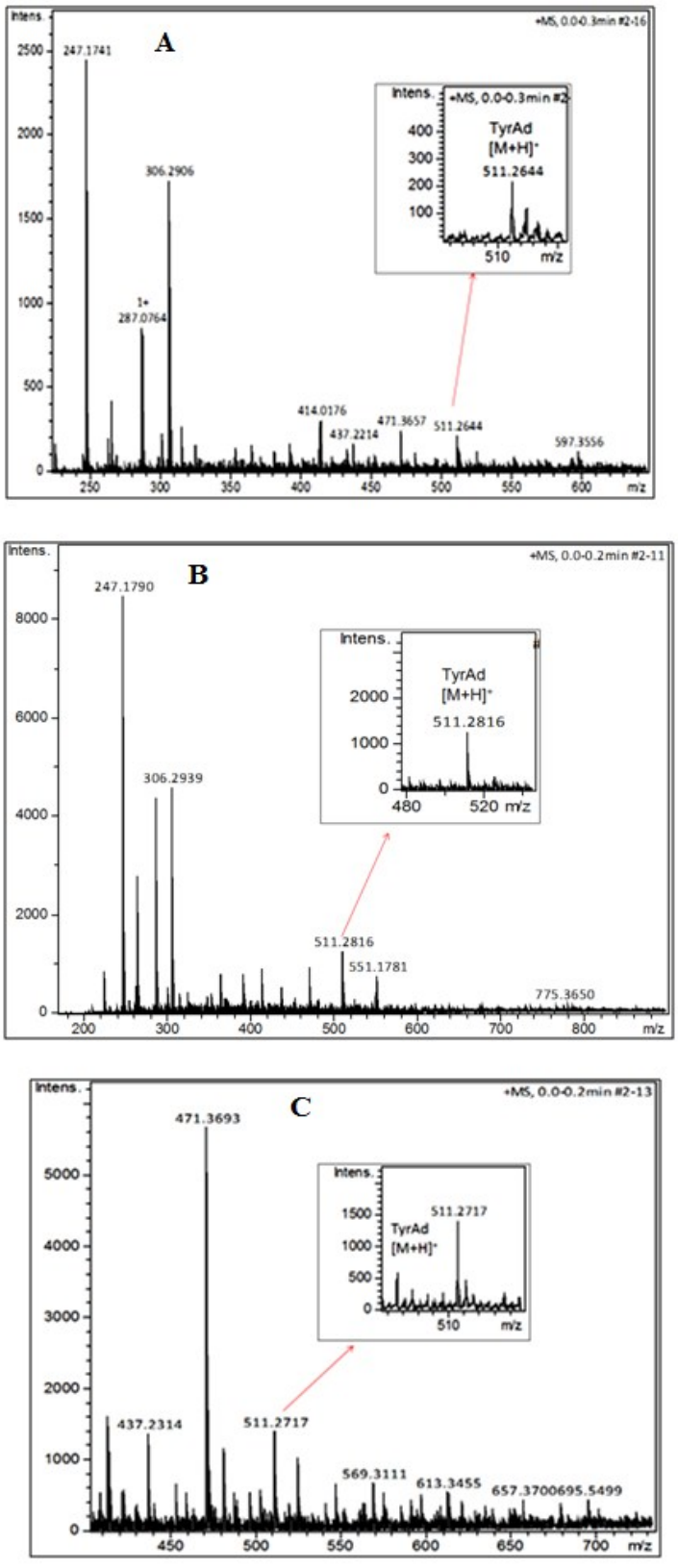

Figure S121. (A) Mass spectrum of solution of tyrosyl adenylate (prepared in lab), 0.53 mM in 3 µM HEPES, 50 mM $MgCl_2$, 80 mM KCl in ultrapure water. Mass peak of tyrosyl adenylate at *m/z* 511.2644 $[M+H]^+$ (calcd *m/z* 511.1336). (B) 7.5 µL of appropriately diluted

tRNA solution was added to the solution of tyrAd and mass spectrum was recorded. Mass peak of tyrosyl adenylate at *m/z* 511.2816 $[M+H]^+$ is visible. (C) 7.5 μL of appropriately diluted tyrosyl synthetase was added to the above solution B and mass spectrum was recorded. TyrAd was found at *m/z* 511.2717 $[M+H]^+$. This experiment indicates that free tyrAd was neither picked up by TyrTS nor by tRNA.

References

1. Zimmerman, J. J.; Arnim, A. V. S. A.-V.; McLaughlin, J. *In Cellular Respiration. Pediatric Critical Care*, Fourth Edition; USA, 2011, Ch 74.